

AD-A127 412

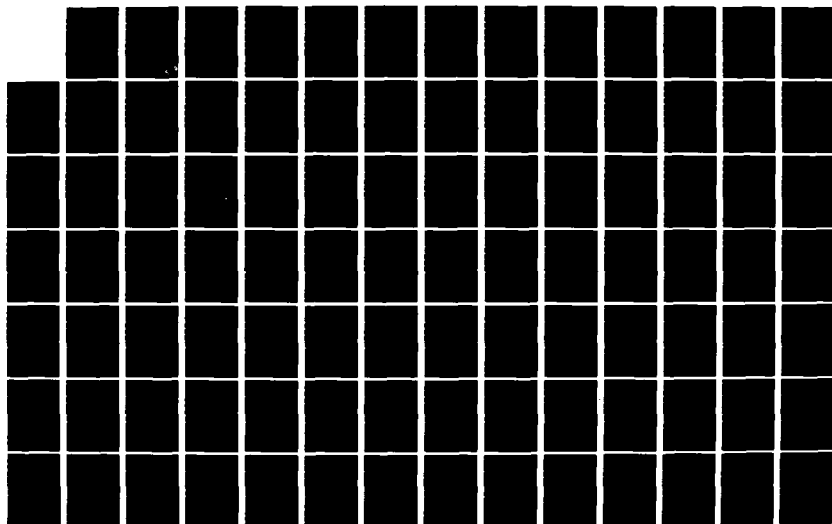
CHARACTERIZATION OF LASER BEAM QUALITY(U) AIR FORCE
INST OF TECH WRIGHT-PATTESSON AFB OH SCHOOL OF
ENGINEERING A T GUMAHAD DEC 82 AFIT/GEO/PH/82D-4

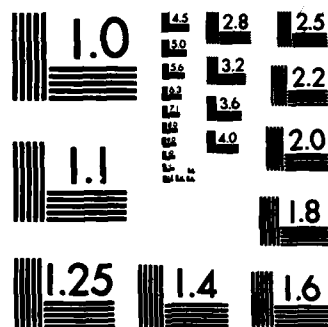
1/2

UNCLASSIFIED

F/G 28/5

NL





MICROCOPY RESOLUTION TEST CHART
NATIONAL BUREAU OF STANDARDS-1963-A

1

AD A127412



CHARACTERIZATION OF LASER BEAM QUALITY

THESIS

AFIT/GEO/PH/82D-4 Arsenio T. Gumahad II
Capt USAF

DTIC FILE COPY

DEPARTMENT OF THE AIR FORCE
AIR UNIVERSITY (ATC)

AIR FORCE INSTITUTE OF TECHNOLOGY

This document has been approved for public release and sale; its use is unlimited.
Wright-Patterson Air Force Base, Ohio

83 04 28 112

DTIC
SELECTED
APR 28 1983
SD
E

①

CHARACTERIZATION OF LASER BEAM QUALITY

THESIS

AFIT/GEO/PH/82D-4 Arsenio T. Gumahad II
Capt USAF

Approved for public release; distribution unlimited

DTIC
ELECTE
S APR 28 1983
E

CHARACTERIZATION OF LASER BEAM QUALITY

THESIS

Presented to the Faculty of the School of Engineering

of the Air Force Institute of Technology

Air University

in Partial Fulfillment of the

Requirements for the Degree of

Master of Science

by

Arsenio T. Gumahad II, B.S.E.E.

Captain

USAF

Graduate Electro-Optics

Dec 1982

Accession For	
NTIS GRA&I	<input checked="checked" type="checkbox"/>
DTIC TAB	<input type="checkbox"/>
Unannounced	<input type="checkbox"/>
Justification	
By _____	
Distribution/	
Availability Codes	
Dist	Avail and/or Special
A	



Preface

This report examines an improved method of laser beam quality characterization. Much of the work done in this report involved computer programming, debugging, and endless simulations, in addition to information gathering on a limited subject matter. Thanks are due to my advisor, Capt R. Cook, and my thesis sponsor, Mr S. Johnson of the Air Force Avionics Laboratory. Their continued support and technical expertise were critical throughout this thesis.

This thesis can not be complete without thanking my fellow students and family. The friendships I have gained here will certainly follow me for years to come with fond memories. My family, even from far-away New Jersey, were certainly instrumental in providing me the needed personal support, through their continued love and understanding. Lastly, my best of thanks to Jamie. Her love and devotion made a very positive contribution throughout this thesis effort, through, certainly one of the hardest times in my life.

Bong Gumahad

Contents

Preface	ii
List of Figures	iv
List of Tables	vi
Abstract	vii
I. Introduction	1
Task	2
Scope and Assumptions.	2
Organization and Approach to the Problem	3
II. Current Methods of Characterizing Laser Beams.	6
Existing Figures of Merit.	6
Power in the Bucket.	7
Beam Divergence and Spot Size Measurements	13
Strehl Ratio	22
III. Modeling Phase Aberrated Laser Beams	25
Theory	26
The Numerical Model.	30
Input	33
Operation	33
Output.	35
IV. Characterizing Phase Aberrated Laser Beams	36
Characteristics of Nondiffraction-limited Beams.	36
Least Squares Method of Curve Fitting.	51
Data Analysis.	54
V. Conclusions and Recommendations.	69
Proposed Procedures.	77
Bibliography.	80
Appendix A: Numerical Model of Nondiffraction-limited Beams	82
Appendix B: Least Squares Method of Curve Fitting	92
Appendix C: Values of Randomly Generated Coefficients.	95

List of Figures

Figure		Page
1	Intensity Distribution of Gaussian Beam.	8
2	Beam Quality P-R Curve	9
3	General Beam quality set-up.	10
4	Transmitted Power vs Aperture and Theoretical Curve.	11
5	Relative widths for ideal and non-ideal Laser Beams.	12
6	Laser Geometry	13
7	Intensity Distribution of a Gaussian beam in which the center is interrupted by an opaque ribbon	16
8	Typical Laser set-up from which beam parameters are determined	17
9	Attenuator method for determining divergence .	20
10	Comparison of waist (w) to the distance from the laser (z) for scanning wire, scanning edge, scanning slit, and theoretical curve from cavity theory	21
11	Wave propagation into the Fresnel region and beyond	23
12	The rectangular function	31
13	Simplified flow diagram of computer model to determine irradiance distributions	34
14	Irradiance profile of phase aberrated beam . .	40
15	Irradiance profile of phase aberrated beam . .	41
16	Irradiance profile of phase aberrated beam . .	42
17	Irradiance profile of phase aberrated beam . .	43
18	Irradiance profile of phase aberrated beam . .	44
19	Comparative plots of diffraction-limited beam and three cases of phase aberrated beams . .	45

20	Irradiance profile.	47
21	Irradiance profile.	48
22	Irradiance profile.	49
23	Irradiance profile.	50
24	Flow diagram of method to calculate F and σ^2 by the least squares solution and using the incremental search method	55
25	Curve fit	57
26	Curve fit	58
27	Curve fit	59
28	Curve fit	60
29	Curve fit	61
30	Quality of fit.	62
31	Quality of fit.	63
32	Quality of fit.	64
33	Quality of fit.	65
34	Quality of fit.	66
35	Total power plot.	72
36	Total power plot.	73
37	Total power plot.	74
38	Total power plot.	75
39	Total power plot.	76

List of Tables

Table		Page
I	Measured values of F and σ^2 for individual terms	67
II	Measured F and σ^2 for twenty random numbers of phase aberration.	68

Abstract

Current methods of characterizing the quality of laser beams were found to be generally insufficient. Since lasers are gaining more use in many applications, an improved set of quality criteria must now be developed. This thesis report investigated characteristics of random phase aberrations and its effects on the far-field irradiance distribution of lasers. A numerical model was developed to simulate non-diffraction-limited beams. Several simulations were done to study the irradiance profiles for varying degrees of aberrations. It was found that phase aberrated beams can be expressed as the sum of two beams: one is the diffraction-limited beam attenuated by a factor F which is a function of the phase distortion, and the second, a much wider beam whose amplitude and lateral extent is a function of the variance and the form of the phase aberration. By assuming the shape of this 'secondary' beam to be Gaussian, its extent can be measured by calculating the variance, σ^2 , of the Gaussian distribution. A numerical code was devised to determine the two parameters by a least squares curve fitting method. A proposed list of procedures is included in the report to measure these parameters experimentally using data derived from the 'power in the bucket' method. The quality of a laser beam is dependent on the degree of phase aberrations introduced into the system. F and σ^2 describes the amount and form of the phase aberration, thus providing a better criteria for beam quality determination.

CHARACTERIZATION OF LASER BEAM QUALITY

I. Introduction

The requirement for precision laser systems is being recognized increasingly in applications involving weapons systems and in medical research. In many applications, this is achieved using advances in state-of-the-art laser technology. However, a persistent problem in engineering applications of laser physics is how to characterize the quality of a laser beam. Although several criteria for beam quality are presently in use, there is no general agreement as to how the relevant Figures of Merit (FOMs) are to be measured. Most existing characterization of beam quality attempt to describe the quality of the beam by specifying a single number, such as the 'number of times diffraction-limited' or the far-field divergence angle. A measure of quality for any system should lie in its ability to reproduce theoretical or ideal expectations. For example, if a beam is propagated through an optical device, the output of this device should reproduce the input exactly. Thus, for optical systems, including lasers, a measure of quality should be a comparison of its measured irradiance profile with the ideal profile. Lack of quality is an inherent result of imperfections or aberrations in the optical device used, e.g. mirrors, apertures, or lenses, as well as the laser medium and atmosphere.

ric turbulence. Therefore a good measure of beam quality is the full description of the aberrations present in the system. Most of the existing and widely used criteria fail to fully describe these aberrations. This thesis report proposes a new set of characterization criteria which will describe beam quality by characterizing the aberrations present in the system.

Tasks

1. Critical survey of existing beam quality criteria and methods of beam quality measurement. Determine the most current and widely accepted criteria for beam characterization.

2. Development of an improved characterization criteria to completely describe the quality of a laser beam. If the current quality characterization methods are found to be inadequate, the thesis will propose an improved set of FOMs which will provide greater accuracy in beam quality description and characterization.

3. Describe standard procedures for the measurement of the FOMs arrived at in task 2.

Scope and Assumptions

This work will be limited to scalar diffraction theory. Only the scalar amplitude of one transverse component of the field will be considered.

Nondiffraction-limited beams are a direct result of imperfections in the optical device as well as beam attenua-

tion due to characteristics of the medium of propagation. Determining beam quality is typically accomplished in an experimental set-up under laboratory conditions. As such, the effects of the medium on the irradiance distribution of the beam are neglected in this report. Only distortions generated within the lasing cavity or imperfections in the mirror surfaces are assumed to result in the nondiffraction-limited nature of the laser beam.

Organization and Approach to the Problem

A systematic approach or plan of attack was devised to ensure that an optimum solution to the thesis problem is reached. These are listed below.

1. Phase I: Critical survey of existing beam quality criteria and methods of beam quality measurements. This phase included an extensive survey of current literature and materials on the subject. Materials from numerous engineering and scientific literatures were used as well as materials from Air Force and Department of Defense published reports.

2. Phase II: Development of a list of currently used methods including an outline of the procedures employed to measure the FOMs. In addition, methods of determining spot size and beam divergence were reviewed and documented. These are listed and discussed in detail in Chapter II.

3. Phase III: Development of a more complete quality characterization criteria for laser beams. The critical sur-

vey of Phase I indicated that the current methods used are generally insufficient to describe the quality of the beam. A more accurate set of criteria was developed during this phase. Phase aberrations and diffraction theory of phase aberrated beams were studied during this phase. A computer code was developed to model the propagation of phase aberrated beams and to allow the study of irradiance profiles in the presence of random phase aberrations.

4. Phase IV: Numerical and analytical methods were investigated, during Phase IV, which were to measure the FOMs derived in Phase III. A code was developed to numerically determine values of the FOMs by fitting the actual aberrated data with a proposed mathematical expression for the nondiffraction-limited beam.

5. Phase V: Development of an experimental procedure to measure the FOMs developed in Phase III and Phase IV of the study.

Chapter II, of this thesis report, examines the various methods of beam quality characterization currently used. It includes a discussion of the theory and procedures practiced when measuring these FOMs. Chapter III discusses the development of a computer model to simulate nondiffraction-limited laser beams, while Chapter IV reviews the results found from several simulations of non-ideal beams. From these results, a new set of FOMs was devised and a numerical method of measuring the FOMs was derived. Chapter V discusses the

merits of the new FOMs when characterizing beam quality and proposes a list of procedures to measure these parameters experimentally.

II. Current Methods of Characterizing Laser Beams

An extensive literature survey was undertaken, during Phase I, to identify currently used methods for characterizing the quality of laser beams. This chapter outlines the various figures of merit used to determine beam quality. The next section lists a number of FOMs currently used (Ref 22), while subsequent sections describe the procedures used to measure the three most widely accepted quality criteria.

Existing Figures of Merit

1. 'Power in the bucket' method- provides a comparison of theoretical and experimental data which is the basis for beam quality determination. Beam quality measurements, involving the 'power in the bucket' method, are normally performed measuring some 'width' of the central maximum of a diffraction pattern at the far-field of a laser beam. This is then compared with some diffraction-limited calculated 'width'. From the comparison of the two widths, one measure of beam quality is obtained (Ref 2).

2. Beam Divergence- a measure of the spread of a laser beam propagating in a medium, as a function of distance from the laser source. A comparison of the experimental divergence and theoretical divergence provides one quality measure. In addition, the smaller the divergence angle, the higher quality the laser is said to be. This is especial-

ly true in applications involving the need to deliver the maximum amount of energy into a very small target area.

3. Strehl Ratio- calculates the ratio of the on-axis irradiance of the aberrated system versus the on-axis irradiance of the diffraction-limited beam. From this ratio, the amount of distortion introduced in the system can be approximated.

4. Focusing Efficiency- indicates the percentage of the total power in the exit pupil which is focused into a specified 'bucket'.

Total Power in the Bucket

For a laser beam with a symmetric Gaussian profile and waist w , the intensity distribution is given by:

$$I(r) = I(0)e^{-2r^2/w^2} \quad (2.1)$$

where $I(r)$ is the beam irradiance as a function of radius r , and $I(0)$ is the maximum on-axis intensity. Figure 1 shows a representation of the Gaussian beam as a function of the beam radius r .

Integrating equation 2.1 over the radius of the beam gives the total power within the entire beam. Thus,

$$P(R) = \int_0^R I(0)e^{-2r^2/w^2} 2\pi r \, dr \quad (2.2)$$

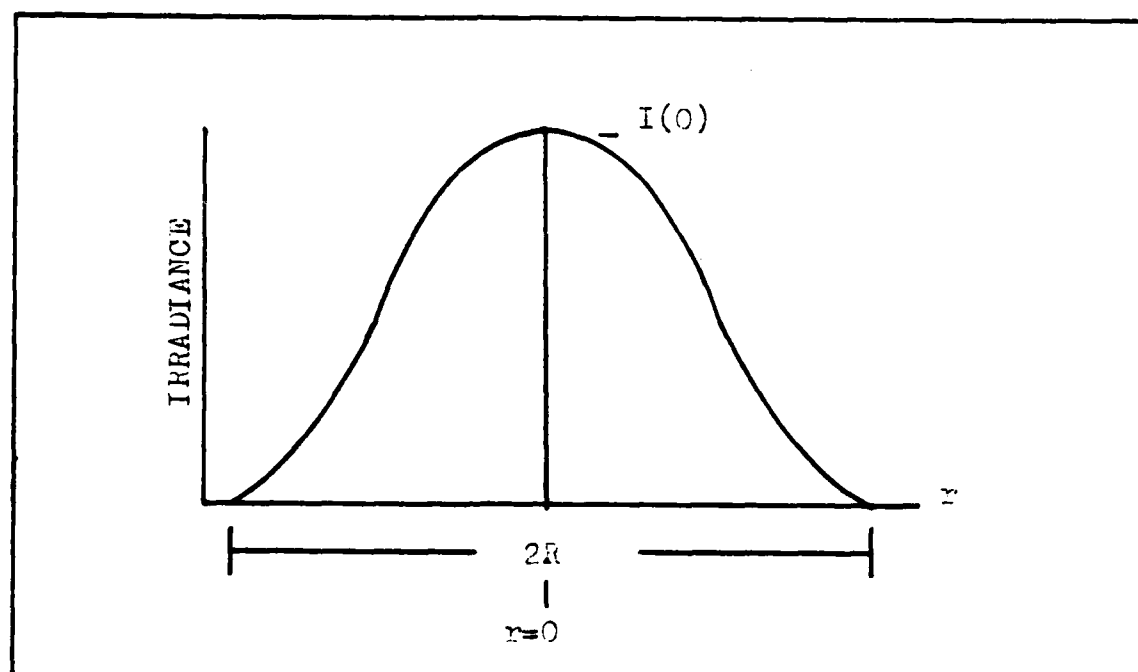


Figure 1. Intensity Distribution of Gaussian Beam.

A solution to this integral results in,

$$P(R) = \frac{\pi w^2 I(0)}{2} (1 - e^{-2R^2/w^2}) \quad (2.3)$$

The ratio of $P(R)$ to the total power $P(\infty)$ is expressed as:

$$\frac{P(R)}{P(\infty)} = 1 - e^{-2R^2/w^2} \quad (2.4)$$

Equation 2.4 gives the normalized power of a Gaussian beam transmitted through an aperture radius of R . When $R \gg w$ the power transmitted is maximized at 1. By varying the values of R , a relationship between total power and aperture size is derived. A typical Power-Radius (P - R) plot is shown in figure 2. If the beam emanating from a laser is

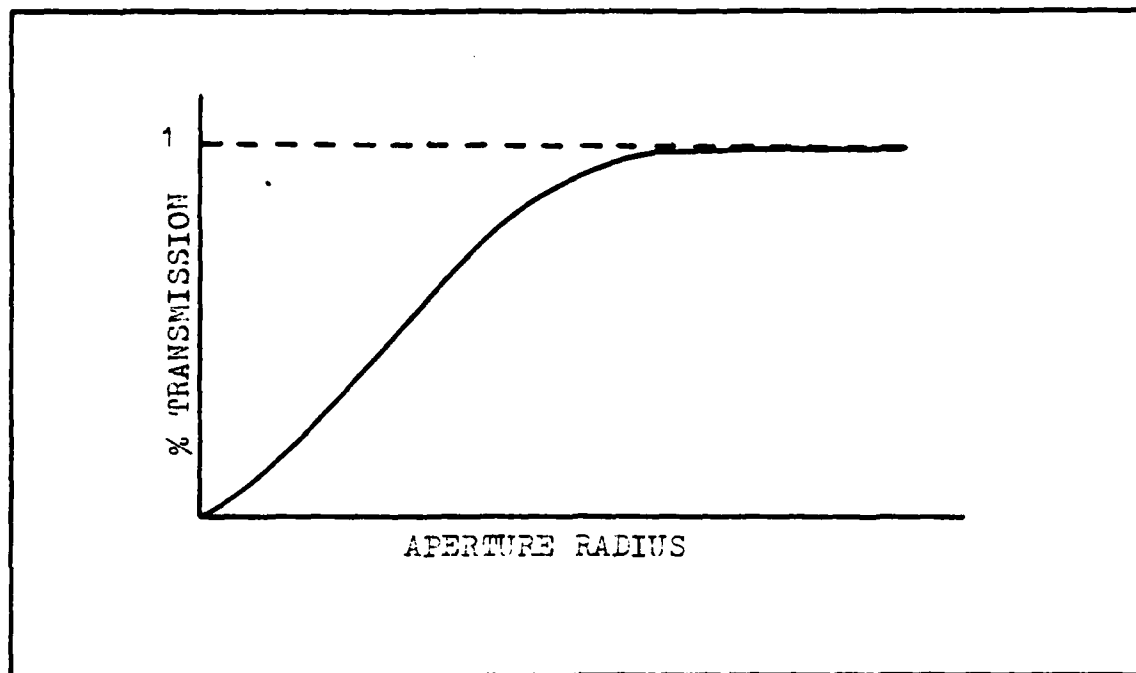


Figure 2. Beam Quality I-R curve

propagated through a series of aperture radii, a comparison of actual measurements with the theoretical diffraction-limited beam provides one measure of beam quality. A 'good' laser beam would closely approximate the P-R plot of the diffraction-limited beam and the numerical results of equation 2.4. Figure 3 shows a typical beam quality measurement arrangement. A lens is used to provide far-field conditions at a reasonable distance from the laser. At the focal plane, a variable iris is placed with a power measurement device immediately behind it. With the iris fully opened, a measure of the total power through the aperture is taken to determine the total power output of the laser. By varying the diameter of the iris or aperture, the relationship between

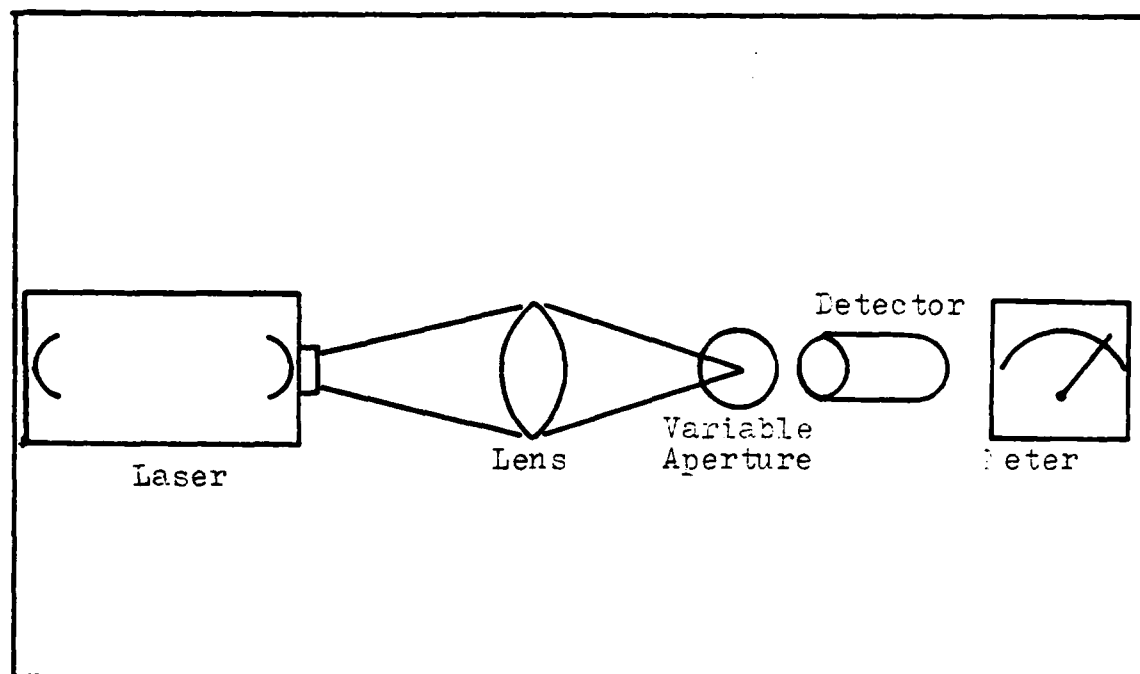


Figure 3. General Beam quality set-up.

transmitted power and aperture radius is determined. The ratio of this power with the total laser power is the normalized transmitted power. Figure 4 is a typical plot showing the P-R curves for non-ideal and diffraction-limited lasers.

Although a comparison of the non-ideal Gaussian P-R curve with the diffraction-limited Gaussian P-R curve provides a quantitative measure of beam quality, a single number is typically associated with this measure. Lasers are often characterized as being ' n times diffraction-limited' (Ref 8). There is no standard way to determine the ' n times diffraction-limited' number. One method of computing the ' n times diffraction-limited' number is dividing the radius corresponding to a measured percentage transmission by the theo-

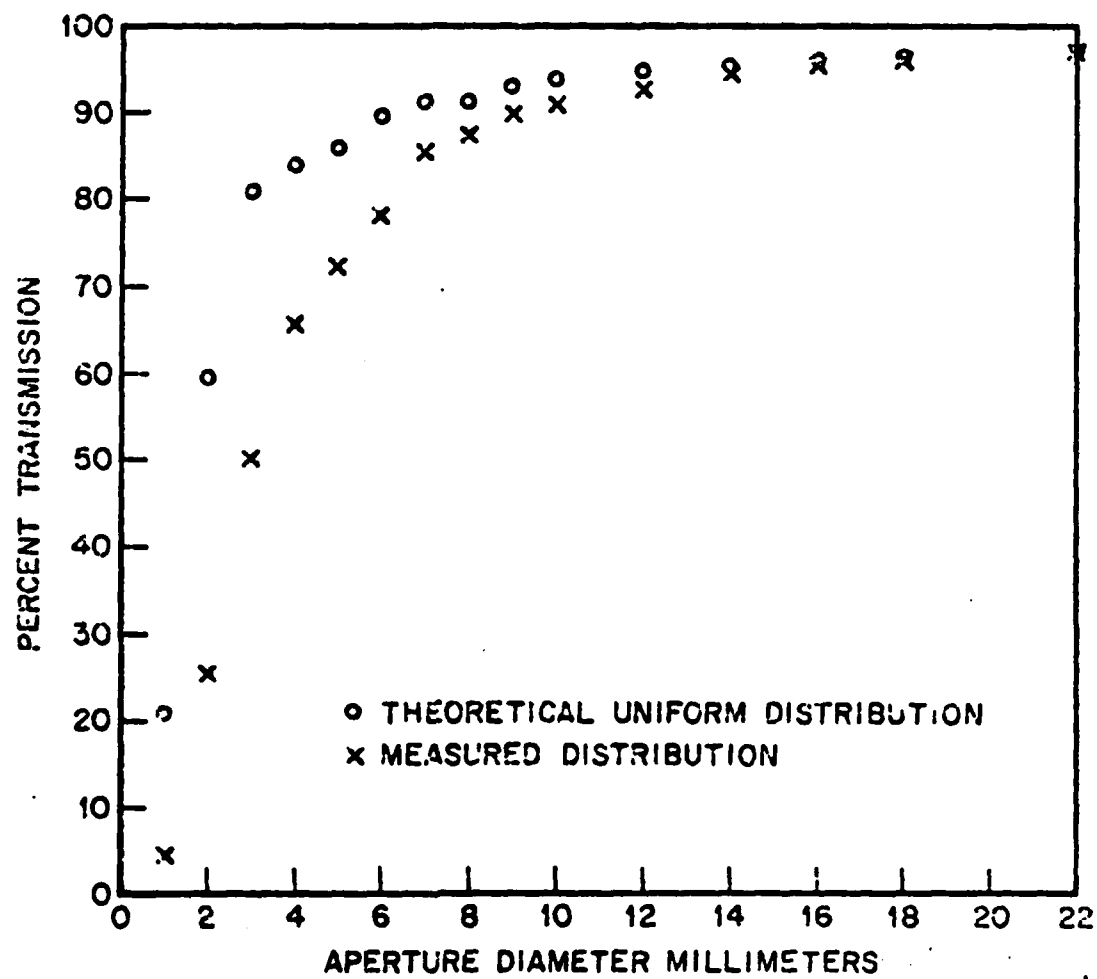


Figure 4. Transmitted power versus aperture and theoretical curve.

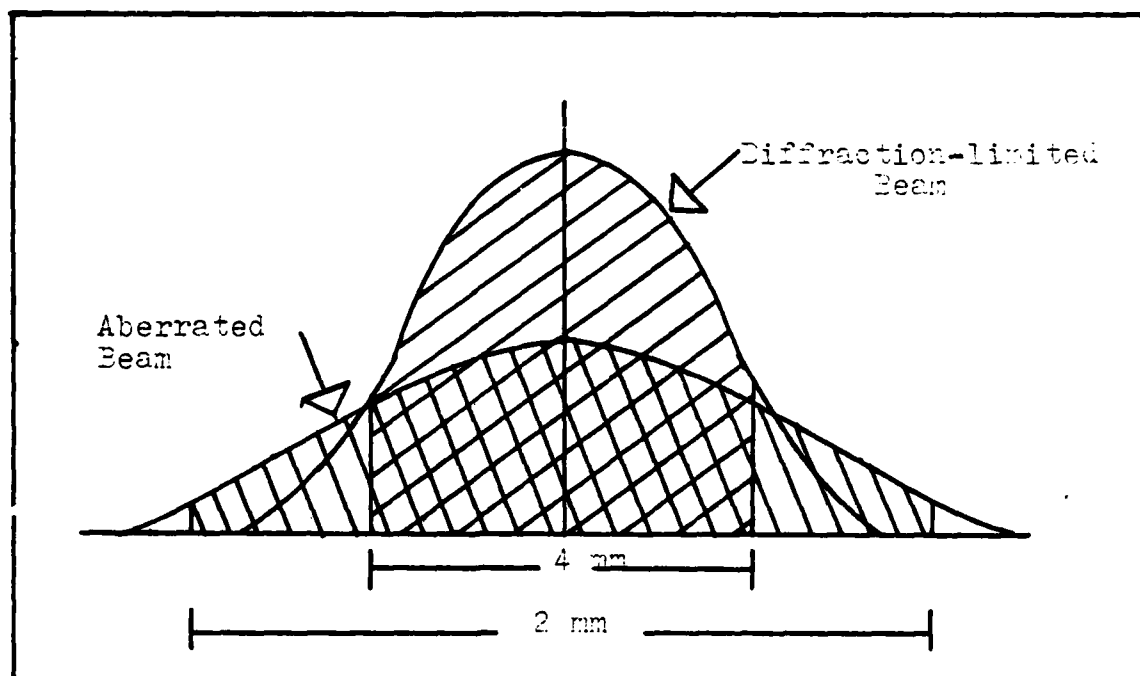


Figure 5. Relative widths for ideal and non-ideal laser beams.

retical radius which would transmit the same measured transmission percentage (Ref 7). For example, figure 5 shows the intensity distribution for a non-ideal laser beam and a Gaussian diffraction-limited laser beam. In the ideal case, an aperture radius of 2 mm is required to transmit 70% of the power while in the non-ideal case, a 4 mm radius is required to achieve the same amount of power. The laser is then said to have a 'diffraction-limited' number of 2. The 'times diffraction-limited' number can also be defined as the ratio of the transmitted power of an ideal beam with that of the non-ideal beam at the radius corresponding to the laser beam waist. For example, if at the beam waist, the diffraction-limited laser was transmitting 86% of the power, while the non-ideal laser 43%, then the corresponding 'number of times

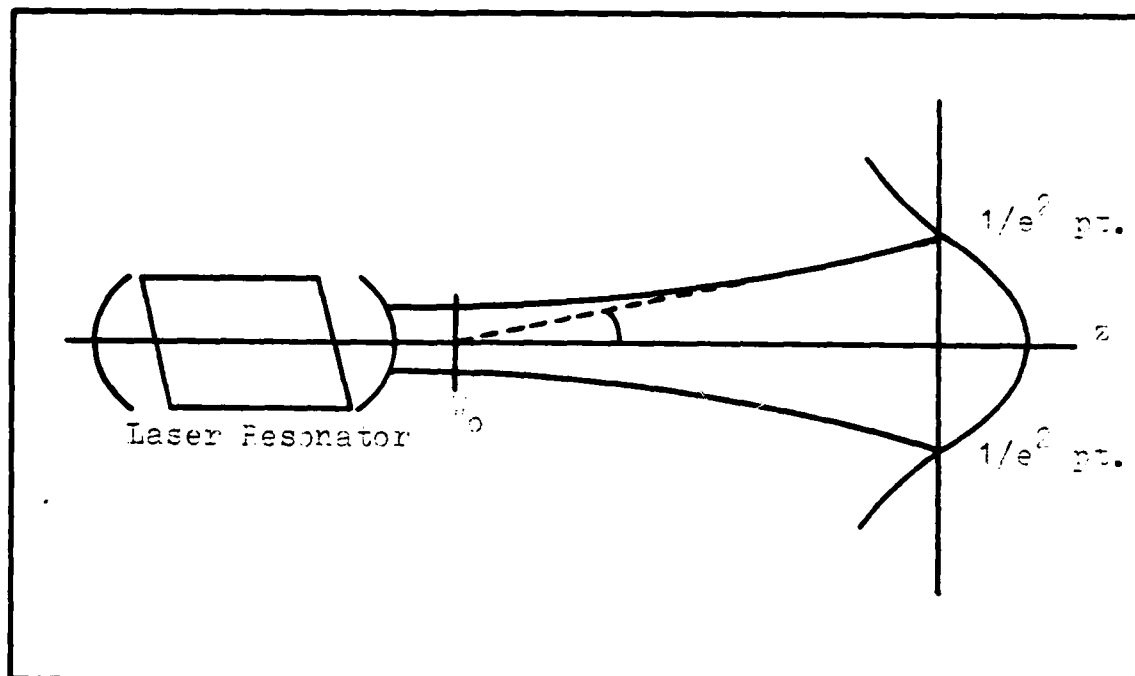


Figure 6. Laser Geometry

diffraction-limited' is 2 .

Beam Divergence and Spot Size Measurements

A generally simple method to characterize a laser beam is by describing its far-field profile. Many use the divergence angle as a measure of this quality. Depending on the application, the divergence angle will vary. For most systems where maximum energy is desired on a small area at possibly great distances away, the divergence angle should be very small. The divergence angle, $\theta(z)$ is the half-angle spread to the point at which the beam irradiance falls to $1/e^2$ of its central value and is described in equation 2.5 and illustrated in figure 6.

$$\theta(z=\infty) = \lambda / \pi w_0 \quad (2.5)$$

One method to determine quality using spot size measurements, is by comparing the measured spot size and the theoretical spot size determined in the far-field. However, measurement of spot size, and for that matter divergence, is not an easy task. This section will now attempt to describe several methods to determine these parameters for lasers with symmetric Gaussian intensity distributions. The most straightforward technique to measure spot size is to scan the beam with a pinhole or slit. However, this technique is now considered unacceptable since in addition to being slow and tedious, it is very sensitive to the scanning path across the beam (Ref 23). The scanning knife-edge method is then used to alleviate these shortcomings. The technique makes use of the waveform generated when the beam is interrupted by a straight-edged chopper moving at a uniform speed (Ref 18). Suzuki and Tachibana (Ref 20) used a rotating chopper with the knife-edge and calculated the beam radius w using equation 2.6.

$$w = 0.7803 \omega r(t_2 - t_1) \quad (2.6)$$

In equation 2.6, ω is the angular velocity of the chopper, r the distance from the rotating center of the rotating chopper to the laser beam axis, and the quantity $t_2 - t_1$ is the time interval for the output to go from 90% to 10% of the total laser power. The spot size given by equation 2.6 was

derived using the result that the normalized power $P(R)/P(0)$ is given by the error function. Thus, w can be found from the curve of $P(R)/P(0)$.

There are still some defects to using the knife-edge scanning technique. The scanning rate must be maintained at a uniformly constant speed and the spot size must be calculated after fitting a variation of the output power from the detector to an error function. Yoshida and Asakura (Ref 23) proposed measuring the spot size of Gaussian laser beams by scanning the beam with an opaque ribbon. The spatial intensity distribution $I(x,y)$ of a Gaussian Laser beam is given by:

$$I(x,y) = \frac{2P(0)}{\pi w^2} e^{-(2x^2+2y^2)/w^2} \quad (2.7)$$

where $P(0)$ is the total laser power, w is the spot size measured at the $1/e^2$ distribution point and x and y are Cartesian coordinates measured from the beam center perpendicular to the axis of propagation. By scanning an opaque ribbon across the beam, the minimum output power from the photodetector is realized when the ribbon reaches the center of the beam. From figure 7 and setting the ribbon width to be $2a$, the minimum power output is given by:

$$P_m = \int_{-\infty}^{\infty} \int_{-\infty}^a \frac{2P(0)}{\pi w^2} e^{-(2x^2+2y^2)/w^2} dx dy + \int_{-\infty}^a \int_a^{\infty} \frac{2P(0)}{\pi w^2} e^{-(2x^2+2y^2)/w^2} dx dy \quad (2.8)$$

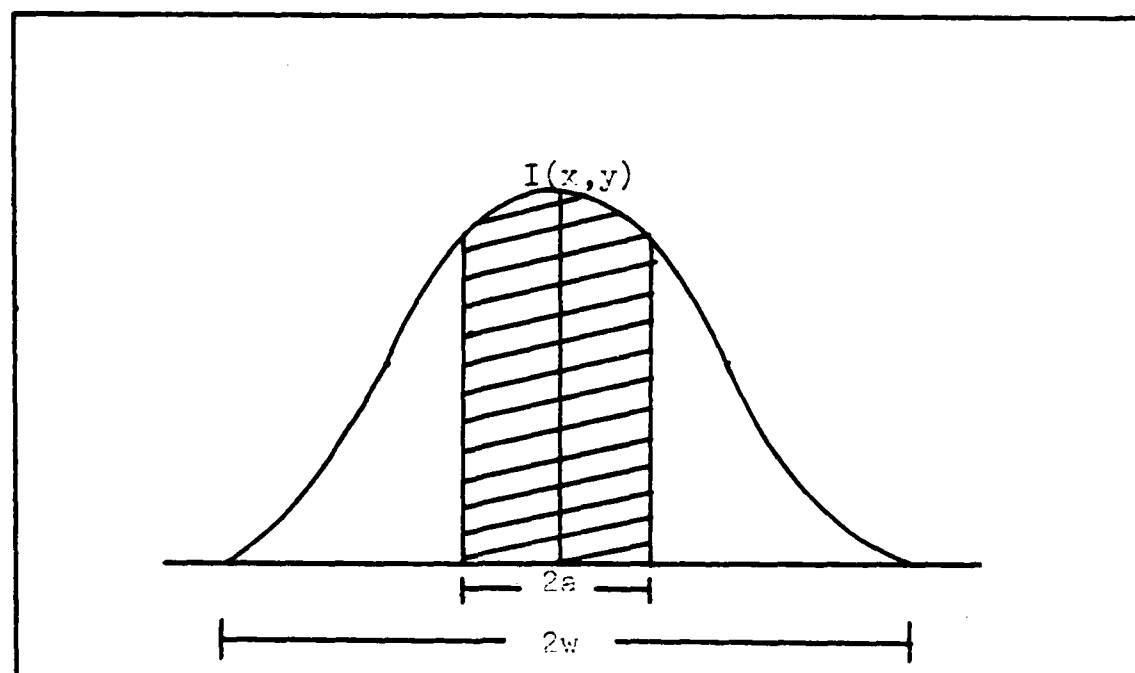


Figure 7. Intensity distribution of a Gaussian beam in which the center is interrupted by an opaque ribbon with width equal to $2a$.

From equation 2.8 the following is derived:

$$\frac{P_m}{P(0)} = \text{erfc} \left(2^{\frac{1}{2}} a/w \right) \quad (2.9)$$

where,

$$\text{erfc}(z) = (2/\pi^{\frac{1}{2}}) \int_z^{\infty} e^{-t^2} dt \quad (2.10)$$

From equation 2.9, if the opaque ribbon width $2a$ is known, then the spot size w can be determined by measuring the value of $P_m/P(0)$. With this technique, the consistency of the speed of scan is not a critical factor to contend with as was the case for the knife-edge method.

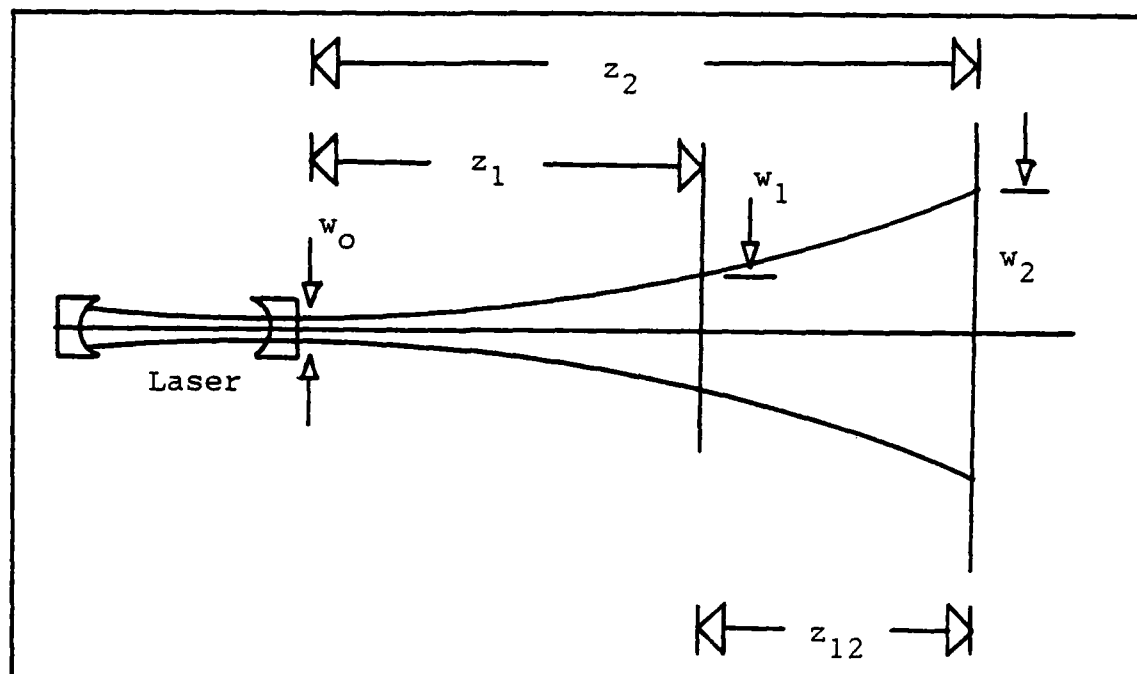


Figure 8. Typical laser set-up from which beam parameters are determined.

By definition, divergence is measured at the $1/e^2$ point of the far-field irradiance distribution. As such, measurement of the divergence for some lasers might be impractical. Therefore, lenses are used, as shown by Suzaki and Tachibana (Ref 21), to determine the divergence by measuring the spot size at the focal plane of the lens and knowing its focal length. When a beam passes through a lens of known focal length, the beam radius in the focal plane w_f is independent of the lens position on the beam axis. This is due to the fact that the field at the focal plane is proportional to the far-field pattern of the incidence beam which depends on the beam waist radius, but not on its location (Ref 1).

Then, $w_f = f \theta(\infty)$ (2.11)

where, f is the focal length of the lens and, $\theta(\infty)$ is the half-angle far-field divergence angle. w_f can be measured using one of the beam spot size measurement techniques outlined above. If f is known, the half-angle far-field divergence angle $\theta(\infty)$ can be found mathematically, by equation 2.11.

Measurements of beam divergence using lenses are, unfortunately, not always accurate. Many times the precise location of the focal plane is difficult to determine. Sollid, et al (Ref 19) proposed a lens-less method to determine beam divergence of Gaussian-shaped laser beams. The propagation of a Gaussian beam is shown in figure 8. Given two values of spot sizes, $w_1(z)$ and $w_2(z)$ and using equation 2.12, the beam waist w_0 can be calculated.

$$w_0^2 = \frac{\frac{1}{2}(w_1^2 + w_2^2) + ((w_1 w_2)^2 - (\lambda z_{12} / \pi)^2)^{\frac{1}{2}}}{2(1 + (\pi/2 \lambda z_{12})^2 (w_2^2 - w_1^2)^2)} \quad (2.12)$$

When the beam waist location is known ($z=0$), and using the expression for extracavity propagation, equation 2.13,

$$\frac{w(z)}{w_0} = (1 + (\theta z / w_0)^2)^{\frac{1}{2}} \quad (2.13)$$

where, $\theta = \lambda / \pi w_0$ (2.14)

the beam waist can be calculated using the reduced equation, 2.15.

$$w_0^2 = \frac{1}{2}w^2(1 \pm (1 - (2\lambda z/\pi w^2)^2)^{\frac{1}{2}}) \quad (2.15)$$

According to Sollid, et al, only one measurement of $w(z)$ is required to calculate w_0 using equation 2.15. The proposed method is to insert beam attenuators of known density in front of the laser, while the energy is exposed at plane z on a sharp-threshold energy sensitive medium. See figure 9 for illustrations. The irradiance distribution produced at the film plane by laser intensity I_0 attenuated by a thickness of material d , with absorption coefficient α is

$$I(r) = I_0 e^{(-2r^2/w^2 - \alpha d)} \quad (2.16)$$

The radius to a given exposure density on the film is measured, corresponding to constant $I(r)$ in a given exposure. From equation 2.16, $w(z)$ can be determined from pairs of measurements involving the same exposure density but different radii $r_i \neq r_j$ and $d_i \neq d_j$. Thus,

$$w(z) = \frac{2(r_i^2 - r_j^2)}{\alpha(t_j - t_i)} \quad (2.17)$$

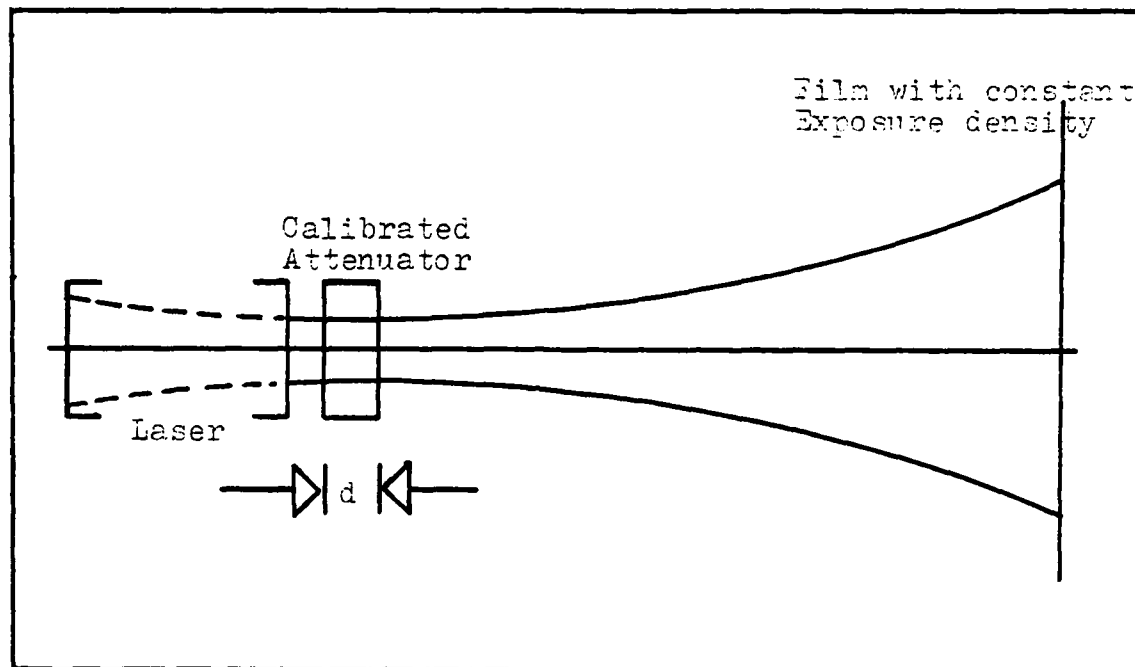


Figure 9. Attenuator method for determining divergence.

where α is the attenuator absorption coefficient. With $w(z)$ known, from equation 2.16, w_0 can now be calculated using equation 2.15. From equation 2.14, the far-field half-angle divergence angle θ can be determined.

Huguley (Ref 12) used a heat-sensitive 'scanning wire' to characterize the laser beam profile and determine laser spot and waist size. The scanning wire, which lies in the direct path of the laser beam, will be heated proportionally to the power density which it intercepts. The heating will result in a proportional change in resistance. When the wire is scanned across the beam, the resistance change will follow the energy profile of the laser beam. The heat sensitive wire method compares very well with the scanning edge and scanning slit methods. Comparative plots of the different methods are shown in figure 10.

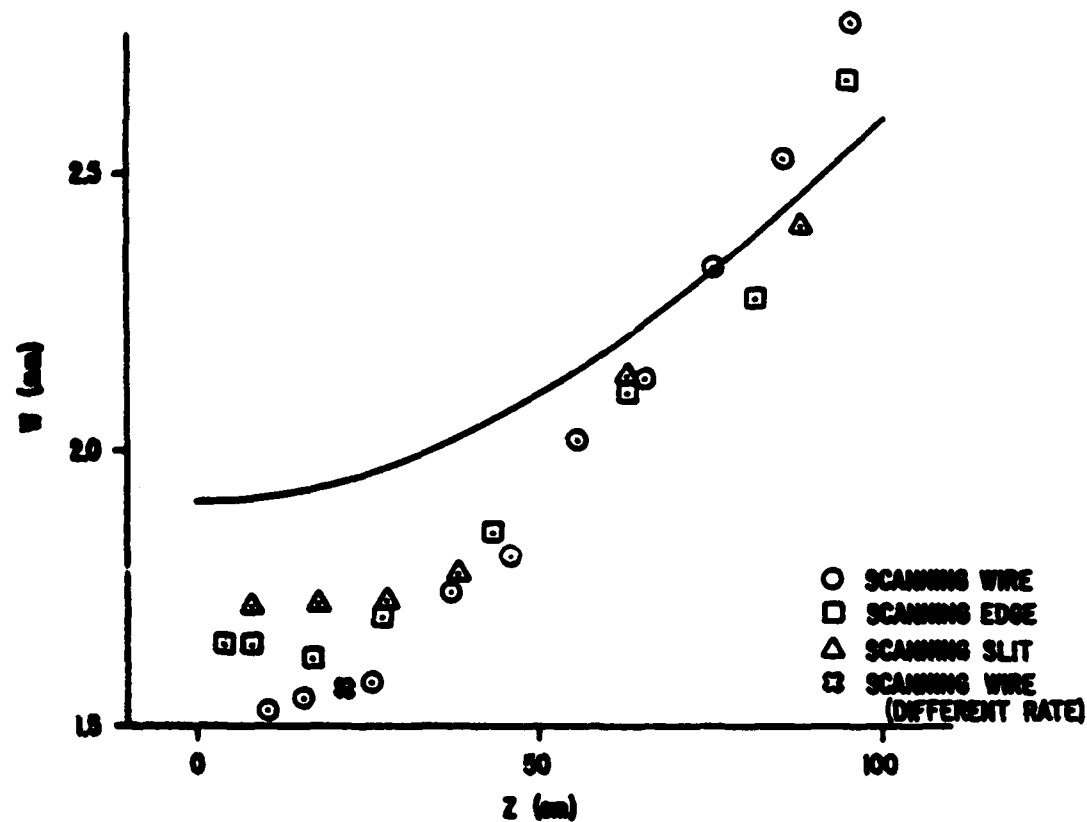


Figure 10. Comparison of waist (w) to the distance from the laser (Z) for scanning wire, scanning edge, scanning slit, and theoretical curve from cavity theory.

Strehl Ratio

It is a well known fact, that the spatial intensity distribution of an imaging system, in the far-field, is completely described by the Fraunhofer approximation to the Huygen-Fresnel principle (Ref 6:57-76). The far-field intensity pattern is expressed, simply, as the Fourier transform of the field immediately behind the diffracting aperture of an optical system. Figure 11 illustrates this point, and designates $U'(x,y)$ as this field. In general, the illuminating field, $U(x,y)$ in figure 11, can be any function. For some lasers, $U(x,y)$ is Gaussian in profile. The field which immediately follows the aperture is expressed as,

$$U'(x,y) = U(x,y) t(x,y) \quad (2.18)$$

where, $t(x,y)$ is the transmittance function associated with the aperture, and $U(x,y)$ the incident field. Then the far-field or Fraunhofer field strength $U(x_1,y_1)$ is given by Goodman (Ref 6:61) as:

$$U(x,y) = \frac{1}{j\lambda z} e^{jkz} e^{jk/2z(x_1^2+y_1^2)} \times \iint_{-\infty}^{\infty} U'(x,y) e^{-j2\pi/\lambda z(xx_1+yy_1)} dx dy \quad (2.19)$$

The associated far-field irradiance is then expressed as:

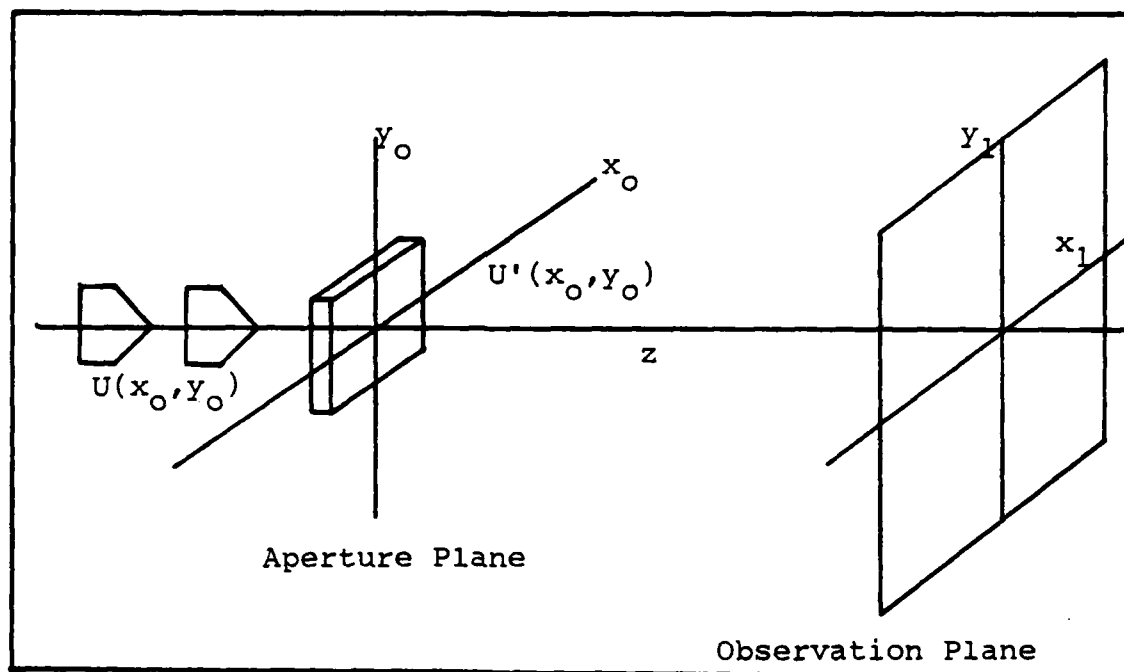


Figure 11. Wave propagation into the Fresnel region and beyond.

$$I(x_1, y_1) = |U(x_1, y_1)|^2 = \left| \frac{1}{\lambda z} \iint_{-\infty}^{\infty} U(x, y) t(x, y) e^{-\frac{j2\pi}{\lambda z}(xx_1 + yy_1)} dx dy \right|^2 \quad (2.20)$$

Equation 2.20 represents the observed intensity distribution, in the far-field, for a diffraction-limited optical system. When wavefront error exists in the system, due to aberrations, the optical system could be thought of as being illuminated by an ideal wave but a phase shifting plate exists within the aperture. The phase error $\phi(x, y)$ can be expressed as:

$$\phi(x, y) = k W(x, y) \quad (2.21)$$

where $k = 2\pi/\lambda$ and $W(x,y)$ is the effective path-length error. With aberration included, equation 2.20 is rewritten as:

$$I(x,y)_{NDL} = \left| \frac{1}{\lambda z} \iint_{-\infty}^{\infty} U(x,y) t(x,y) e^{j\phi(x,y)} e^{-\frac{j2\pi}{\lambda z}(xx_1 + yy_1)} dx dy \right|^2 \quad (2.22)$$

Chapters III and IV, of this report, will investigate aberration effects on diffraction theory in more depth. When an optical system suffers from aberrations, the peak value of its intensity distribution is less than the peak value of the same system in the diffraction-limited case. The ratio of these peak values, known as the Strehl ratio, indicates the amount of aberration present in a system, thus providing a powerful measure of laser quality. The Strehl ratio is given as,

$$S.R. = \frac{I_{\text{aberrated}}}{I_{\text{diffraction-limited}}} \bigg|_{\text{on-axis}} \quad (2.23)$$

According to Gaskill (Ref 5), a Strehl ratio of 0.8 or higher is often considered characteristic of an optical system which is effectively unaberrated.

III. Modeling Phase Aberrated Laser Beams

Imperfections in the optical system, called aberrations, are the major contributors to the nondiffraction-limited nature of a laser beam. Specific sources of optical aberrations that produce nondiffraction-limited beams range from distortions generated within the lasing cavity to imperfect mirror surfaces encountered in the exterior (and interior) optical trains. In characterizing laser beams, it is necessary to describe the nature and the form of these aberrations. To do this, effects of aberrations must first be studied. Two types of aberrations reduce the quality of optical systems and hence, the output of these systems. These are amplitude and phase aberrations. Studies have indicated, however, that the aberrations due to purely amplitude distortions are not as severe compared to effects due to random phase aberrations (Ref 8).

In order to study the effects of random phase aberrations on the irradiance profile of laser beams, a numerical model was developed to simulate the propagation of nondiffraction-limited laser beams. The function of the code is to numerically integrate the Huygen-Fresnel integral to determine irradiance. The code was devised to allow for two-dimensional numerical integration. The need for two-dimensional integration was realized to allow for flexibility in choosing aperture type and dimension. The model determines irradiance distributions for both circular and rectangular

apertures. The following sections will discuss the generalities and assumptions used in developing the model in more detail, and reviews the theory of phase aberrations and also, the theory of diffraction in the presence of phase aberrations.

Theory

The general form of the Huygen-Fresnel integral is shown in equation 3.1:

$$U(x_1, y_1) = \frac{e^{jkz}}{j\lambda z} e^{jk/2z (x_1^2 + y_1^2)} \times \iint_{-\infty}^{\infty} U'(x_o, y_o) e^{\frac{jk}{2z}(x_o^2 + y_o^2)} e^{-\frac{j2\pi}{\lambda z}(x_o x_1 + y_o y_1)} dx_o dy_o \quad (3.1)$$

where $U(x_1, y_1)$ is the field strength at the observation plane with Cartesian coordinates x_1 and y_1 , and $U'(x_o, y_o)$ is the field strength at the aperture plane with coordinates x_o and y_o . The distance between the aperture and the plane of observation is z and the wavelength of the signal is λ . By applying the Fraunhofer approximation to equation 3.1 the field strength at the far-field reduces to:

$$U(x_1, y_1) = \frac{e^{jkz}}{j\lambda z} e^{\frac{jk}{2z}(x_1^2 + y_1^2)} \iint_{-\infty}^{\infty} U'(x_o, y_o) e^{-\frac{j2\pi}{\lambda z}(x_o x_1 + y_o y_1)} dx_o dy_o \quad (3.2)$$

Hence, at the far-field or Fraunhofer region, the field strength is simply the Fourier transform of the aperture plane field strength multiplied by constant phase terms. The irradiance $I(x_1, y_1)$ is the square of the absolute of equation 3.2, or,

$$I(x_1, y_1) = \frac{1}{(\lambda z)^2} \left| \iint_{-\infty}^{\infty} U'(x_0, y_0) e^{-\frac{j2\pi}{\lambda z}(x_0 x_1 + y_0 y_1)} dx_0 dy_0 \right|^2 \quad (3.3)$$

Notice that in equation 3.3, the phase terms of equation 3.2 disappear.

As briefly discussed in Chapter II, the aperture plane field strength $U'(x_0, y_0)$ can be expressed as:

$$U'(x_0, y_0) = U(x_0, y_0) t(x_0, y_0) \quad (3.4)$$

where, $U(x_0, y_0)$ is the field strength incident on a limiting aperture with transmittance $t(x_0, y_0)$. In order to achieve far-field conditions, the Fraunhofer condition must be satisfied. At optical frequencies, the conditions required for satisfying these conditions can be severe. For example, at a wavelength of 0.6 micrometer and an aperture width of 2.5 cm, the observation distance must be $z \gg 1600$ meters. In many instances, meeting the condition is not readily realized and, in most cases, impractical. As will now be shown, the use of ideal lenses will alleviate these deficiencies

and provide far-field conditions at the focal plane of the lens.

The phase transformation function of a lens is given by Goodman as:

$$U_1(x_o, y_o) = e^{jknD} e^{-\frac{jk}{2f}(x_o^2 + y_o^2)} \quad (3.5)$$

where, D is the width of the lens at the center and f , the focal length. If the incident field $U(x_o, y_o)$ is truncated by a limiting aperture with transmittance $t(x_o, y_o)$ and focused with an ideal lens of focal length f , then the field at the aperture plane can be expressed as:

$$U'(x_o, y_o) = U(x_o, y_o) t(x_o, y_o) e^{jknD} e^{-\frac{jk}{2f}(x_o^2 + y_o^2)} \quad (3.6)$$

Substituting equation 3.6 into equation 3.1 will result in the cancellation of the quadratic term within the integral when $z=f$, thus, simplifying equation 3.1 into:

$$U(x_1, y_1) = \frac{e^{jkf}}{j\lambda f} e^{\frac{jk}{2f}(x_1^2 + y_1^2)} \iint_{-\infty}^{\infty} U(x_o, y_o) t(x_o, y_o) e^{-\frac{j2\pi}{\lambda f}(xx_o + yy_o)} dx_o dy_o \quad (3.7)$$

The irradiance is simply the square of the Fourier transform of the product of the incident field and the aperture transmittance function.

In the presence of aberrations, the irradiance function becomes,

$$I(x_1, y_1) = \frac{1}{(\lambda_f)^2} \left| \iint_{-\infty}^{\infty} U(x_0, y_0) t(x_0, y_0) e^{j\phi(x_0, y_0)} e^{-j\frac{2\pi}{\lambda_f}(x_0 x_1 + y_0 y_1)} dx_0 dy_0 \right|^2 \quad (3.8)$$

where, $\phi(x_0, y_0)$ represents the aberration function.

Amplitude distortions can be a contributing source to the nondiffraction-limited nature of a laser beam. However, their comparative contribution is much less than the contribution arising from phase aberrations (Ref 8). In this report, only small-distortion random phase aberrations will be assumed to contribute to the nondiffraction-limited nature of the beam.

The contribution of the aberration function to the on-axis irradiance at the focal plane can be assessed using the Strehl criterion (Ref 3:464),

$$\frac{I(x=0)}{I(x=\infty)} = 1 - (\Delta\phi)^2 \quad (3.9)$$

where, $(\Delta\phi)^2$ is the variance of the phase aberration function. When phase distortions are small (less than $1/5 \lambda$), the normalized intensity at the center of the observation plane at focus is independent of the nature of the aberrations.

tion and is proportional to the variance of the aberration function.

Phase aberrations are generally due to imperfections in the optical device such as a laser. In this report, phase aberration will be represented as the Fourier series expansion of a function which satisfies the condition:

$$f(x,y) = \text{rect}(x)\text{rect}(y) = \begin{cases} 1 & -\frac{1}{2}l_x < x < \frac{1}{2}l_x \\ & -\frac{1}{2}l_y < y < \frac{1}{2}l_y \\ 0 & \text{elsewhere} \end{cases} \quad (3.10)$$

A graphical representation of this function is shown in figure 12. Thus, the phase aberration function for non-diffraction-limited beams can be represented as:

$$\phi(x,y) = \frac{2\pi}{\lambda} \left[\sum_{n=1}^N A_n \cos(n\pi \frac{2x}{l_x}) \cos(n\pi \frac{2y}{l_y}) \right] \quad (3.11)$$

where, A_n is a randomly generated coefficient representing the amplitude of the phase distortion, and l_x and l_y are the corresponding aperture widths in the x and y directions. The coefficients are randomly generated by a random number generator.

The Numerical Model

In developing the computer model, the incident field

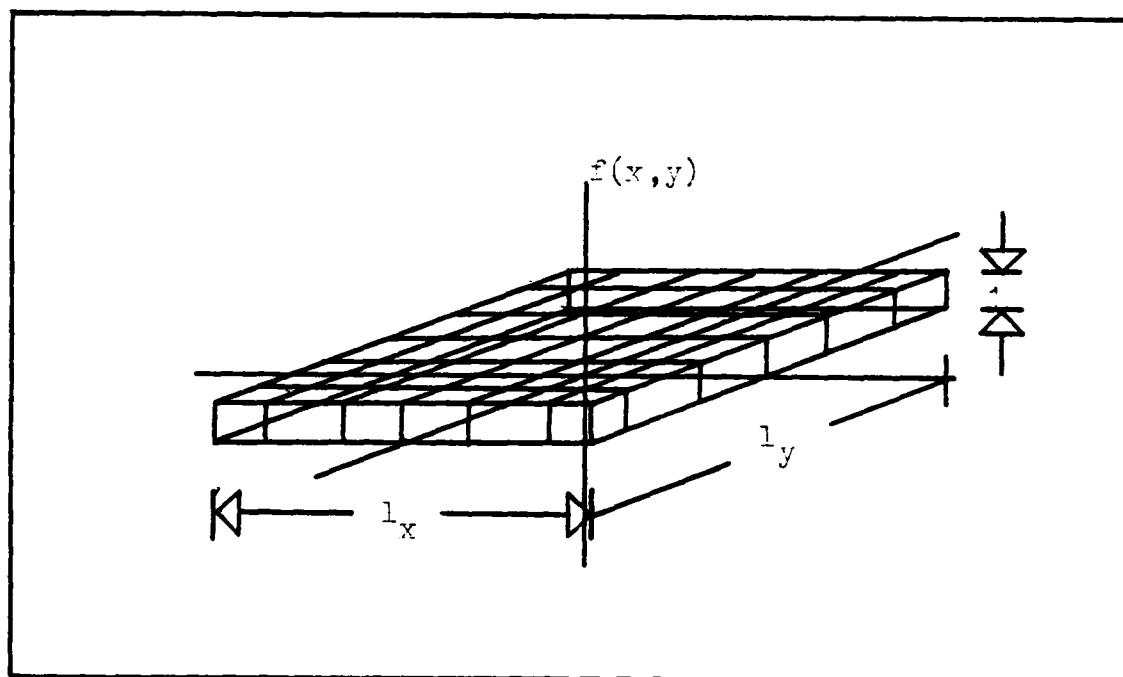


Figure 12. The rectangular function.

is assumed to be Gaussian in intensity, truncated by an aperture (either rectangular or circular), and focused by a perfect thin lens. The system is assumed to be aberrated by the function $\phi(x,y)$ of equation 3.11. For the sake of simplicity, however, only the x-component of equation 3.11 is considered to contribute to the aberration. Thus, $U'(x_o, y_o)$ of equation 3.1 becomes:

$$U'(x_o, y_o) = e^{\frac{-(x_o^2 + y_o^2)}{w^2}} e^{jknD} e^{\frac{-jk}{2f}(x_o^2 + y_o^2)} e^{j\phi(x_o)} \text{rect}(x_o, y_o) \quad (3.14)$$

where, w is the spot size at the aperture. For a rectangular aperture, with transmittance function described by equation 3.10, the limits of integration can be changed, thereby

reducing the form of the nondiffraction-limited irradiance profile to:

$$I(x_1, y_1) = \frac{1}{(\lambda z)^2} \left| \int_{-\frac{1}{2}l_y - \frac{1}{2}lx}^{\frac{1}{2}l_y + \frac{1}{2}lx} \int_{-\frac{1}{2}l_x - \frac{1}{2}ly}^{\frac{1}{2}l_x + \frac{1}{2}ly} e^{-\frac{j2\pi}{\lambda z} (x_0 x_1 + y_0 y_1)} e^{-\frac{jk}{2f} (x_0^2 + y_0^2)} e^{j\phi(x_0)} dx_0 dy_0 \right|^2 \quad (3.15)$$

The function of the computer code is to numerically integrate equation 3.15. For circular apertures, only the integration limits of equation 3.15 are changed. Note that the quadratic terms are left inside the integral since z is not necessarily always equal to f . This is especially convenient when the irradiance profile of beams not at lens focus is desired. Numerical integration is accomplished using a modified form of the trapezoid rule (Ref 14).

Modeling nondiffraction-limited beams in two dimensions provides greater flexibility in studying non-symmetrical laser beams. In addition, the form of the phase aberration function is not necessarily separable in x and y . Such is the case with the aberration function of equation 3.11. The x component of the aberration cannot be separated and treated independently from its y component.

Figure 13 shows a simplified flow diagram of the code. Appendix A includes the program listing and a sample data

output from this numerical code. The following sections will briefly describe the three main parts of the code: input, output, and operation.

- Inputs.
1. Laser wavelength.
 2. Aperture type- circular or rectangular.
 3. Aperture dimension-
 - if rectangular, the width of the aperture in x and y directions.
 - if circular, the radius of the aperture.
 4. Extent of the observation plane.
 5. z - distance of the observation plane to the aperture.
 6. f - the focal length of the lens.

Operation. The code determines the irradiance distribution of an aberrated optical system. Only the distribution in the x axis at the $y=0$ reference point of the observation plane is calculated. The integration process arranges the aperture plane into a 20×20 array. A bigger array is certainly more desirable, but due to constraints in computer time and cost, this is not possible. However, for the purpose of this study, the array size chosen was found to be sufficiently accurate. Accuracy of the computer model was determined by comparing results derived from the model with theoretical results. Two important points were compared. They are:

1. Axial distance of zero points from the central axis ($x=0$), and

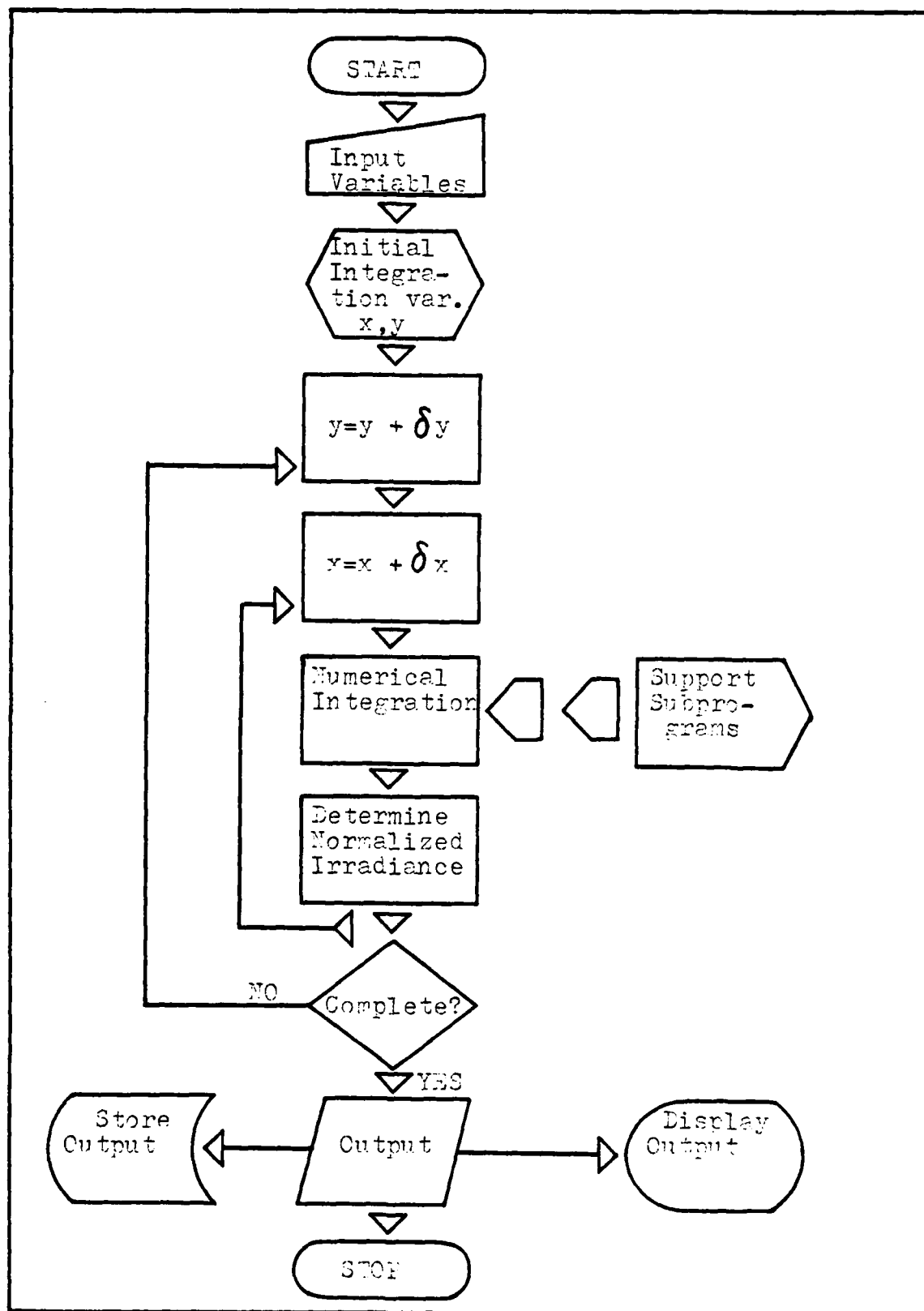


Figure 13. Simplified flow diagram of computer model to determine irradiance distributions.

2. Relative values of maximums and their points of occurrences, e.g. 1st side lobe, 2nd side lobe, etc.

The model was found to be accurate to within 2% of the theoretical results.

Fifty data points, in the observation plane, are calculated. This number of points was found to be adequate in describing the irradiance distributions of simulated nondiffraction-limited laser beams. For each point in the observation plane, integration over the entire extent of the aperture is necessary. As mentioned earlier, integration is done using a modified form of the trapezoid numerical integration rule. All points in the plane of observation are normalized with respect to the on-axis ($x=0, y=0$) irradiance of the diffraction-limited case.

Output. In this thesis, data points of irradiance versus the axis of observation were stored to tape. Plots were generated by attaching the data tape into available Air Force Institute of Technology computer/plotter packages. In this report, data plots were generated using the HPLOTTER.

IV. Characterizing Phase Aberrated Laser Beams

Chapter II of this thesis report reviewed the current methods used to characterize laser beams and the procedures used to measure them. Chapter III discussed the development of a computer model to numerically simulate nondiffraction-limited beams at the focal plane of a lens. From this model, certain characteristics of phase aberrated beams were found to contribute to the overall quality measure of laser beams. When describing the quality of beams, it is important that these characteristics are measured. Most of the existing characterization criteria do not attempt to describe these characteristics. This chapter proposes measuring these parameters when characterizing the quality of laser beams. A method to measure these parameters by a least squares curve fitting method will also be discussed.

Characteristics of Nondiffraction-limited Beams

The Strehl criterion of equation 3.9 determines the on-axis normalized irradiance of a nondiffraction-limited beam. An important parameter which the Strehl criterion do not describe, however, is the lateral extent of the aberrated beam. The energy removed from the on-axis beam is re-distributed into the outskirts of the main beam. This scattered energy forms a 'halo' around the main beam. Hogge, Butts, and Burlakoff (Ref 8) showed that the nondiffraction-limited beam can be expressed as the sum of two beams. One beam is

the attenuated diffraction-limited beam, the other is a much wider beam whose amplitude and lateral extent depend on both the variance and the functional form of the aberration.

By assuming the shape of the 'halo' to be Gaussian, a mathematical expression is hereby introduced describing the nature of the nondiffraction-limited beam. The form of this expression is:

$$F I_0(x) + \frac{(1 - F)}{\sqrt{2\pi\sigma^2}} e^{-x^2/2\sigma^2} \quad (4.1)$$

where, $FI_0(x)$ is the 'first' beam described as the diffraction-limited beam attenuated by a factor F . The second term of equation 4.1 represents the 'secondary' beam or 'halo' which is Gaussian in shape with variance σ^2 .

Using the computer model described in Chapter III, resulting irradiance distributions at the focal plane of the lens were analyzed. In these simulations, the laser beam was assumed to have a waist of 0.45 mm, truncated by a rectangular aperture (1 mm x 1 mm), and focused by a lens with a focal length of 20 cm.

To simulate the effects of random phase aberration, the first twenty terms of the series expansion of the aberration function (equation 3.11) were considered. For the sake of simplicity, only the x component of equation 3.11 is included. The y component, in this model, is assumed constant. The coefficients in each term of the series are ran-

dom numbers. In the study of random phase aberration and its effects on the irradiance distribution of nondiffraction-limited beams, five different sets of random coefficients were multiplicatively scaled to reflect new strengths of phase distortion. The variance for each set is proportional to the sum of the squares of the coefficients. The form of the variance is derived below:

If the aberration function is expressed as:

$$\phi(x) = 2\pi/\lambda A \cos 2\pi \frac{x_0}{lx} \quad (4.2)$$

where, A is the amplitude or distortion of the aberration function, then the variance of this function is:

$$\Delta\phi^2 = \overline{\phi(x)^2} - \overline{\phi(x)}^2 = \frac{\int_{-\frac{1}{2}lx}^{\frac{1}{2}lx} \phi^2(x) dx}{\int_{-\frac{1}{2}lx}^{\frac{1}{2}lx} dx} - \left[\frac{\int_{-\frac{1}{2}lx}^{\frac{1}{2}lx} \phi(x) dx}{\int_{-\frac{1}{2}lx}^{\frac{1}{2}lx} dx} \right]^2 \quad (4.3)$$

or

$$\Delta\phi^2 = (2\pi/\lambda)^2 \frac{1}{2} A^2 \quad (4.4)$$

Let the square of the coefficient be represented as C^2 , and let $C^2 = (2\pi A/\lambda)^2$, then equation 4.4 reduces to:

$$\Delta\phi^2 = \frac{1}{2} C^2 \quad (4.5)$$

For two or more terms of the aberration function, the variance takes the form,

$$\Delta\phi^2 = \frac{1}{2}C_1^2 + \frac{1}{2}C_2^2 + \dots \frac{1}{2}C_n^2 \quad (4.6a)$$

or

$$\Delta\phi^2 = \frac{1}{2} \left[\sum_{i=1}^N C_i^2 \right] \quad (4.6b)$$

If the variance of the first set of coefficients is represented by $\frac{1}{2} \sum_{i=1}^{20} C_i^2$ or $\frac{1}{2} \text{sum}(C_i^2)$ then the subsequent sets are $\frac{1}{2} \sum_{i=1}^{20} (\frac{1}{2}C_i)^2$ or $\frac{1}{2} \text{sum}(\frac{1}{2}C_i^2)$, $\frac{1}{2} \text{sum}(C_i/3)^2$, $\frac{1}{2} \text{sum}(C_i/6)^2$, and $\frac{1}{2} \text{sum}(C_i/8)^2$. $\frac{1}{2} \text{sum}(C_i)^2$ is the most aberrated case, while $\frac{1}{2} \text{sum}(C_i/8)^2$ the least. Appendix C lists the randomly generated values of coefficients. Figures 14 to 18 show individual irradiance distribution plots for the five different sets of coefficients studied, while figure 19 show a comparative irradiance plot of a diffraction-limited beam and three cases of aberrated beams. It is evident, from these plots and equation 4.1, that as the variance of the phase aberration increases, the on-axis irradiance decreases, while increasing the amplitude of the 'secondary' beam or 'halo'. An increase in the variance of the function indicates an increase in the coefficients of the individual terms in the series expansion representing aberration.

The lateral extent of the 'secondary' beam is a function of the individual terms in the series expansion of the aberration function. To study this relationship, several

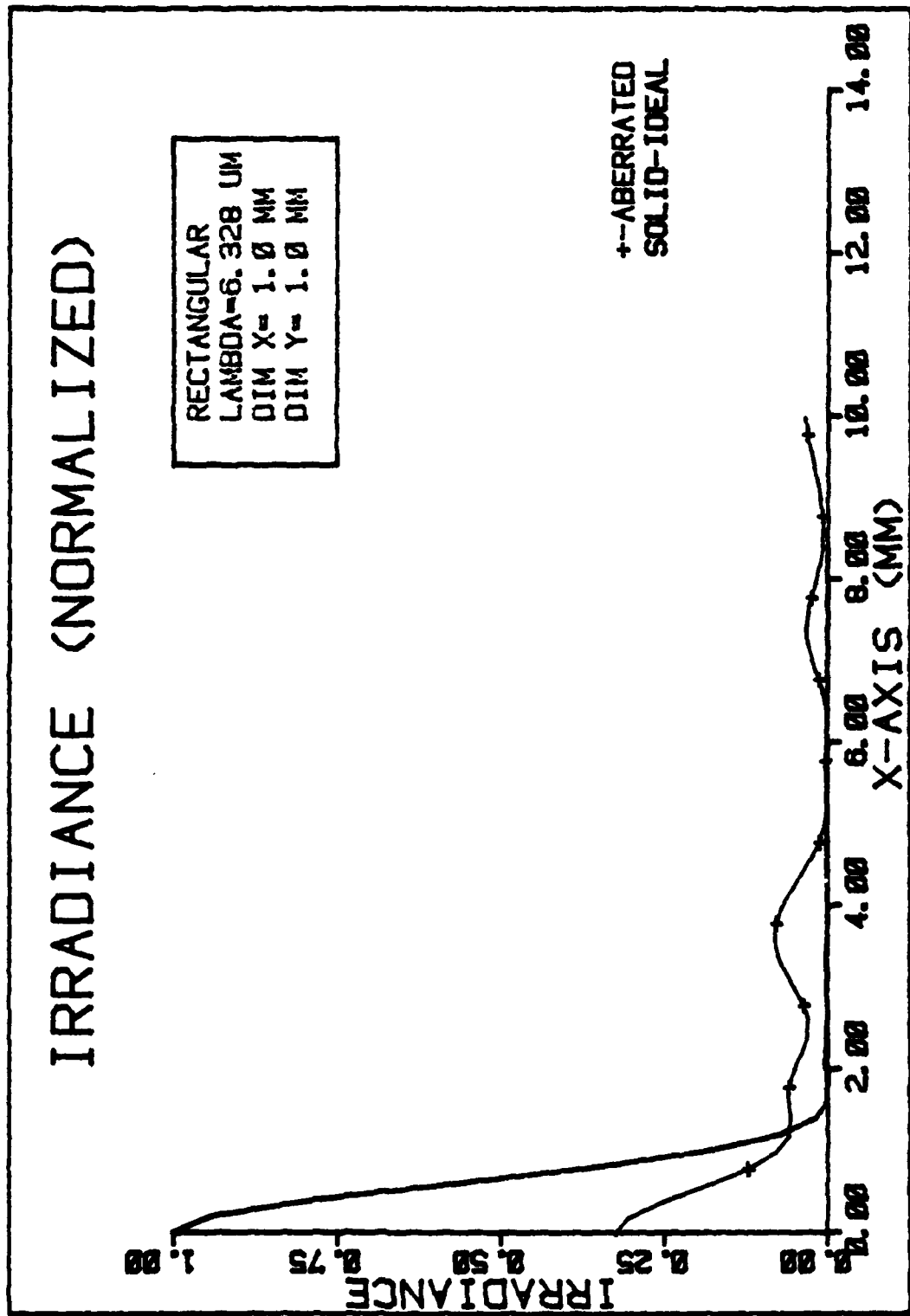


Figure 14. Irradiance profile of phase aberrated beam with variance $\frac{1}{2}\sum(C_i)^2$.

IRRADIANCE (NORMALIZED)

RECTANGULAR
 LAMBDA=6.328 UM
 DIM X= 1.0 MM
 DIM Y= 1.0 MM

+--ABERRATED
 SOLID--IDEAL

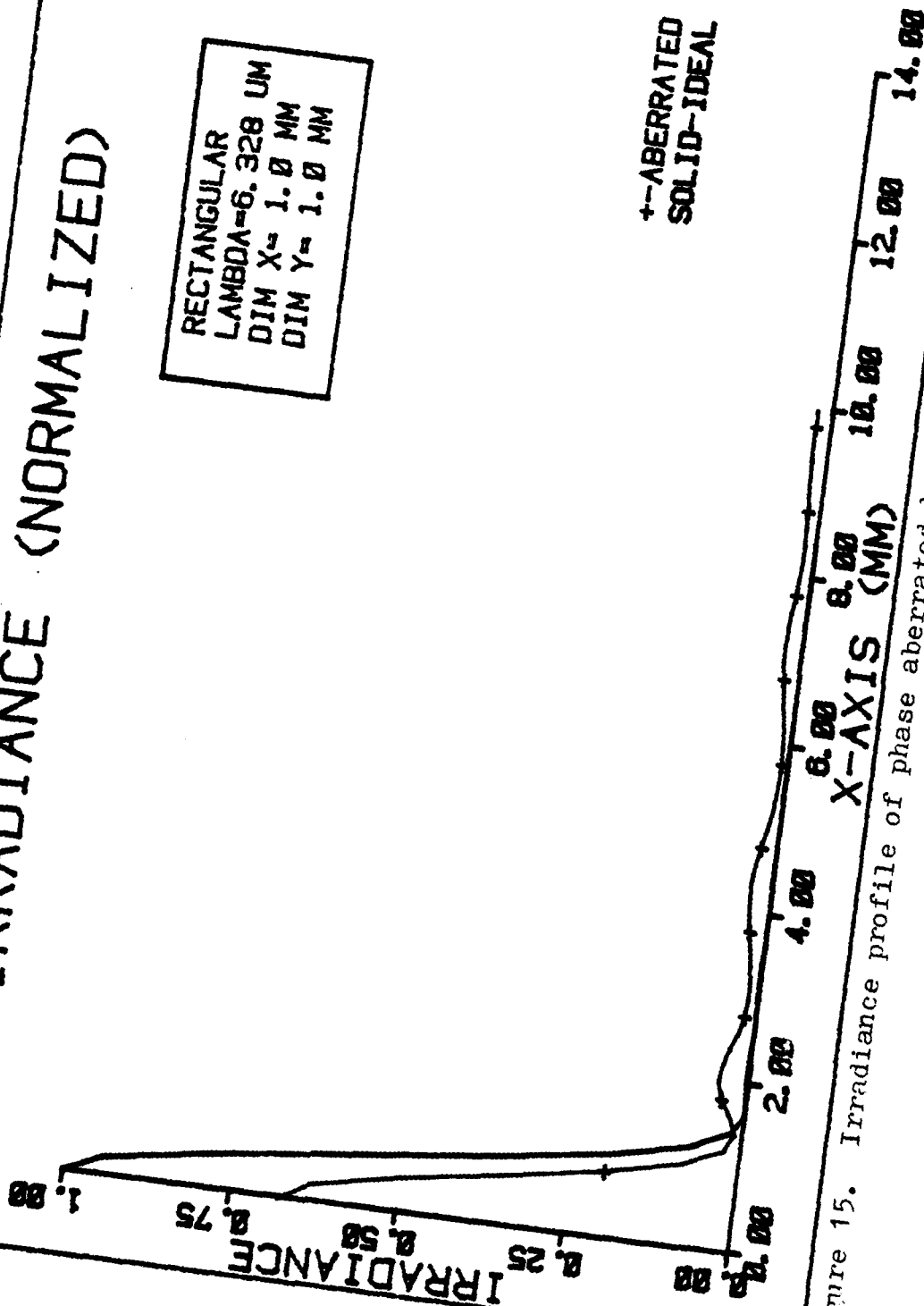


Figure 15. Irradiance profile of phase aberrated beam with variance $\frac{1}{2} \sum (C_i)^2$.

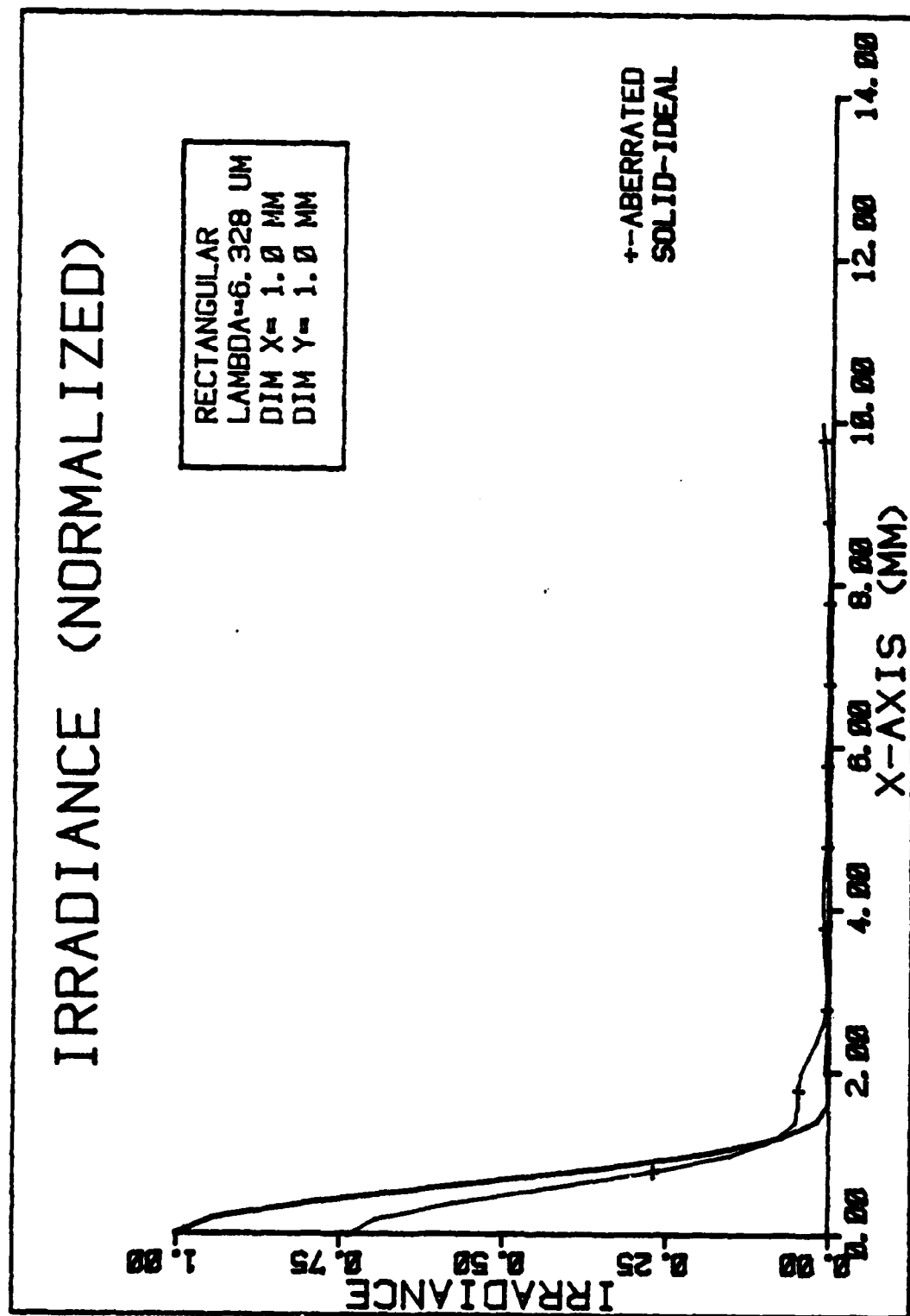


Figure 16. Irradiance profile of phase aberrated beam with variance $\frac{1}{2} \sum (C_1/3)^2$.

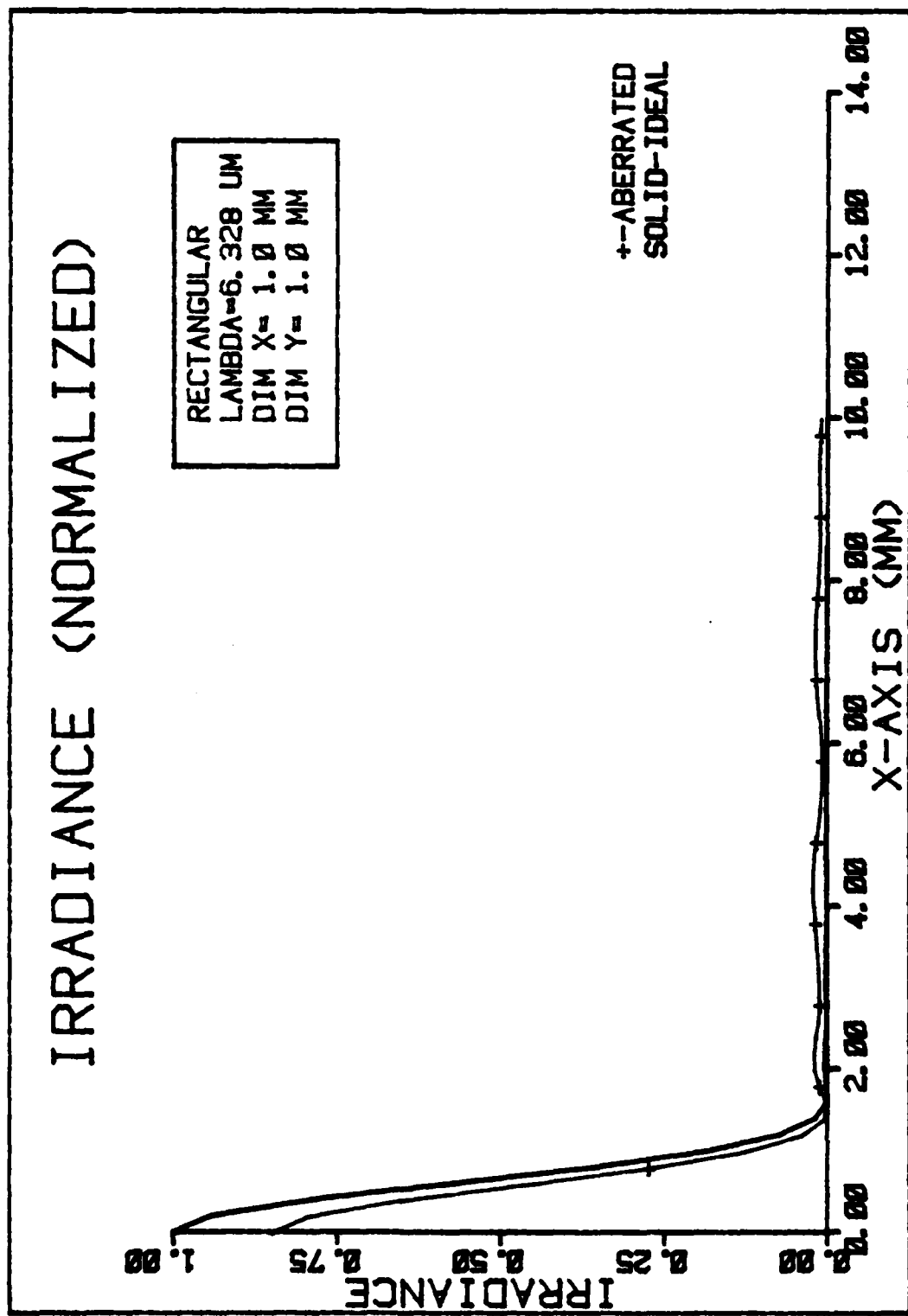


Figure 17. Irradiance profile of phase aberrated beam with variance $\frac{1}{2} \sum (C_i/6)^2$.

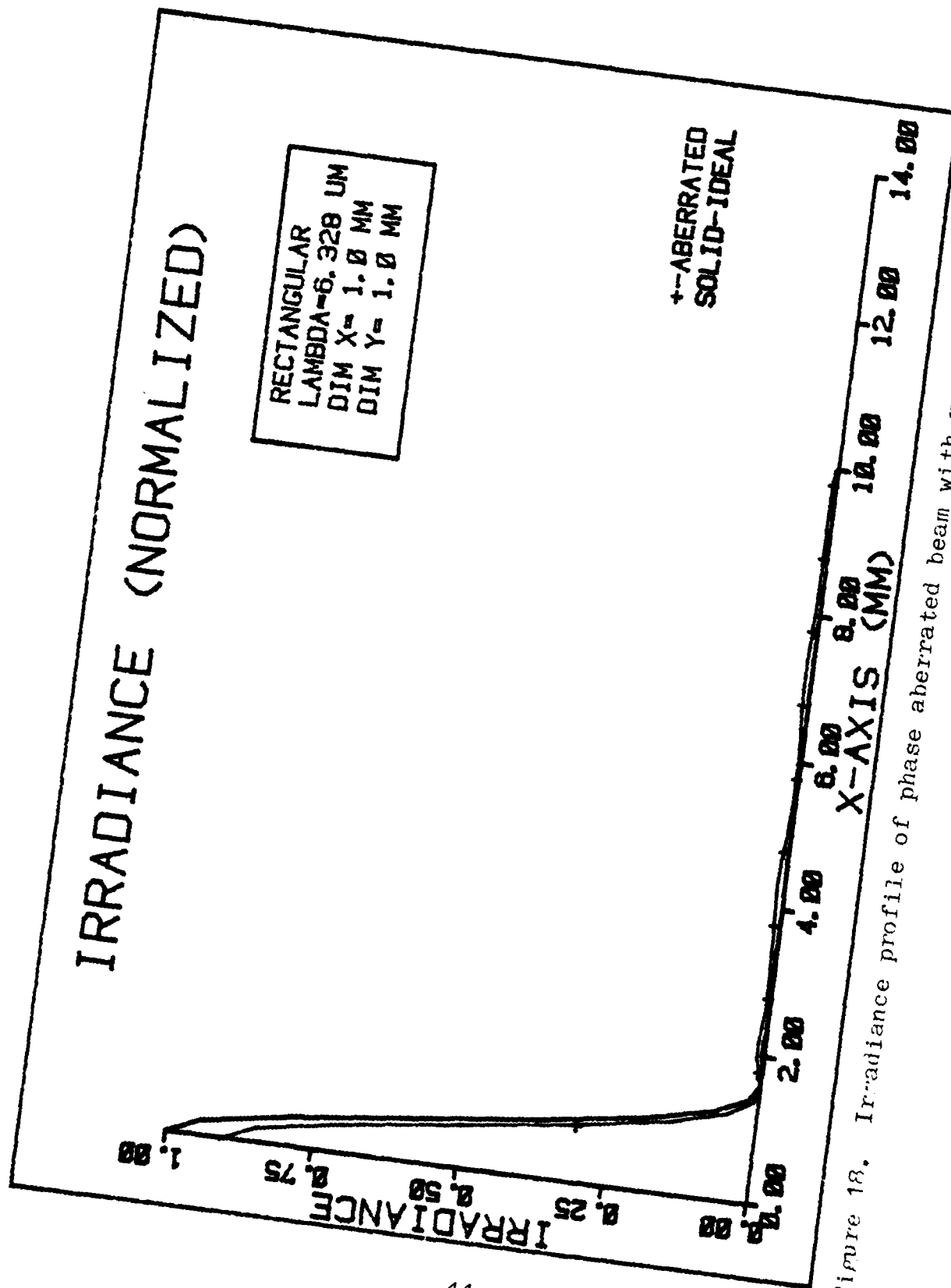


Figure 18. Irradiance profile of phase aberrated beam with variance $\frac{1}{2} \sum (C_i/8)^2$.

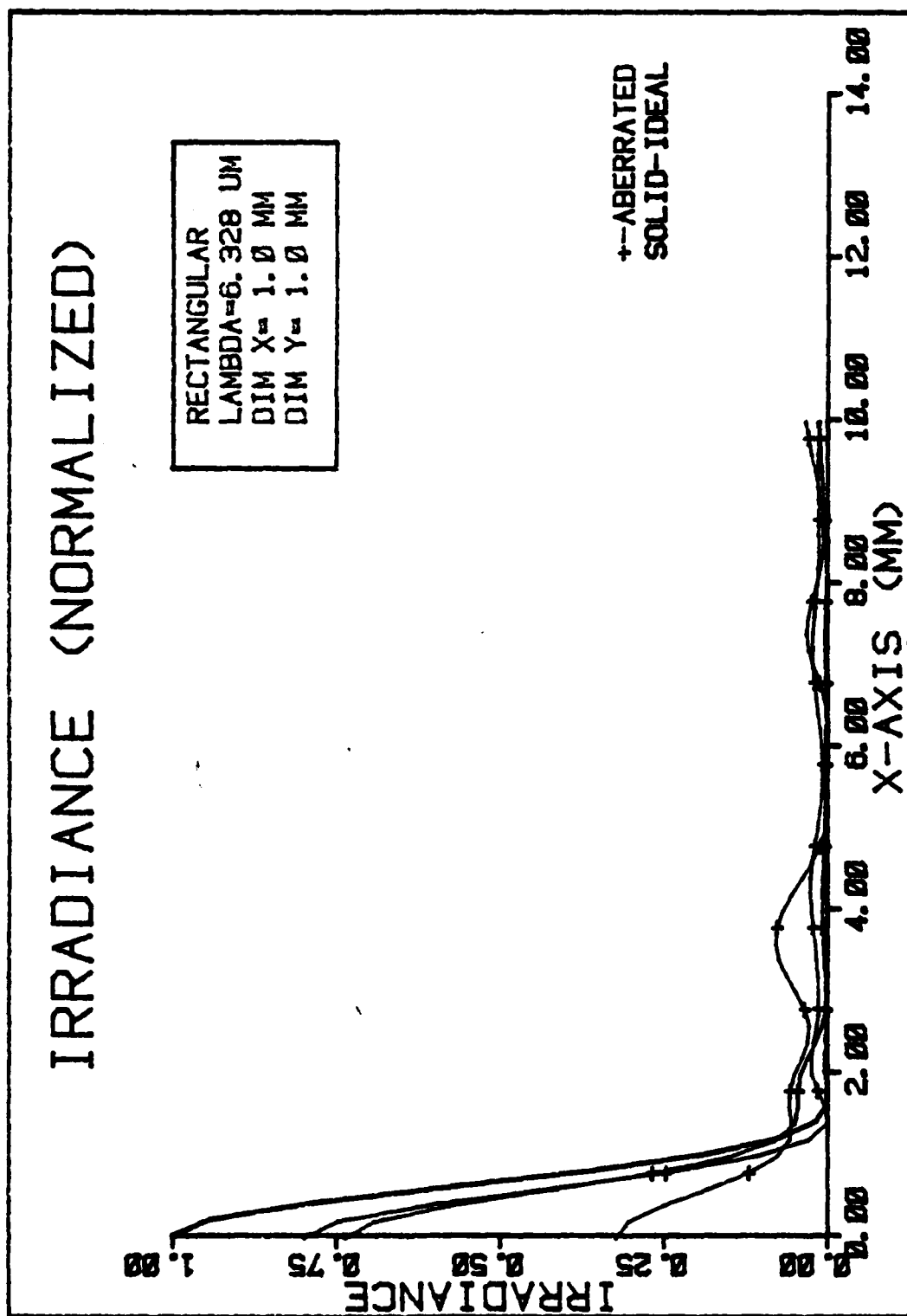


Figure 19. Comparative plot of diffraction-limited beam and three cases of phase aberrated beams.

simulations were done, whereby only specific terms of the series expansion were considered. By doing this, it is assumed that the specific term considered is the major contributing term in the expansion. All the other terms are zero or very small in amplitude and thus, negligible. In all cases, the variance of the phase aberration function was kept constant. In one set of simulation, the fundamental mode, the second, third, and fifth harmonics or terms of the series were individually considered. A phase distortion amounting to 0.095λ was assumed for each one. The results of these simulations are shown in figures 20 to 23. Notice that the extent of the aberrated beam increases with increasing harmonics of the aberration function.

By representing the 'secondary' beam or 'halo' with a Gaussian distribution function, the extent of the nondiffraction-limited beam can be conveniently determined by measuring the variance, σ^2 , of the distribution.

Most of the current methods of beam characterization do not attempt to describe the attenuating factor and the lateral extent of the aberrated beam. In most cases, only one parameter is measured. For example, the 'power in the bucket' method measures the 'number of times diffraction-limited' value. There is no basis of quantitative development for this measure to which it might be shown that the measure alone completely describes the beam quality. The Strehl

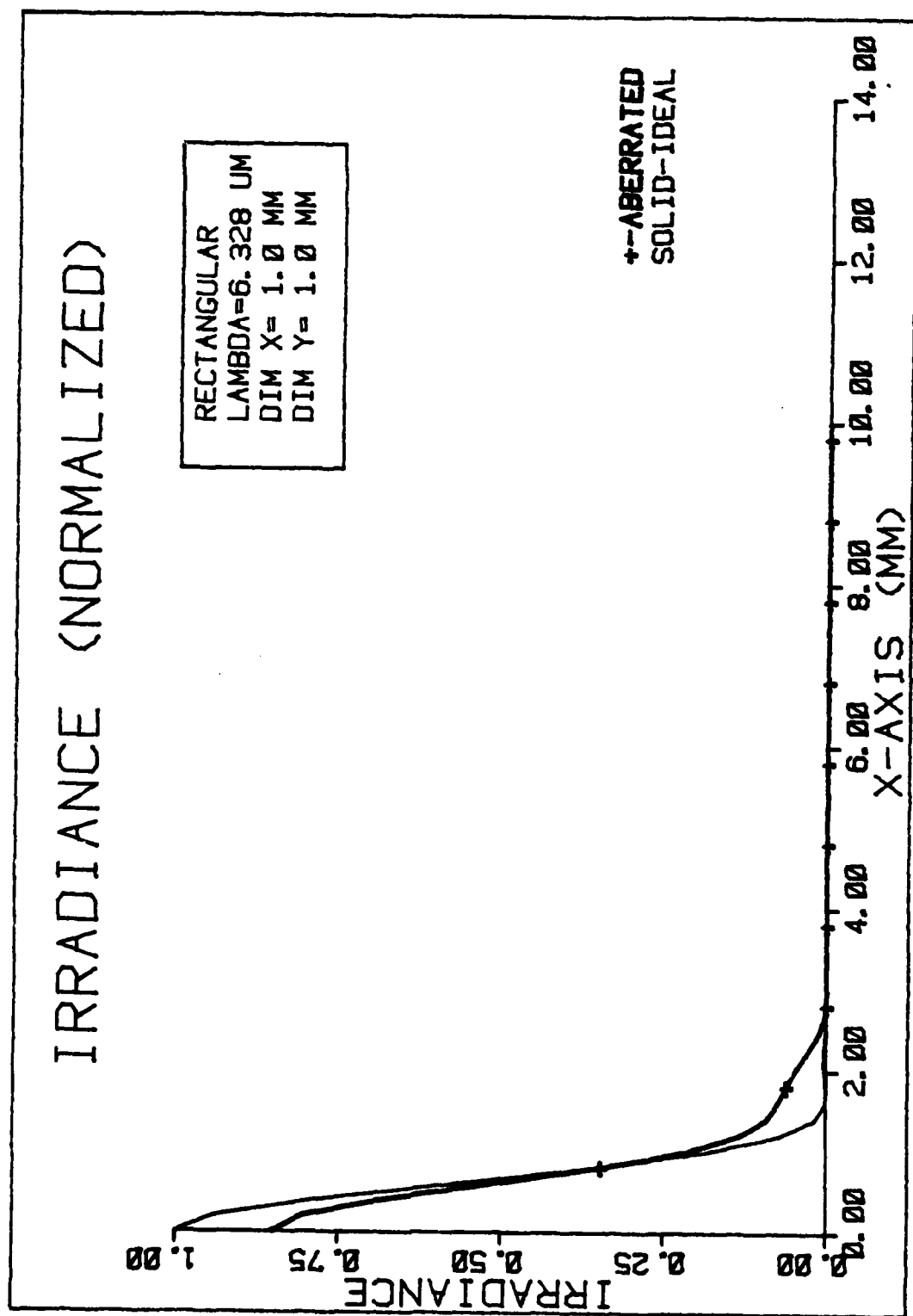


Figure 20. Irradiance profile for the function $\frac{\pi(0.095\lambda)}{\lambda} \cos(2\pi x)$.

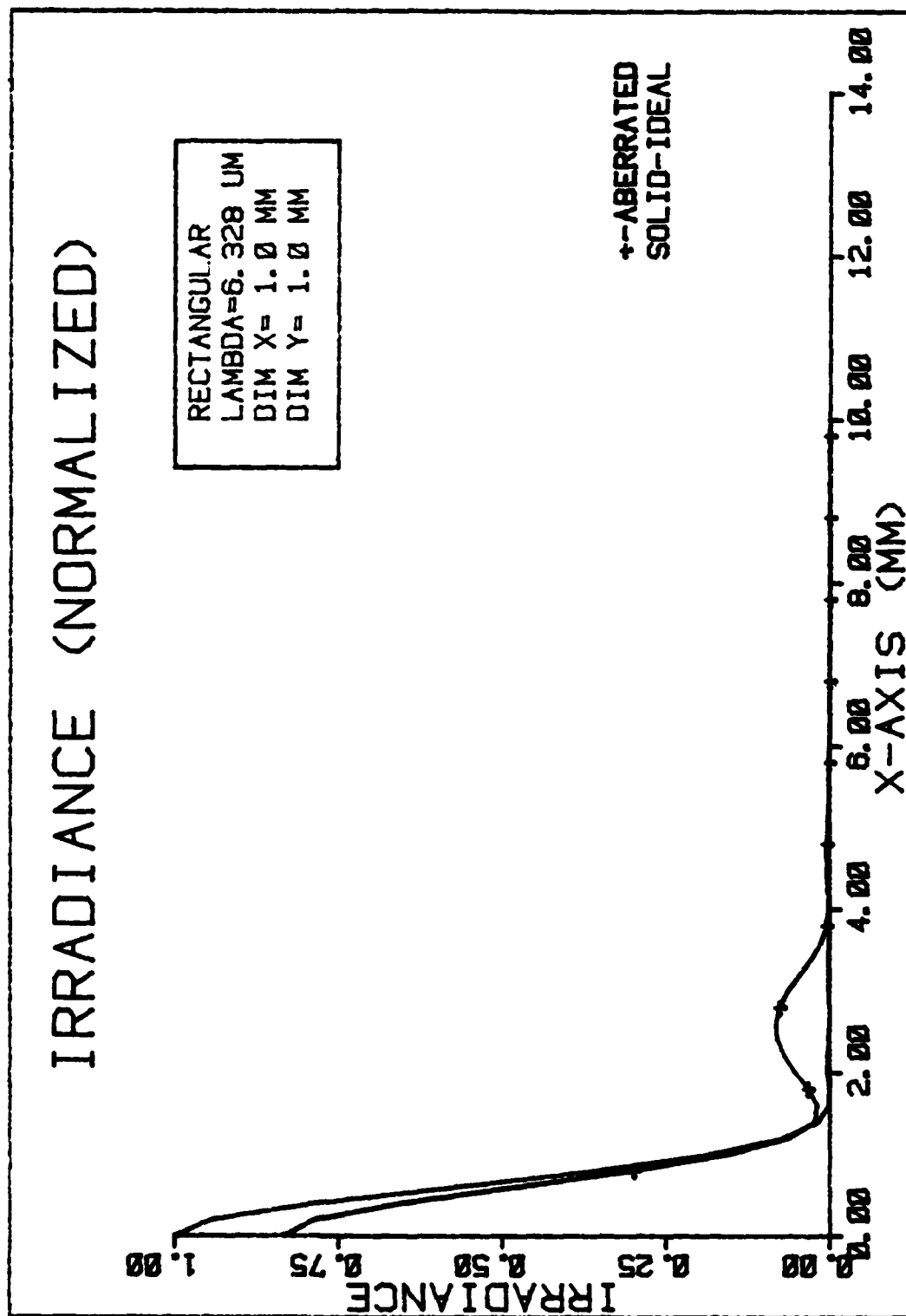


Figure 21. Irradiance profile for the function $\frac{2\pi(0.095\lambda)}{\lambda} \cos(4\pi x)$.

IRRADIANCE (NORMALIZED)

RECTANGULAR
 LAMBDA=6.328 UM
 DIM X= 1.0 MM
 DIM Y= 1.0 MM

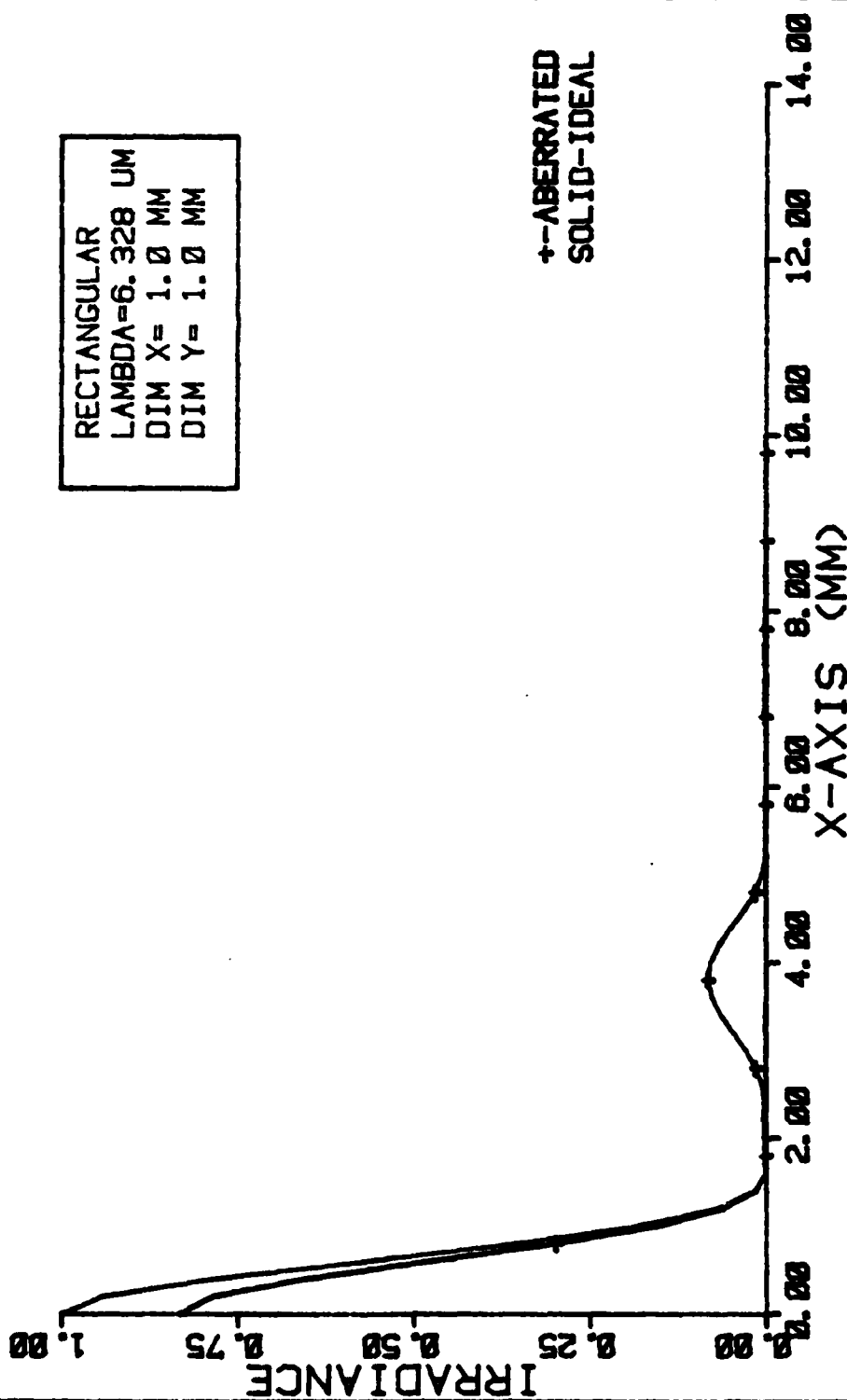


Figure 22. Irradiance profile for the function $\frac{2\pi}{\lambda}(0.095\lambda)\cos(\pi x)$.

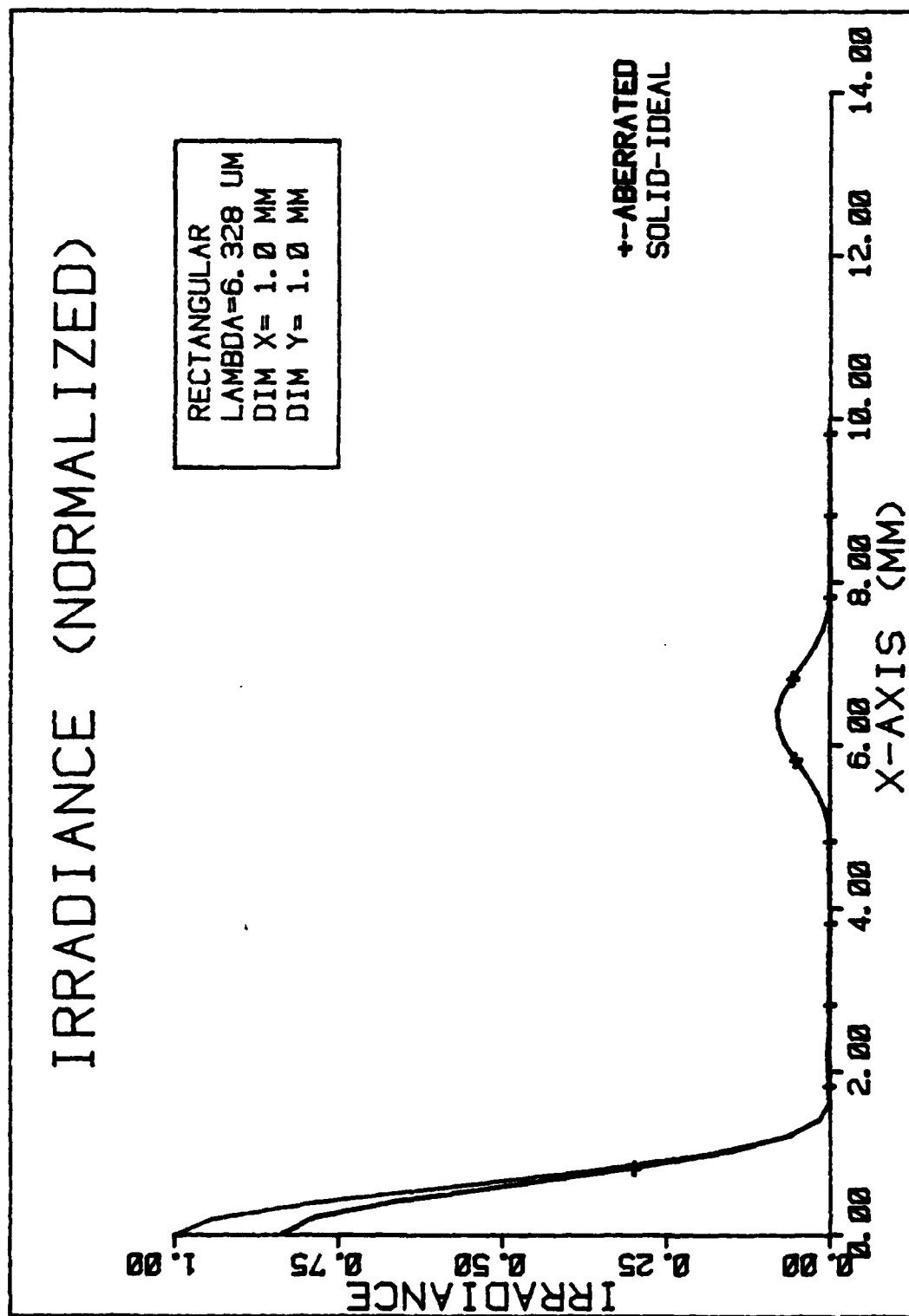


Figure 23. Irradiance profile for the function $\frac{2\pi(0.095\lambda)\cos(10\pi x)}{\lambda}$.

criterion also lends itself to a singular measure for beam quality. Although, it is important to determine the on-axis irradiance of an aberrated beam, it is also important to know how the scattered energy is distributed beyond the central axis. A better measure of beam quality, therefore, is one which determines both the attenuating factor imposed on the ideal beam, and the lateral extent of the aberrated beam. It is proposed, that in characterizing beam quality of some Air Force lasers, the attenuating factor F and the extent, represented by the variance σ^2 are measured. The following section will now discuss a method of numerically measuring these important beam quality parameters.

Least Squares Method of Curve Fitting

To determine the parameters F and σ^2 , the aberrated irradiance $I(x)$ was numerically fitted to the mathematical expression of equation 4.1. Corresponding to each of the observed values of x , there are two values of irradiance, namely, the observed value of irradiance $I(x)$ and the irradiance of equation 4.1

$$I'(x) = I_0(x)F + \frac{(1-F)}{\sqrt{2\pi\sigma^2}} e^{-x^2/2\sigma^2} \quad (4.1)$$

The difference between $I(x)$ and $I'(x)$ is called the deviation.

$$d = I(x) - I_0(x)F - \frac{(1-F)}{\sqrt{2\pi\sigma^2}} e^{-x^2/2\sigma^2} \quad (4.7)$$

Each deviation measures the amount by which the predicted value of irradiance falls short of the observed value $I(x)$. The set of all deviations,

$$[d_1 = I(x_1) - I_0(x_1)F - \frac{(1-F)}{\sqrt{2\pi}\sigma^2} e^{-x_1^2/2\sigma^2}] , \dots ,$$

$$[d_n = I(x_n) - I_0(x_n)F - \frac{(1-F)}{\sqrt{2\pi}\sigma^2} e^{-x_n^2/2\sigma^2}] \quad (4.8)$$

gives a picture of the closeness of fit of the mathematical expression, equation 4.1, to the observed data. The mathematical expression is a perfect fit only if all deviations are zero. By squaring each term in the set, positive and negative values of d are weighted equally. Thus,

$$J(F, \sigma) = \sum_{n=1}^N d_n^2 = \sum_{n=1}^N \left[I(x_n) - I_0(x_n)F - \frac{(1-F)}{\sqrt{2\pi}\sigma^2} e^{-x_n^2/2\sigma^2} \right]^2 \quad (4.9)$$

The sum of the squares of the deviation depends upon the choice of F and σ .

The method of least squares fit takes as the solution, $I_0(x)F + (1-F)/(2\pi\sigma^2)^{1/2} e^{-x^2/2\sigma^2}$ of best fit that one for which the sum of the squares of the deviation is a minimum. Thus, values for F and σ are determined for which the surface $H=J(F, \sigma)$ in F, σ, H -space has a low point. To find this minimum, the following partial differential

equations are solved simultaneously:

$$\frac{\partial J(F, \sigma)}{\partial F} = 0 \quad \text{and} \quad \frac{\partial J(F, \sigma)}{\partial \sigma} = 0 \quad (4.11)$$

or,

$$\frac{\partial}{\partial F} [I(x_n) - I_o(x_n)F - \frac{(1-F)}{\sqrt{2\pi\sigma^2}} e^{-x_n^2/2\sigma^2}]^2 = 0 \quad (4.12a)$$

and,

$$\frac{\partial}{\partial \sigma} [I(x_n) - I_o(x_n)F - \frac{(1-F)}{\sqrt{2\pi\sigma^2}} e^{-x_n^2/2\sigma^2}]^2 = 0 \quad (4.12b)$$

The solution was derived rather extensively, and the steps taken will not be shown here. Two expressions were derived from the solution of equations 4.12a and 4.12b. The expressions are given below:

$$F = \frac{\sum_{n=1}^N [I_o(x_n)I(x_n) - \frac{(I_o(x_n) + I(x_n))}{\sqrt{2\pi\sigma^2}} e^{-x_n^2/2\sigma^2} + \frac{e^{-x_n^2/\sigma^2}}{2\pi\sigma^2}] }{\sum_{n=1}^N [I_o^2(x_n) - \frac{2I_o(x_n)}{\sqrt{2\pi\sigma^2}} e^{-x_n^2/2\sigma^2} + \frac{e^{-x_n^2/\sigma^2}}{2\pi\sigma^2}] } \quad (4.13)$$

and,

$$G(F, \sigma) = \sum_{n=1}^N [(I_o(x_n)F - I(x_n)) \frac{(1-F)}{\sqrt{2\pi\sigma^2}} e^{-x_n^2/2\sigma^2} + \frac{(1-F)^2}{2\pi\sigma^3} e^{-x_n^2/\sigma^2}] \\ \times [(x_n^2/\sigma^2) - 1] = 0 \quad (4.14)$$

To determine F and σ , a numerical method of approxima-

ting the root of $G(F, \sigma)$ via the incremental search method was used. Figure 24 depicts the flow diagram of this numerical process.

The numerical codes works in this manner. An initial value for σ is assigned and equation 4.13 is calculated for F . F is then substituted into equation 4.14 and $G(F, \sigma_{\text{initial}})$ is calculated. A next value of σ is considered repeating the process outlined above until a value for $G(F, \sigma_{\text{next}})$ is determined. The two values for G are multiplied and this product is analyzed. If the product is zero, the root has been found. If it is negative, then a solution very close to the root has been reached. Small increments are added to σ , repeating the process until a predetermined level of accuracy is achieved. If the product is positive, σ is incremented until a negative product or a zero product is attained. Appendix B lists the numerical code of least squares curve fitting used to determine F and σ .

Data Analysis

In the preceding sections of this chapter, it was shown that the lateral extent of the 'secondary' beam varied as a function of the harmonics of the aberration function. As higher terms in the series expansion were considered, the lateral extent of the nondiffraction-limited beam increased accordingly. Now a numerical code is available to determine the relationship between F , σ , and the aberration function.

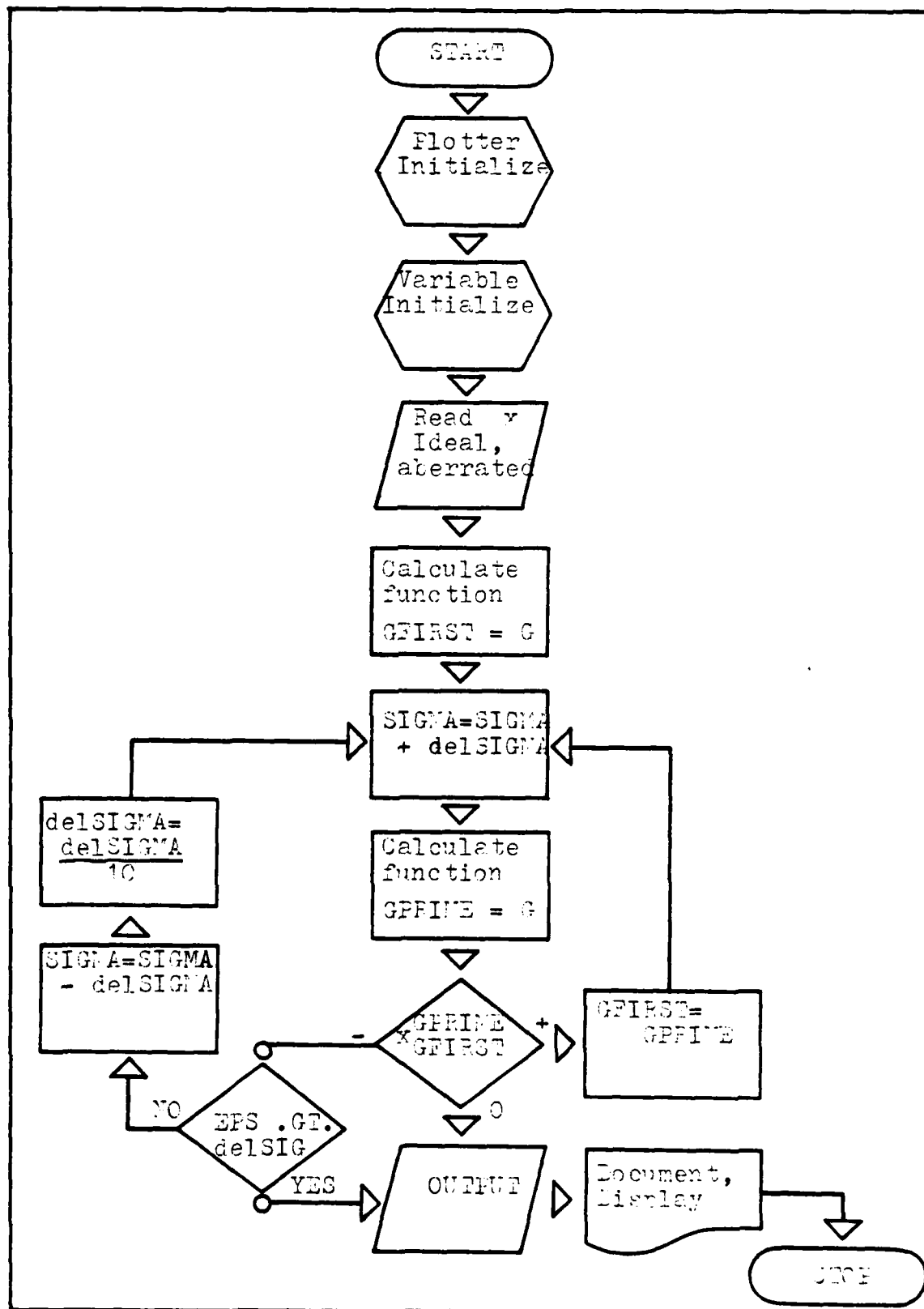


Figure 24. Flow diagram of method to calculate σ and its error by the LS solution using incremental search method.

Several simulation runs were done to investigate this relationship. First, the relative strengths of the phase distortion were varied while considering only the fundamental mode of the aberration. F and σ were derived by the numerical least squares curve fitting method discussed above. Next, the second, third, and fourth harmonics were individually considered. Results of these analyses are shown in table I. Figures 25 to 29 show the 'quality' of some of the fits. As predicted, the lateral extent or the variance of the 'secondary' beam increased as a function of the harmonic term considered.

From the data, an important observation is made regarding the relationship between F and σ^2 . They are independent of each other and must be treated separately. From table I, the variance is shown to be relatively constant over a wide range of phase distortions for the specific term considered. F approximates the value of the on-axis irradiance as the amount of aberration becomes smaller. The amplitude of the secondary beam or 'halo' becomes small, but the lateral extent remains the same. Thus the measured variance reflects, in general, the lateral extent owing to the more dominant term in the series expansion.

Next, curve fitting of irradiance profiles generated by simulating random phase aberrations containing the first twenty terms of the series expansion was done. Various strengths of phase distortion were considered. Figures 30 to 34 show the quality of these fits, yielding values for F and σ^2 , which are listed in table II.

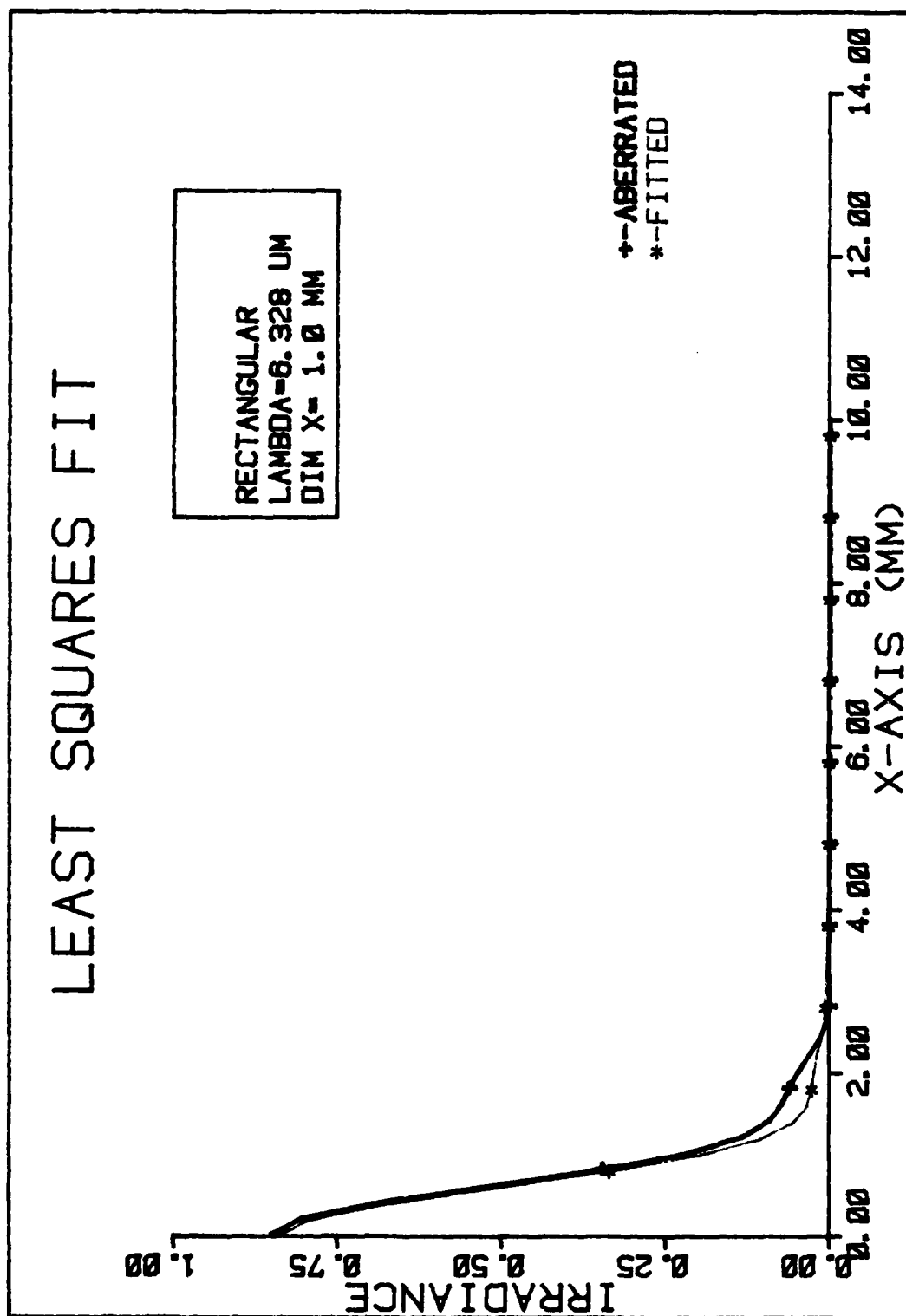


Figure 25. Curve fit of the function $\varphi=0.6\cos^2\pi x$, resulting in $F=0.76, G^2=1.48$.

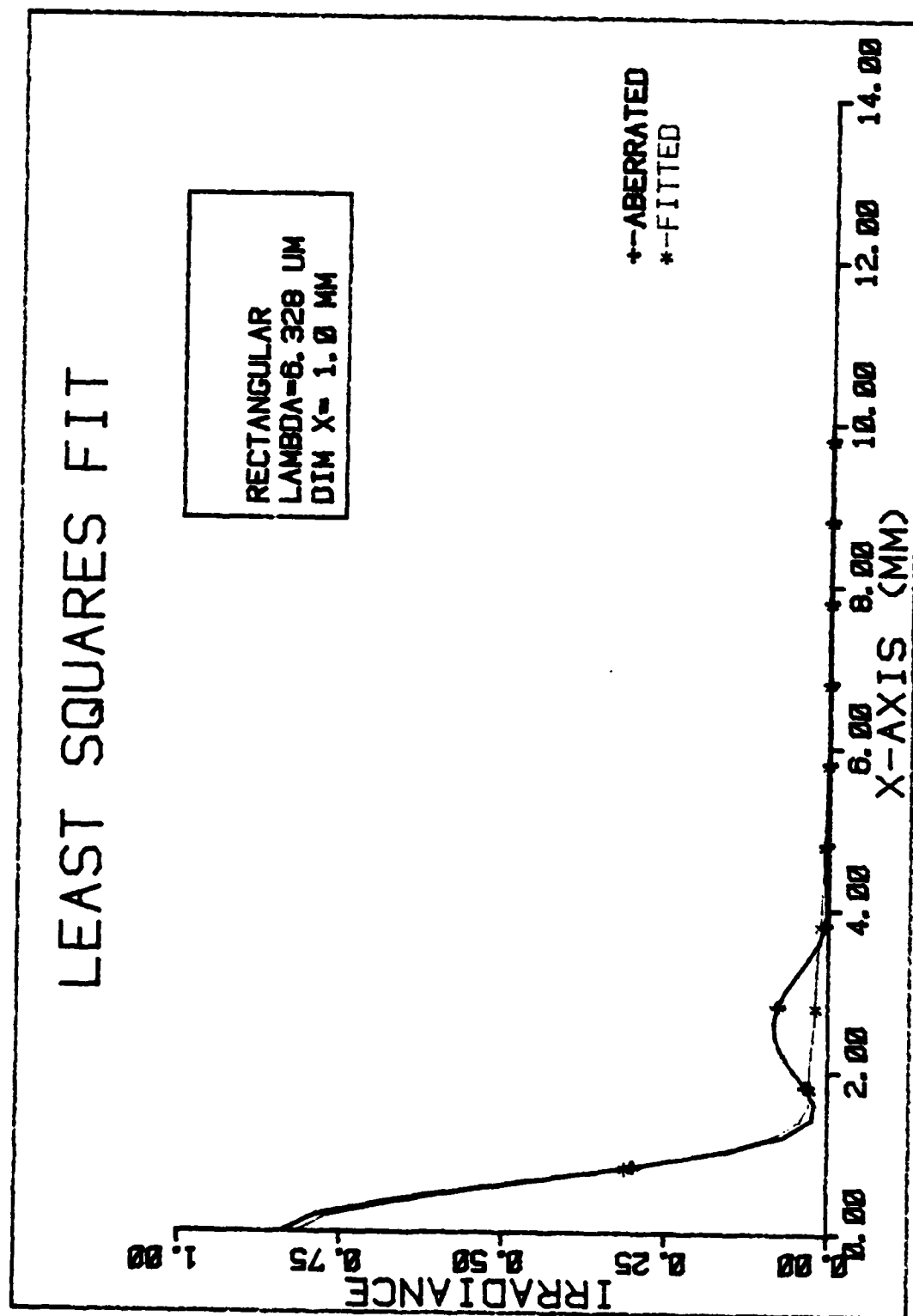


Figure 26. Curve fit of the function $\varphi = 0.6 \cos 4\pi x$, resulting in $F=0.78, \sigma^2=6.91$.

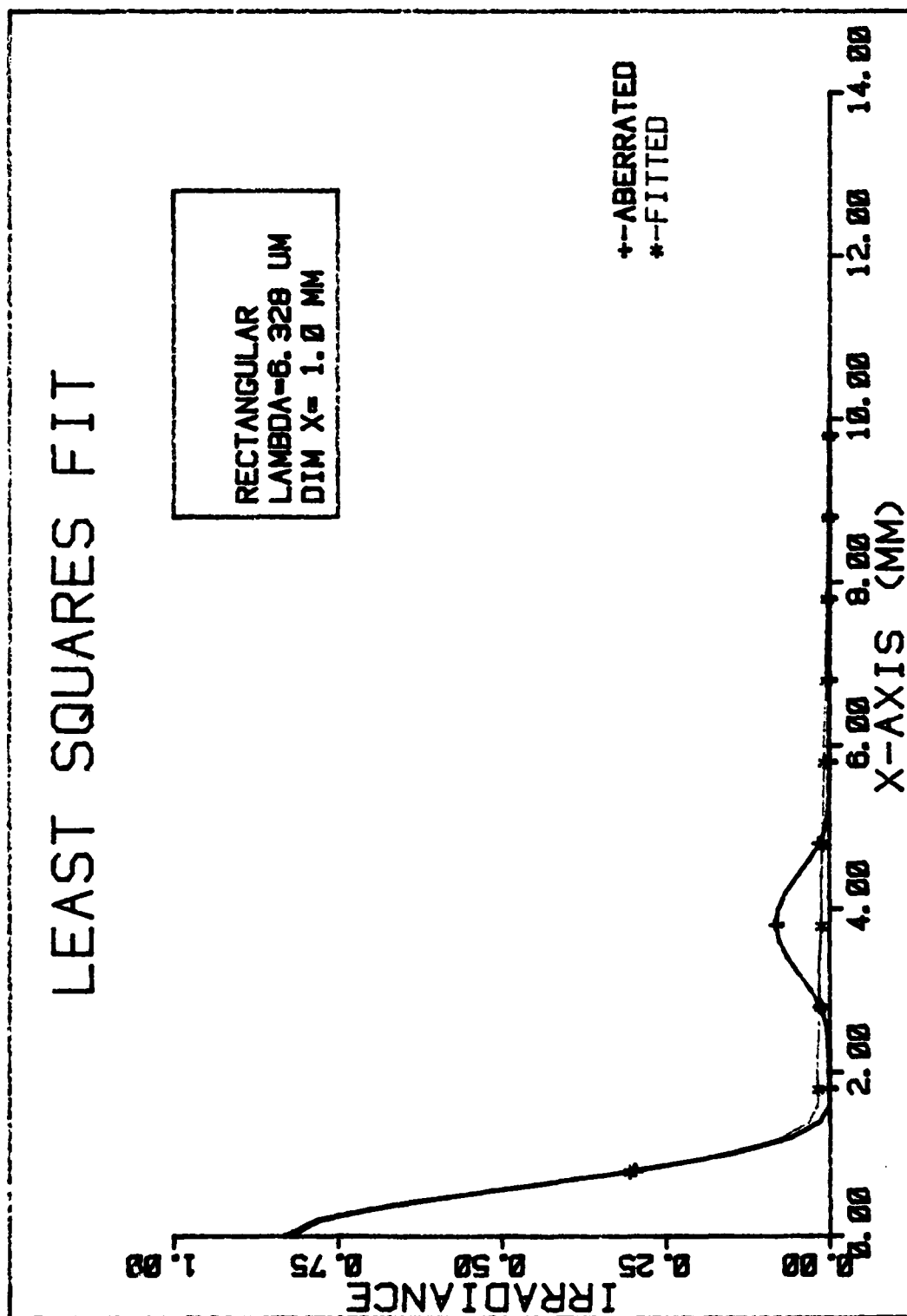


Figure 27. Curve fit of the function $\varphi = 0.6 \cos \sqrt{x}$, resulting in $F=0.8, \sigma^2=18.3$

LEAST SQUARES FIT

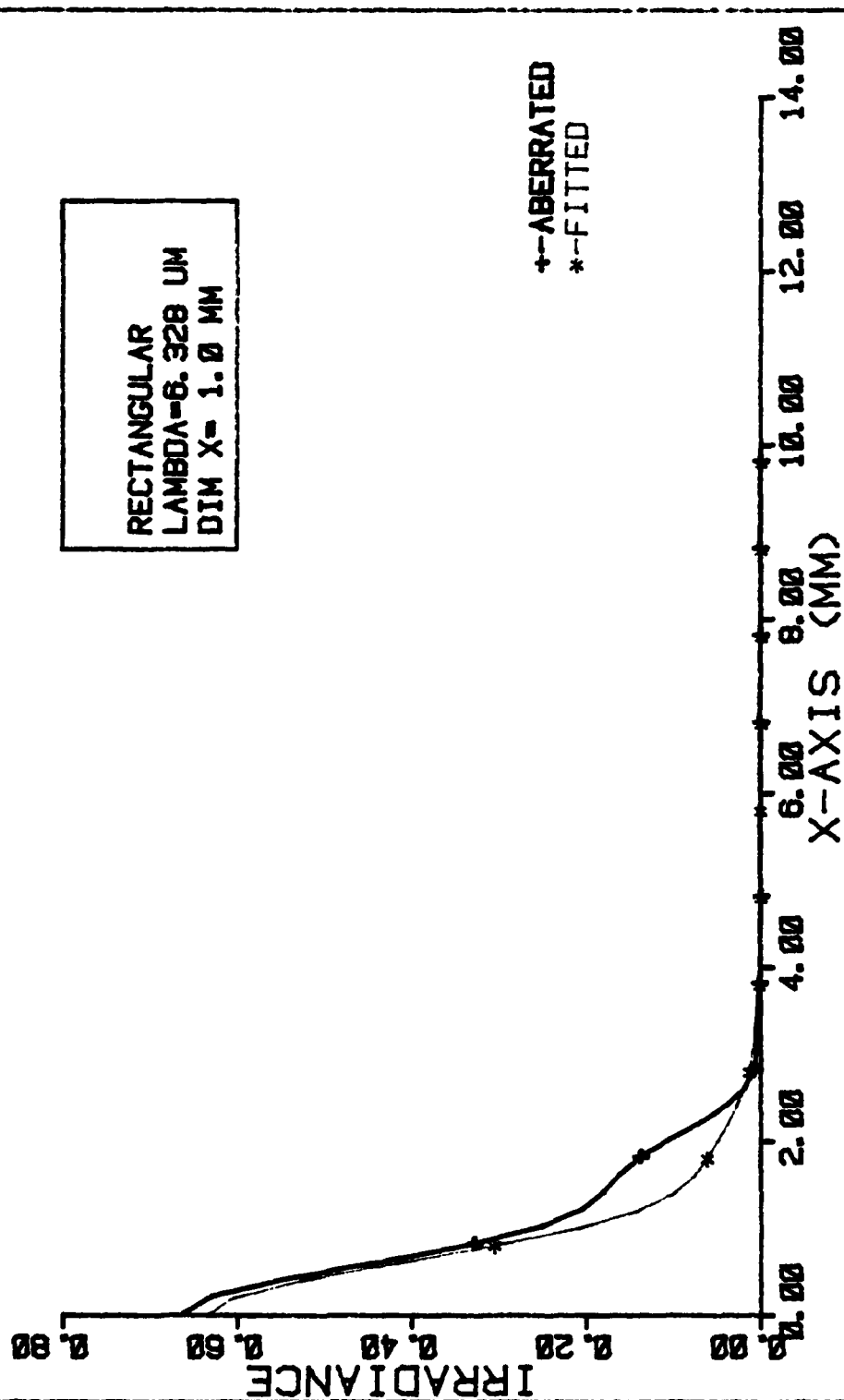


Figure 28. Curve fit of the function $\varphi = 0.4 \cos 2\sqrt{b}x$, resulting in $R=0.88, \sigma^2=1.47$

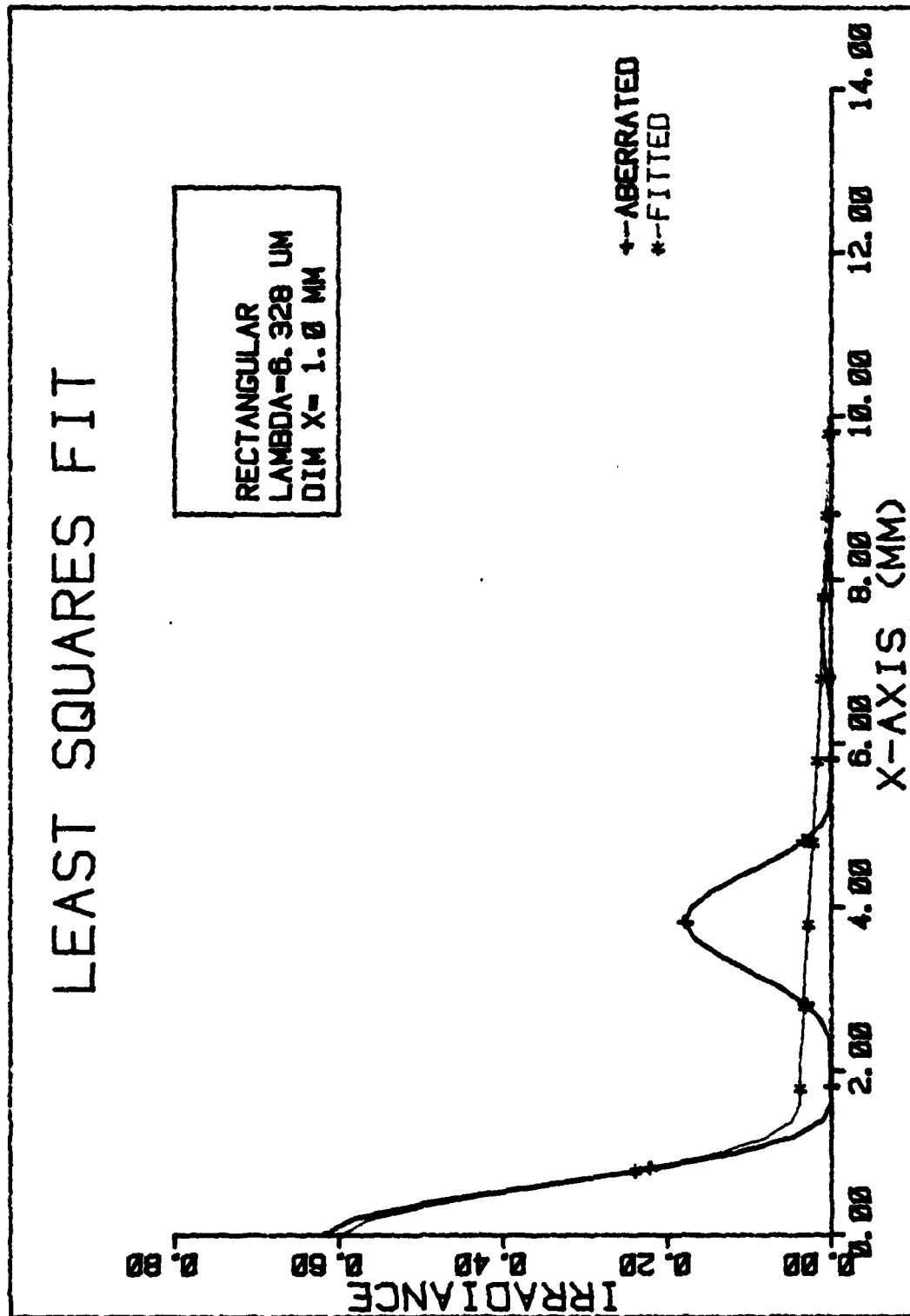


Figure 29. Curve fit of the function $\varphi = 0.95 \cos 6\sqrt{x}$, resulting in $F=0.56, \sigma^2=19.2$.

LEAST SQUARES FIT

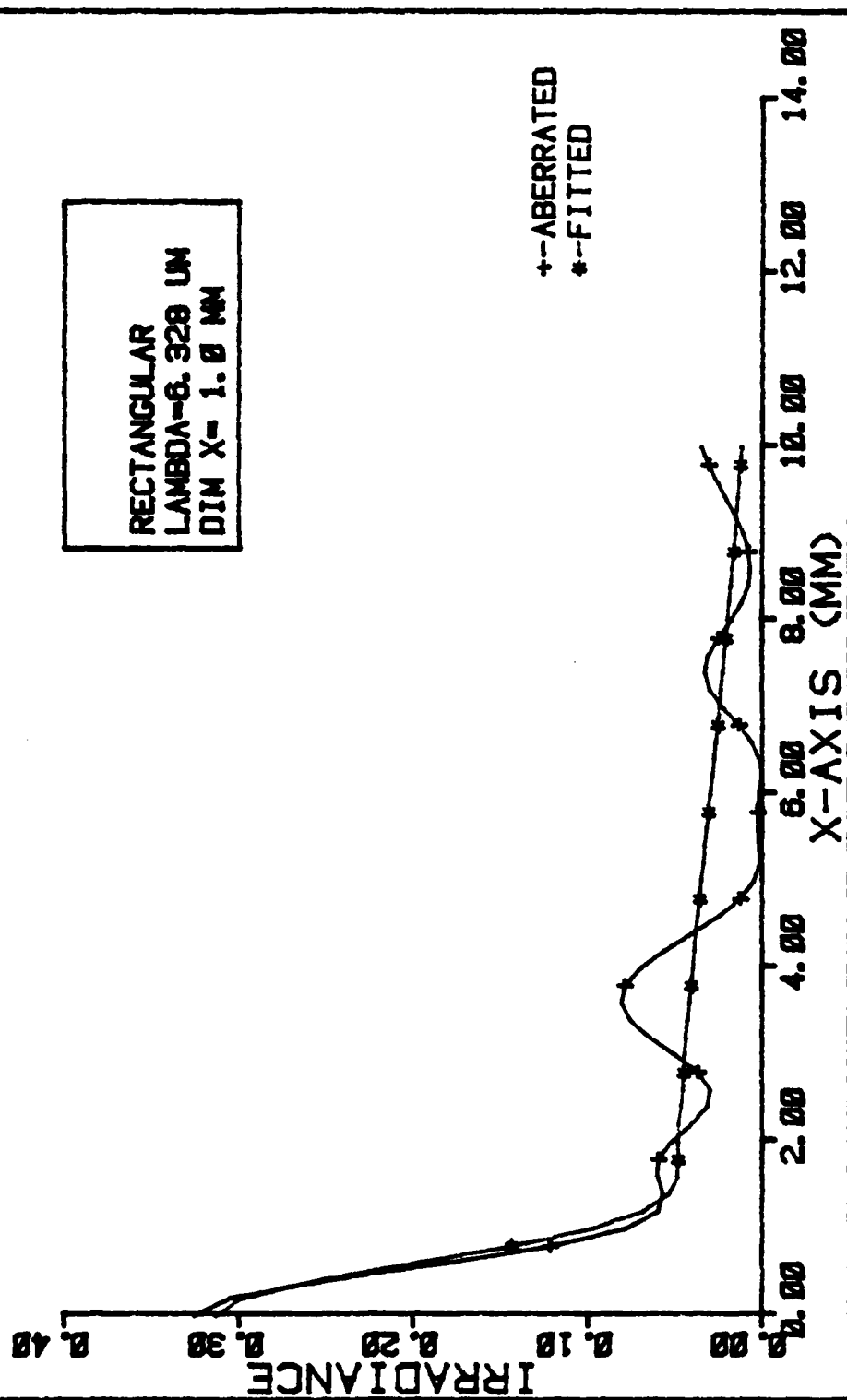


Figure 30. Quality of fit, variance of the aberration function is $\frac{1}{2} \sum (C_i)^2$.
 Results: $F=0.263, G^2=34.28$.

LEAST SQUARES FIT

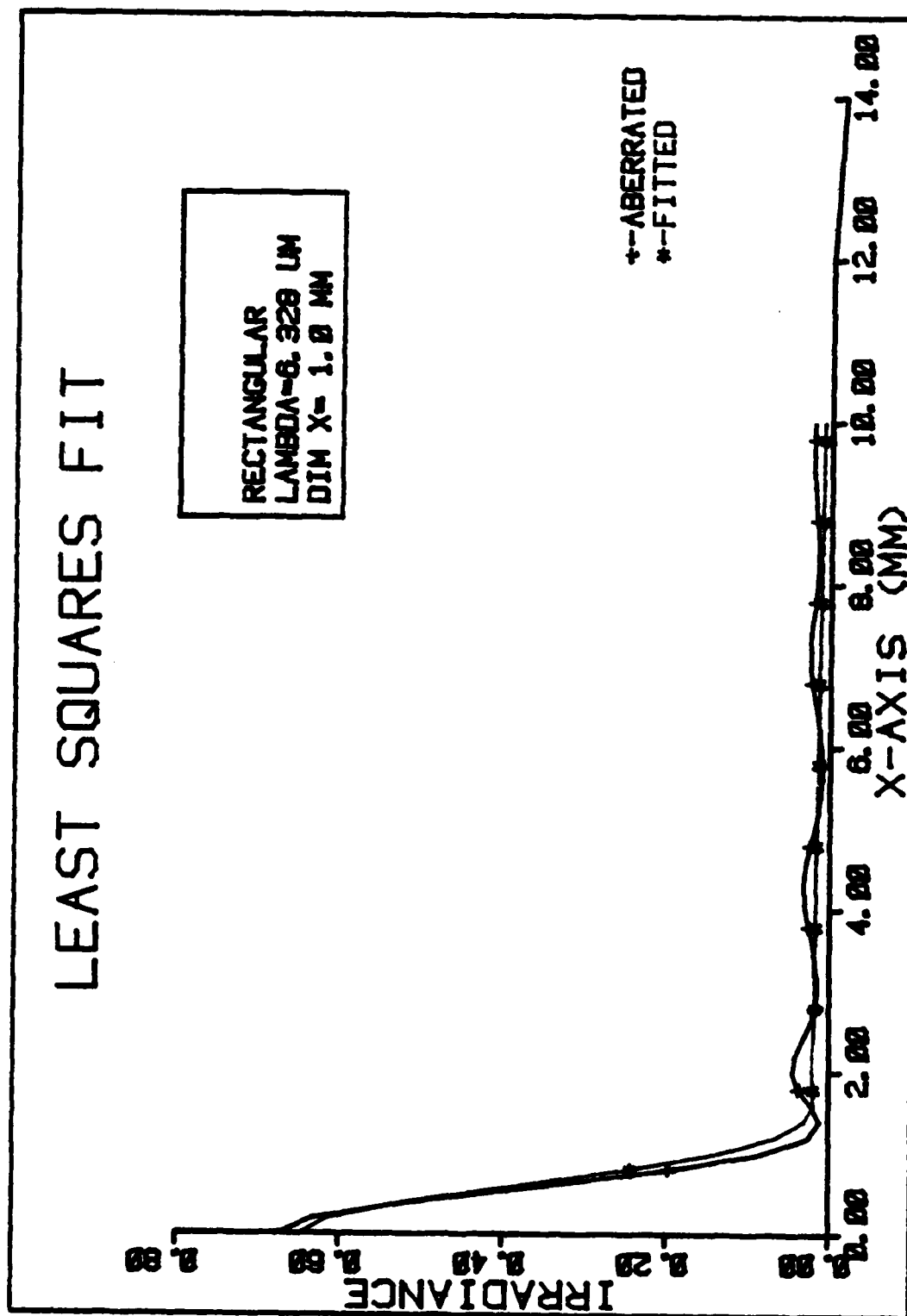


Figure 31. Quality of fit, variance of the aberration function is $\frac{1}{2} \sum (\frac{1}{2} C_i)^2$.
 Results: $F=0.628, \sigma^2=66.03$.

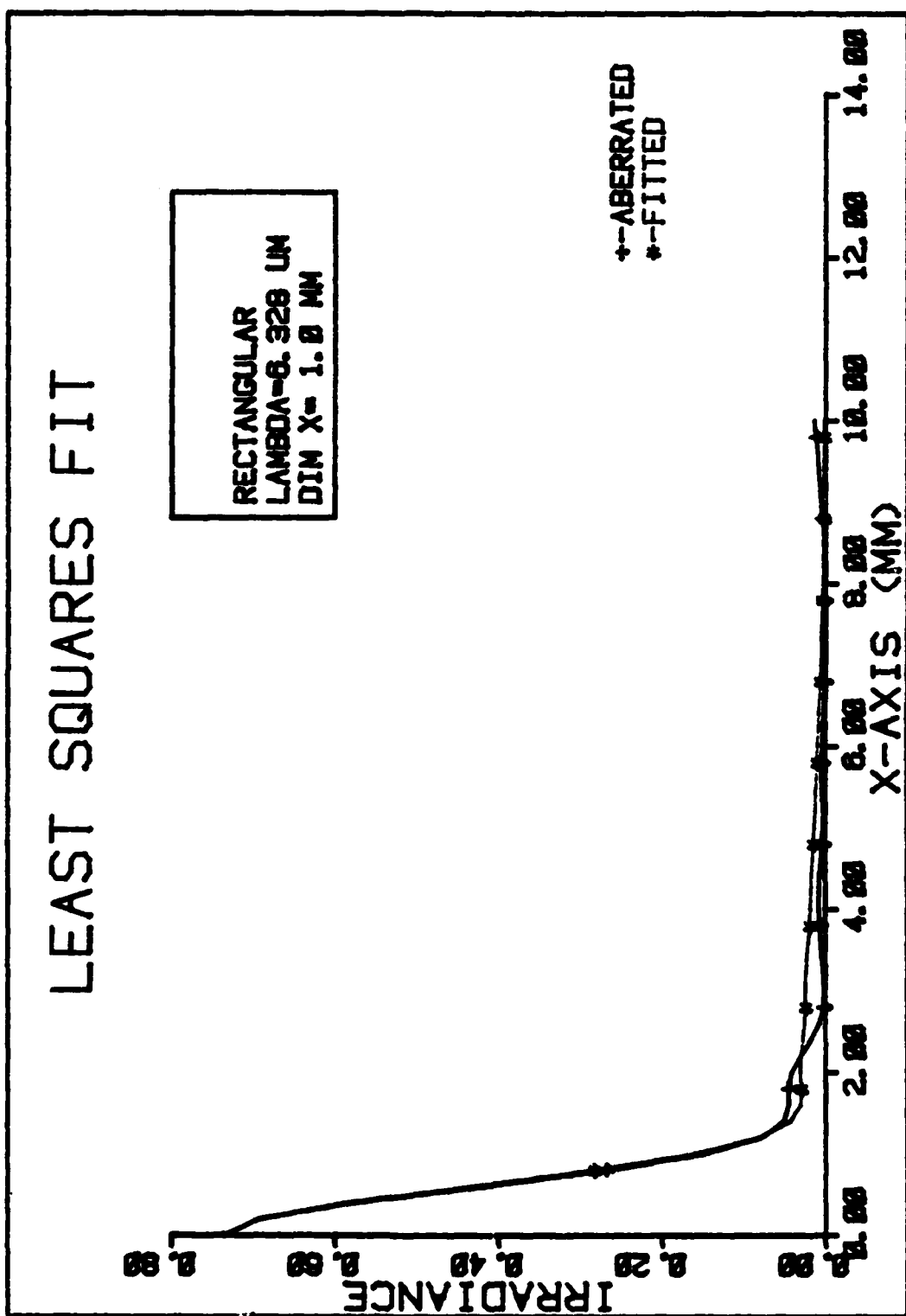


Figure 32. Quality of fit, variance of the aberration function is $\frac{1}{2} \sum (C_i/3)^2$.
 Results: $F=0.701, \sigma^2=13.79$.

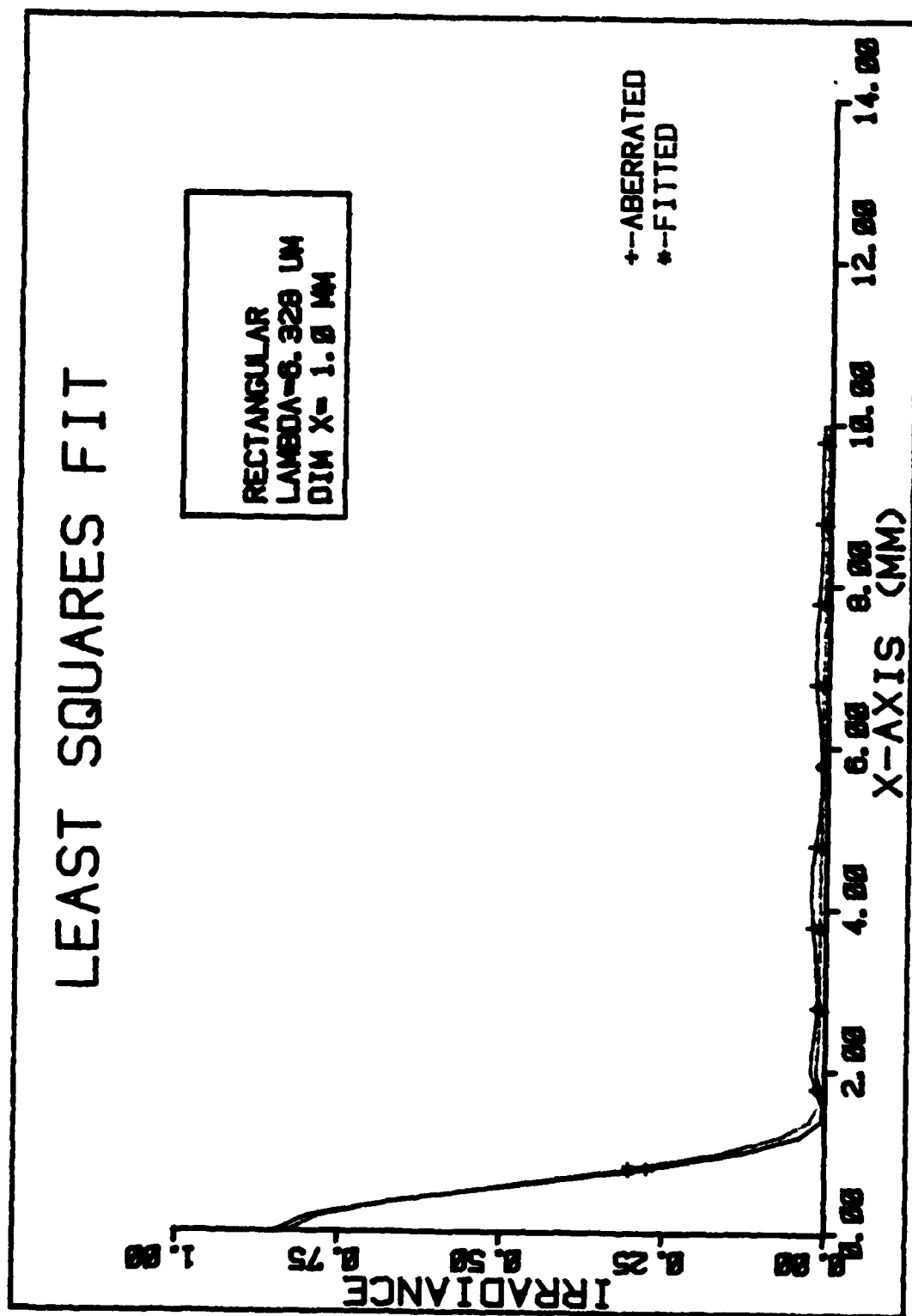


Figure 33. Quality of fit, variance of the aberration function is $\frac{1}{2} \sum (C_i/6)^2$.
 Results: $F=0.82, \sigma^2=65.68$.

LEAST SQUARES FIT

RECTANGULAR
 LAMBDA=0.328 UM
 DIM X= 1.0 MM

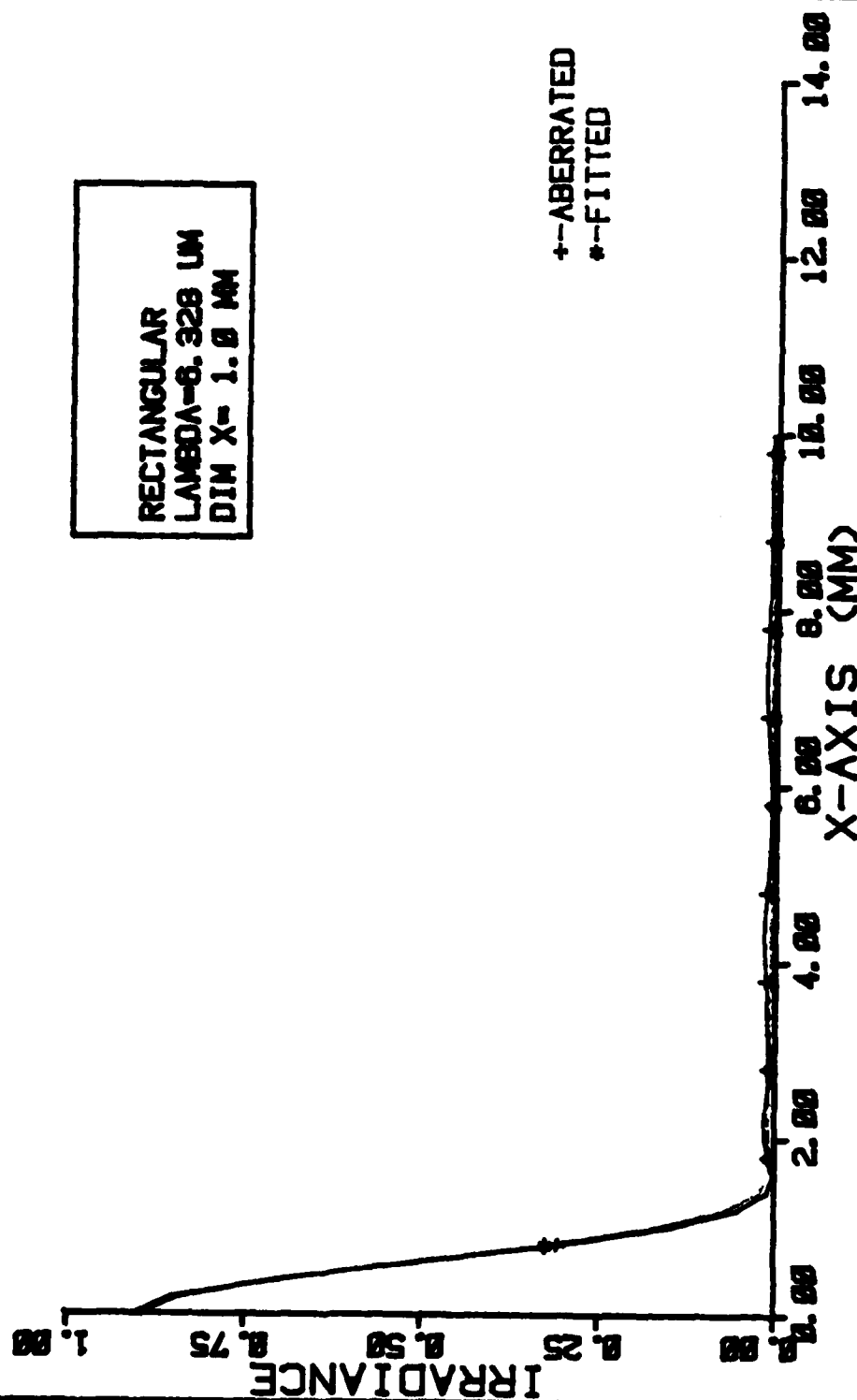


Figure 34. Quality of fit, variance of the aberration function is $\frac{1}{2} \sum (C_i/8)^2$.
 Results: $F=0.89$, $\sigma^2=65.48$.

Table I

Measured values of F and σ^2 for Individual Terms

Mode	Aberration function $2\pi/\lambda \text{Acos}(n2\pi x)$	σ^2 -extent	F	I(x=0)
Fundamental	0.15 cos $2\pi x$	1.45	0.98	0.99
	0.40 cos $2\pi x$	1.47	0.88	0.93
	0.50 cos $2\pi x$	1.48	0.83	0.89
	0.60 cos $2\pi x$	1.49	0.76	0.85
	0.75 cos $2\pi x$	1.51	0.64	0.78
	0.95 cos $2\pi x$	1.55	0.46	0.66
2nd Harmonic	0.40 cos $4\pi x$	6.81	0.90	0.92
	0.60 cos $4\pi x$	6.91	0.78	0.83
	0.95 cos $4\pi x$	7.23	0.51	0.62
3rd Harmonic	0.40 cos $6\pi x$	18.02	0.91	0.92
	0.60 cos $6\pi x$	18.31	0.80	0.83
	0.95 cos $6\pi x$	19.19	0.56	0.62
4th Harmonic	0.40 cos $8\pi x$	35.57	0.91	0.92
	0.60 cos $8\pi x$	36.04	0.81	0.83
	0.95 cos $8\pi x$	37.44	0.576	0.62

Table II

Measured F and σ^2 for twenty random numbers of aberration

Variance of Aberration	σ^2 -extent	F	$I(x=0)$
$\frac{1}{2}\text{sum}(C_i)^2$	34.28	0.26	0.33
$\frac{1}{2}\text{sum}(\frac{1}{2}C_i)^2$	13.79	0.70	0.74
$\frac{1}{2}\text{sum}(C_i/3)^2$	66.03	0.63	0.68
$\frac{1}{2}\text{sum}(C_i/4)^2$	66.09	0.69	0.74
$\frac{1}{2}\text{sum}(C_i/6)^2$	66.68	0.82	0.85
$\frac{1}{2}\text{sum}(C_i/7)^2$	65.56	0.86	0.88
$\frac{1}{2}\text{sum}(C_i/8)^2$	65.48	0.89	0.91
$\frac{1}{2}\text{sum}(C_i/2.5)^2$	63.38	0.64	----

V. Conclusions and Recommendations

Two important characteristics of laser beams in the presence of random phase aberrations were discussed in Chapter IV. The amount of attenuation and the lateral extent of the nondiffraction-limited beam describe the amplitude and form of the aberration and provide a better measure of laser beam quality.

Phase I of this study identified several currently used methods to characterize the quality of laser beams. In general, these methods and the figures of merit associated with them are insufficient. As already mentioned, a single parameter is often used when assigning a quality measure for a laser system. However, this singular parameter is insufficient since it does not describe the lateral extent of the phase aberrated beams. For example, in the 'power in the bucket' method, the 'times diffraction-limited' number is the quality number, and this is measured at an arbitrary point in the P-R curve. Similarly, only the normalized on-axis irradiance is determined from the Strehl criterion.

The far-field irradiance distribution and the total power curve (P-R curve) contains far greater information than what a singular measure would indicate. A single point in these curves simply cannot give a quantitative description of the overall quality of a laser beam. In the developing sections of this report, it was found that

two quantities, namely the attenuating factor F and the measure of lateral extent, σ^2 provided a better measure of quality for aberrated beams. Therefore, as a result of this thesis analysis, it is recommended that when characterizing the quality of laser beams, these two quantities are measured.

In describing beam quality using the 'times diffraction-limited' number, a number equal to 1, indicated a laser beam which is diffraction limited. Using the Strehl ratio, a ratio of 0.8 or better reflects a laser beam which is effectively unaberrated. Using the newly derived FOMs, an F equal to 1, defines an ideal or diffraction-limited beam. Examining equation 4.1, it is noted that at this limit, the second term representing the amplitude and spread of the 'halo' disappears. When the laser beam is phase aberrated, F becomes less than unity, and the 'secondary' beam appears. The spread of the 'secondary' beam, as discussed in Chapter IV, is a function of the form of the aberration and not its variance. Thus, for one form of aberration, the lateral extent of the beam remains the same for varying amounts of distortion. As the beam becomes more aberrated, the amplitude of the 'secondary' beam increases since more energy is scattered into this beam, while the spread remains constant. In attempting to approximate the form of the diffraction-limited beam, it is important, therefore, to minimize both the amount of attenuation and the spread or lateral extent of the 'secondary' beam.

The total power plots of figures 35 to 39 were the result of integrating the irradiance of the diffraction-limited beam, the aberrated beam and the 'fitted' beam. (The power plots of the normal and 'fitted' aberrated beams were included to show, once again, the closeness of the numerical fit discussed in the last chapter.) The total power plots are no more than the P-R curves, discussed in Chapter II, and derived from the 'power in the bucket' method. Figures 35 to 36 show the power plot of an aberrated beam whose spread, σ^2 was measured at approximately 65mm. While figures 37 to 39 are for aberrated beams with a spread of about 1.5 mm. Each plot represents different amounts of attenuation. An important observation is made from these power plots which supports an earlier hypothesis. Aberrated beams with high F values and small 'secondary' beam spread closely approximates the diffraction-limited case moreso than beams with low F values and wider dispersions. Thus, as a result, the ultimate design goal for laser systems is an attenuation factor of unity. Since, for practical systems this is not achieved readily, then a realistic design objective must be a laser system whose beam is characterized with an F very close to 1 and a 'secondary' beam with a small lateral extent.

F and σ^2 are derived from the overall far-field irradiance profile. As already mentioned above, the total power plots of P-R curves are the result of integrating

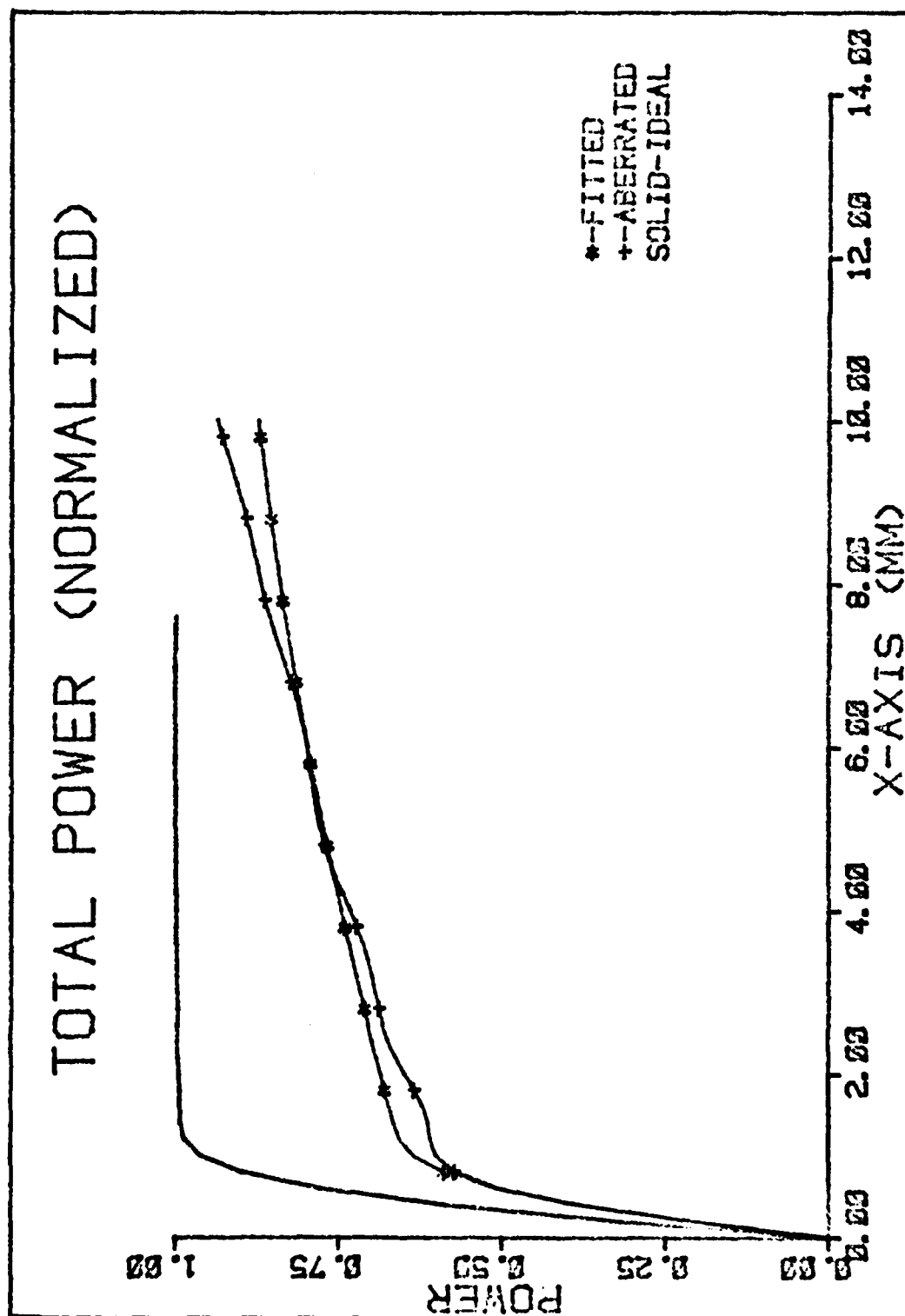


Figure 35. Total Power plot. $R=0.628$, $\sigma^2=66.03$.

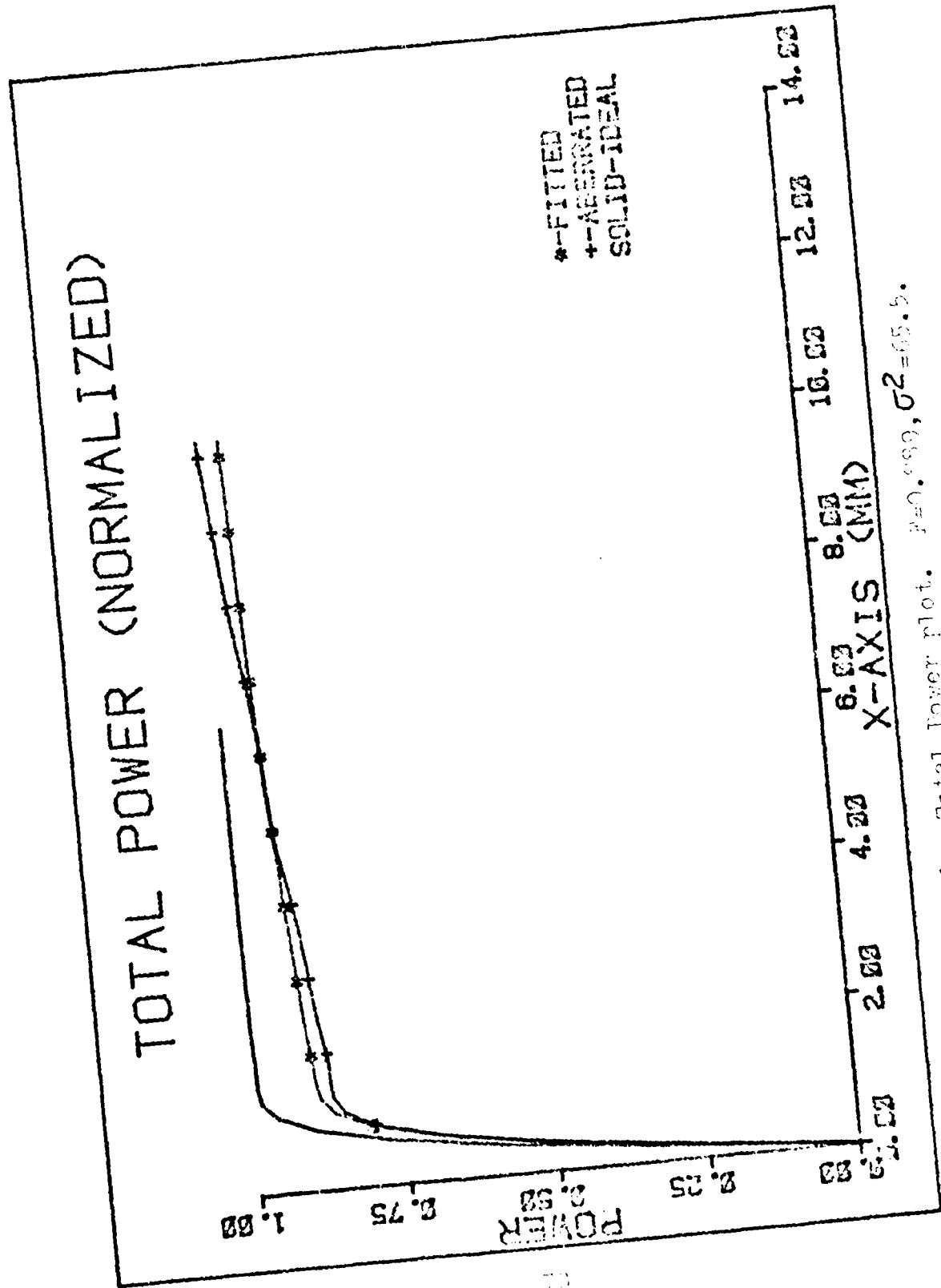


Figure 36. Total Power plot. $R=0.999$, $\sigma^2=0.5$.

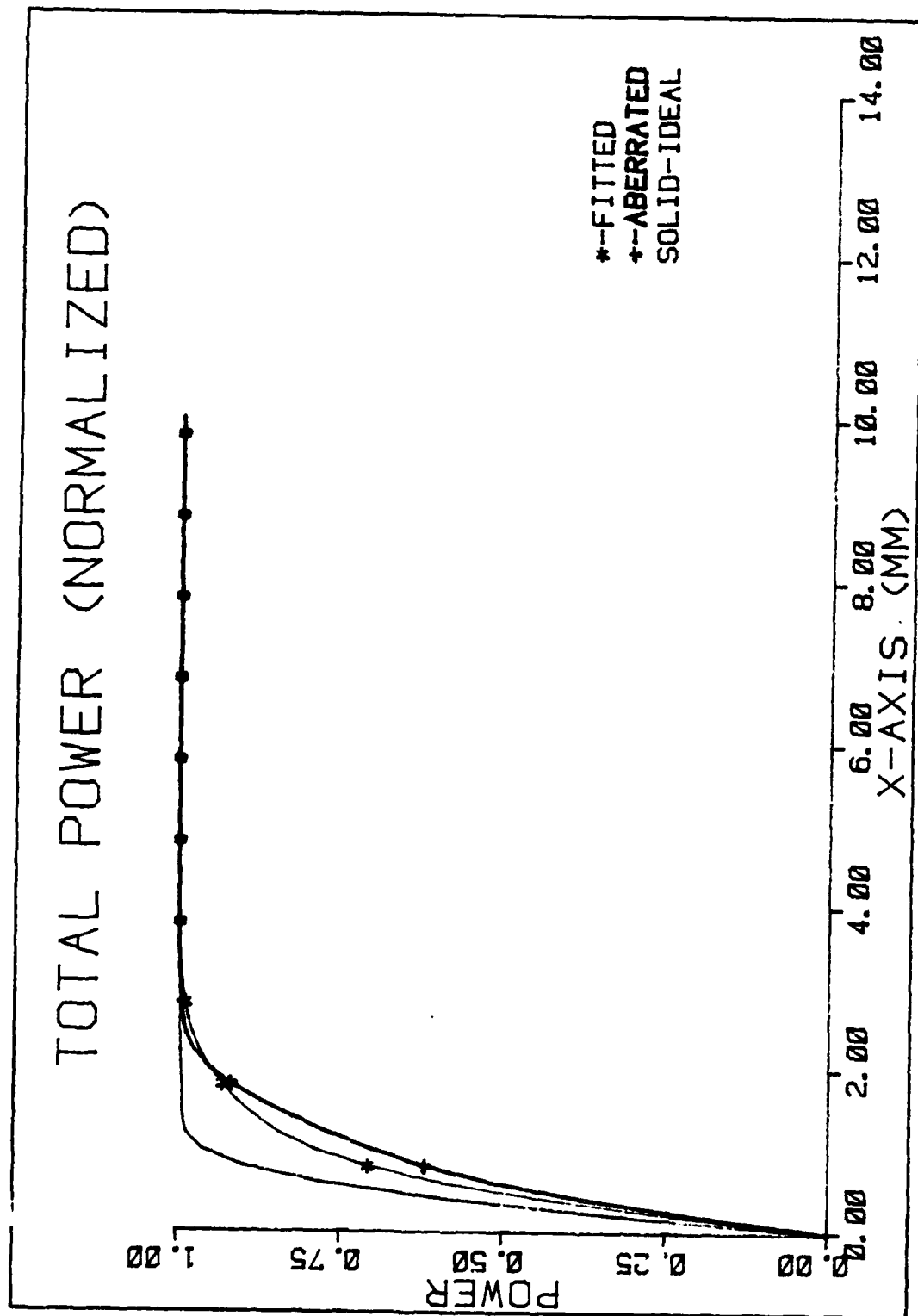


Figure 37. Total Power plot. $R=0.46, \sigma^2=1.55$.

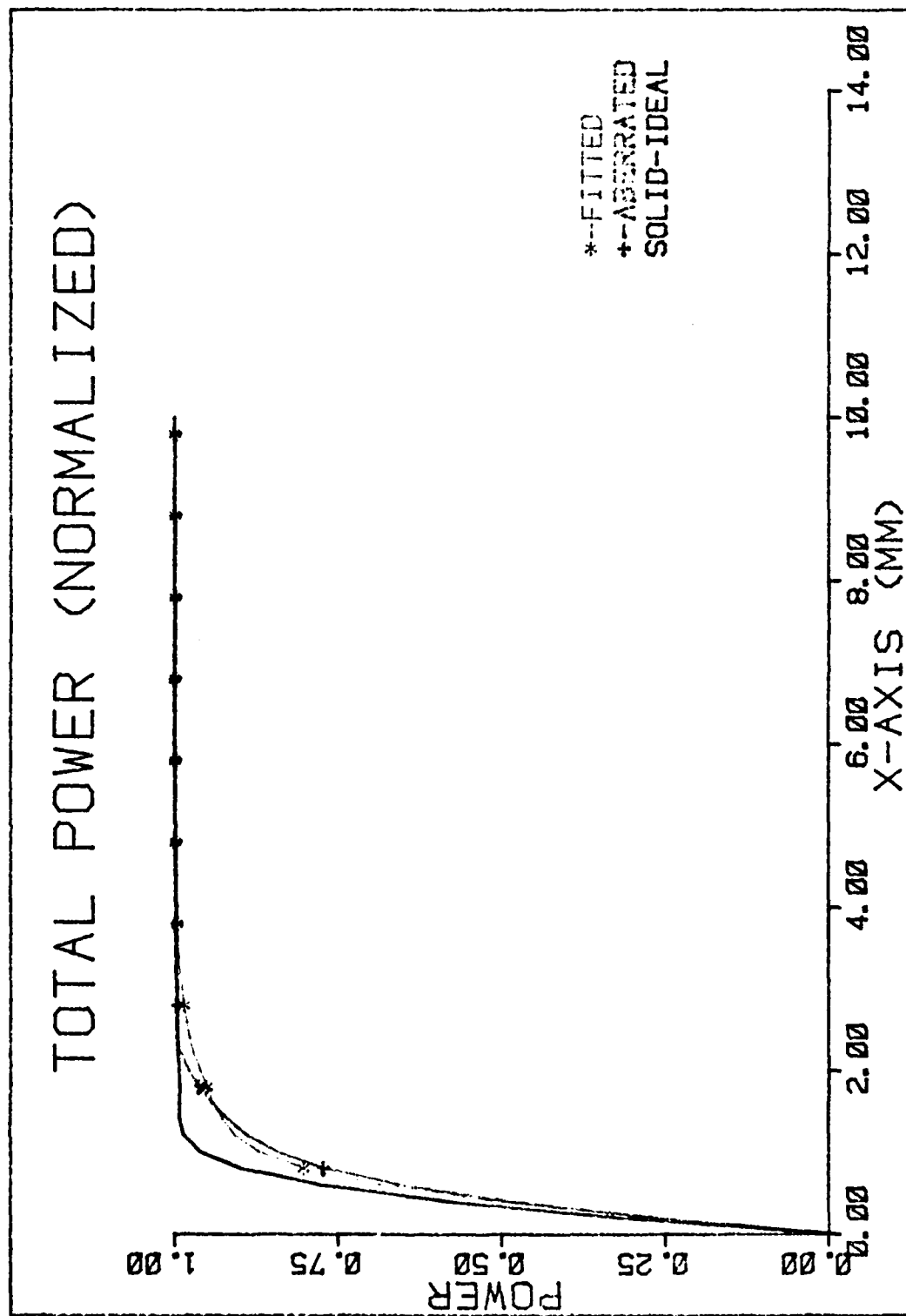


Figure 38. Total Power plot. $F=0.769, \sigma^2=1.49$.

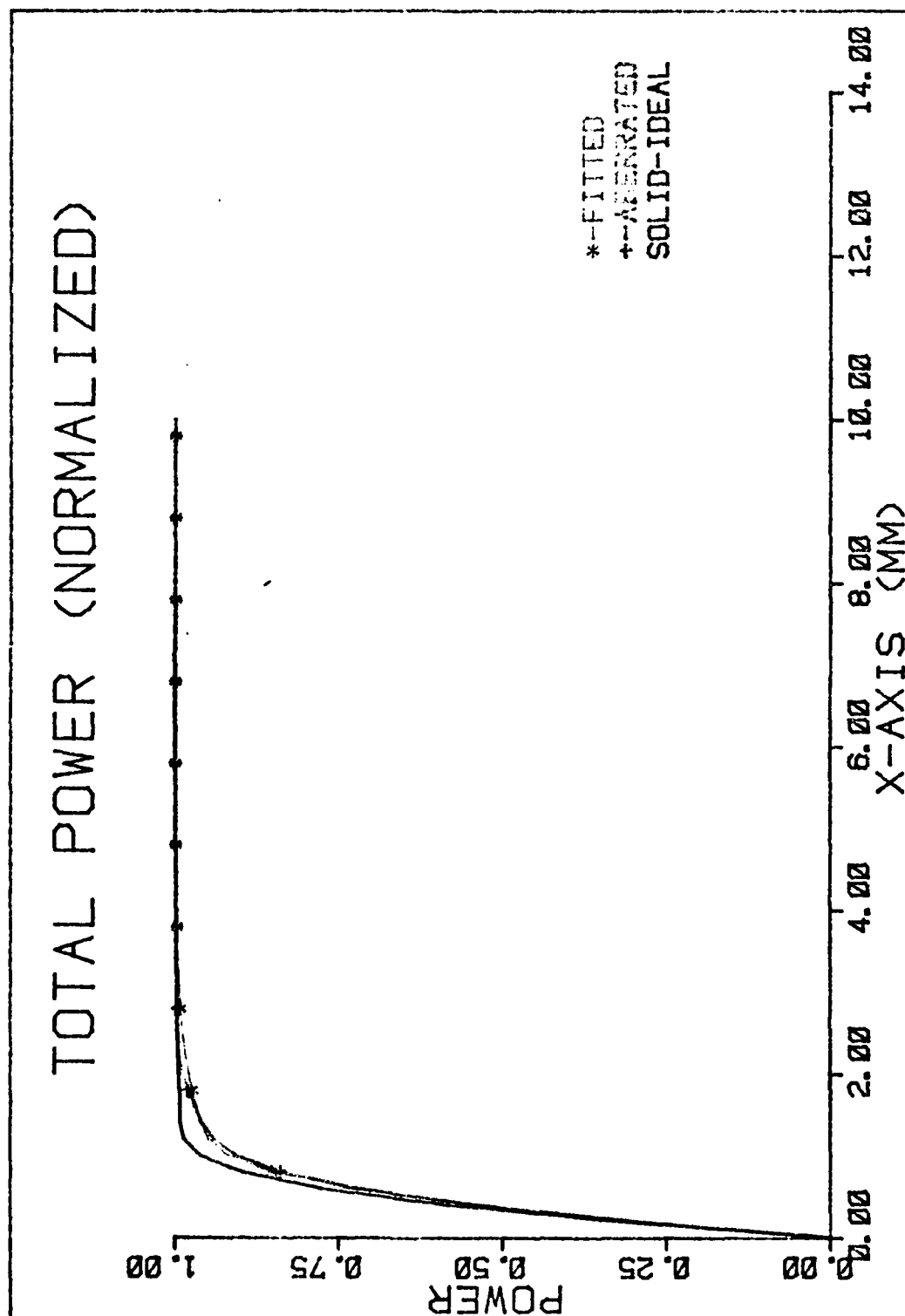


Figure 29. Total Power plot. $R=0.002$, $\sigma^2=1.47$.

this irradiance distribution. Therefore, the attenuating factor and the extent of the aberrated beam can be derived from differentiating the total power P-R curve. No special method or apparatus is required, since these two quantities can be measured from the P-R curve generated by the 'power in the bucket' method. The next section describes a proposed procedure to do this measurement.

Proposed Procedures

The process of experimentally determining F and σ^2 is divided into five different steps. These are set-up, beam alignment, P-R curve generation, derivation of the irradiance profile from the P-R curve, and finally, measurement of the attenuating factor and lateral extent.

Apparatus Set-up. The experimental set-up of figure 3 will be used. A lens system of focal length, f , will be inserted between the laser and an adjustable aperture with a power detector immediately behind it. To achieve far-field conditions at the input of the power detector, it is vital that the variable aperture is placed exactly at the focus of the lens.

Beam Alignment. The position of the center of the beam, at the plane of the variable aperture, is required in order to optimize power measurement. Exact beam center must be known since the central point of the variable aperture is

aligned with this beam center. A method of determining laser beam center was outlined in Chapter II. Briefly, this required the use of an opaque ribbon of finite width 2a. By scanning this ribbon across the beam, the minimum output power is realized when the ribbon reaches the center of the beam. For a more detailed discussion of this technique see Ref. 23. The center of the adjustable aperture is then aligned with this beam center.

P-R Curve Generation. In the conventional 'power in the bucket' method, the variable aperture is opened to its maximum diameter, to measure the total output power of the laser. Power measurements are then taken for various aperture diameter. This value is normalized with respect to the laser's total output power and plotted with the normalized power plot of the diffraction-limited case.

However, the degree of phase aberration, present in the laser system, is not known at the outset and, hence, the total power measured the conventional way may be inaccurate. The amount of energy falling on the surface of the detector is limited by the maximum size of the variable aperture, and also, the entrance window of the detector itself. If the extent of the aberrated beam is beyond the physical limit of the variable aperture/detector system, the energy contained in the outskirts is then lost. Thus, the measured power does not reflect the true total power

of the laser. A convenient solution to the problem is a numerical fit of the measured absolute power values (for different aperture diameter) with some mathematical expression. From this expression, the total power of the laser can be mathematically approximated simply by setting the independent variable of the expression equal to infinity. The measured values of absolute power as a function of aperture diameter can now be normalized with respect to the calculated total laser power.

Irradiance Distribution. The nondiffraction-limited P-R curve is the result of integrating the irradiance distribution of a test laser. Thus, by taking the derivative of the total power, irradiance can be determined. Since the form of the irradiance distribution for the diffraction-limited case is known from theory, only the nondiffraction-limited power must be differentiated to obtain the aberrated irradiance distribution.

Determine F and σ^2 . With both the diffraction-limited and aberrated irradiance known, the attenuation factor F and the nondiffraction-limited beam's lateral extent σ^2 can now be found by the least squares method of curve fitting discussed earlier in Chapter IV. The program listing of this method is listed in Appendix B.

Bibliography

1. Arnaud, J.A., W.M. Hubbard, et al. "Techniques for Fast Measurement of Gaussian Laser Beam Parameters," Applied Optics, 10: 2775-2776 (December 1981).
2. Avizonis, P.V. and D. Holmes. "Determination of Beam Quality for Gaussian Beams from the Far-Field Diffraction Pattern," Laser Digest, 8-15. (AD 900 204 L)
3. Born, M. and E. Wolf. Principles of Optics, (fifth edition), New York: Pergamon Press, 1975.
4. Buck, A.L. "The Radiation Pattern of a Truncated Gaussian Aperture Distribution," Proceedings IEEE, 55: 448-450 (March 1967).
5. Gaskill, J.D. Linear Systems, Fourier Transforms, and Optics, New York: Wiley, 1978.
6. Goodman, J.W. Introduction to Fourier Optics, New York: McGraw-Hill Book Company, 1968.
7. Hanley, S.T. Beam Quality Measurement on the NTSL, Interim Report, Naval Research Lab, Washington, D.C., (August 1974). (AD 922 179)
8. Hogge, C.B., R.R. Butts, and M. Burlakoff. "Characteristics of Phase Aberrated Non-diffraction Limited Laser Beams," Applied Optics, 13: 1065-1070 (May 1974).
9. Holmes, D.A., H.V. Winsor, D.A. Maier, and J.R. Baumgardner. Diffraction of a Square Beam by a Circular Aperture," Laser Digest, 16-18. (AD 900 204 L)
10. Holmes, D.A., J.E. Karka, and P.V. Avizonis. "Parametric Study of Apertured Focused Gaussian Beams," Applied Optics, 11: 565-574 (March 1972).
11. Holmes, D.A., J.R. Baumgardner and M.L. Bernabe. "A Simple Approximate Formula for Estimating on-axis far-field Irradiance in the Presence of near-field Phase Aberrations," Laser Digest, 8-13. (AD 919 135 L)

12. Huguley, C. "Characterization of Laser Beam Profiles by a Scanning Wire," Laser Digest, 103-108. (AD 922 964 L)
13. Humphreys, R.P. and W.E. Thompson III. "Diffraction Effects of a Circular Aperture upon Rectangular and Square Annular Beams," Laser Digest, 14-23. (AD 922 964 L)
14. James, M.L. Applied Numerical Methods for Digital Computation with FORTRAN and CSMP, New York: Harpet & Row Pub., 1977.
15. Loomis, J.S. "On-axis Intensity of Phase Aberrated Gaussian Beams," Laser Digest, 33-40. (AD 919 135 L)
16. Munch, J., K.T. Yano, E.C. Rea, and D. Miller. Chemical Laser Evaluation, Final Report, TRW Defense and Space Systems Group (October 1978). (AD B031 3332).
17. Schell, R.G. and G. Tyros. "Irradiance from an Aperture with a Truncated-Gaussian Field Distribution," Journal of the Optical Society of America, 61: 31-35, (January 1971).
18. Skinner, D.R. and R.E. Whitcher. "Measurement of the Radius of a High Power Laser from Near the Focus of a Lens," Journal of Physics, E5: 237-238, 1972.
19. Sollid, E., C.R. Phipps, S.J. Thomas, and E.J. Mclellan. "Lensless Methods of Measuring Gaussian Laser Beam Divergence," Applied Optics, 17: 3527-3528 (November 1978).
20. Suzaki, Y. and A. Tachibana. "Measurements of the μ m Sized Radius of Gaussian Laser Beam using the Scanning Knife-Edge," Applied Optics, 12: 2809-2810 (December 1975).
21. Suzaki, Y. and A. Tachibana. "Measurement of the Gaussian Laser Beam Divergence," Applied Optics, 16: 1481-1482, (June 1971).
22. Vogelsang, K.R., et al. System Optical Quality Study Phase I, Final Report, Hughes Aircraft Company, Culver City, CA, (June 1974). (AD 922 535 L)
23. Yoshida, A. and T. Asakura. "A Simple Technique for Quickly Measuring the Spot Size of Gaussian Laser Beams," Optics and Laser Technology, 273-274 (December 1976).

Appendix A

Numerical Model of Non-Diffraction Limited Beam

```

100=    PROGRAM DIFGEN(INPUT,OUTPUT,TAPE5=INPUT,TAPE6=OUTPUT,TAPE9)
110=    DOUBLE PRECISION DSEED
120=    DIMENSION PX(105,105),PXA(105,105)
130=    DIMENSION PLOG(105,105),PLOGA(105,105),AX1(105),AY1(105)
140=    DIMENSION DFF(105)
150=    DIMENSION RNDM(50)
160=    COMPLEX ARG,EA,EB,EA1,EB1
170=    COMPLEX CZ
180=    COMPLEX FX,SUM,FXA,SUMA,FXI,FXMAX,FXAI,FXAMAX
190=    COMPLEX ABERR,AREA1,AREA,AREA1A,AREAA,VOL,VOLA
200=    COMPLEX V,VA,CX,CXA,CPX,CPXA,FXP,SPX,PMA,PMI,A1,A,VPO,VP,C
210=    COMPLEX EFCS,EAFCs
220=    COMPLEX ANUM,ANUM3
230=C
240=C    THIS PROGRAM DETERMINES THE IRRADIANCE DISTRIBUTION OF
250=C    DIFFRACTION-LIMITED & ABERRATED SYSTEMS. BOTH THE FRESNEL
260=C    REGION AND THE FRAUNHOFER DIFFRACTION PATTERN CAN BE DE-
270=C    TERMINED THROUGH THE SOLUTION OF THE FRESNEL-HUYGEN IN-
280=C    TEGRAL. THE SOLUTION IS DONE NUMERICALLY USING THE TRAPE-
290=C    ZOID RULE OF INTEGRATION. THE POINTS GENERATED IN THE
300=C    PRINTOUTS AND PLOTS REPRESENT THE NORMALIZED INTENSITY
310=C    DISTRIBUTION.
320=C    IN THIS THESIS, IT IS ASSUMED THAT THE SYSTEM IS FOCUSED
330=C    BY A PERFECT THIN LENS WITH FOCAL LENGTH F.
340=C
350=C    *****
360=C
370=    WRITE(6,500)
380=500    FORMAT(* *,20X,*NUMERICAL SOLUTION TO  FRESNEL INTEGRAL*)
390=    WRITE(6,501)
400=501    FORMAT(* *,15X,*THIS PROGRAM CALCULATES THE FRESNEL *)
410=    WRITE(6,502)
420=502    FORMAT(* *,15X,* FAR-FIELD INTENSITY DISTRIBUTION FOR A*)
430=    WRITE(6,503)
440=503    FORMAT(* *,15X,*DIFFRACTION-LIMITED AND ABERRATED SYSTEM*)
450=    WRITE(6,505)
460=505    FORMAT(* *,15X,*+++++MASTER'S THESIS PROJECT+++++)
470=    WRITE(6,5105)
480=5105    FORMAT(* *,20X,*+++++SYSTEM IS FOCUSED+++++)
490=C
500=C    *****
510=C
520=C    INPUT PARAMETERS
530=C
540=C    *****INITIALIZATION OF INTEGRATION VARIABLES*****
550=CCCCCCCCCCCCCCCC INTEGRATION INCREMENTS CCCCCCCCCCCCCCCCCC
560=C    HUB=INCREMENT OF INTEGRATION

```

```

570=C          NBCD=INTEGER EQUIVALENT OF BCD
580=          BCD=20.0
590=          NBCD=20
600=CCCCCCCCCCCC OBS PLANE INCREMENT CCCCCCCCCCCCCCCCCC
610=C          XX1=INCREMENT
620=C          NN=INTEGER EQUIVALENT OF C
630=C          NNN=NN+1
640=          XX1=50.0
650=          NN=50
660=          NNN=NN+1
670=          WRITE(6,570)
680=570       FORMAT(* *,20X,*INPUT THE WAVELENGTH IN 0.XXXXXXXX MM *)
690=          READ(5,400)BLAMDA
700=400       FORMAT(1F10.8)
710=          WRITE(6,1750)
720=1750     FORMAT(* *,20X,*BEAM WAIST IN MM *)
730=          READ(5,401)W0
740=401       FORMAT(1F10.4)
750=750       WRITE(6,571)
760=571       FORMAT(* *,20X,*INPUT Z-DISTANCE FROM SOURCE, IN METERS*)
770=          READ(5,401)Z1
780=          WRITE(6,5171)
790=5171     FORMAT(* *,20X,*INPUT FOCAL LENGTH, METERS*)
800=          READ(5,401)F1
810=          F=F1*1000.0
820=          Z=Z1*1000.0
830=          WRITE(6,572)
840=572       FORMAT(* *,20X,*APERTURE TYPE:,0-RECT,1-CIRC*)
850=          READ(5,402)ITYPE
860=402       FORMAT(I2)
870=C
880=C          *****
890=C
900=C          WHEN THE APERTURE IS RECTANGULAR, THE FOLLOWING IS
910=C          ENTERED:
920=C          XRECT-WIDTH OF APERTURE IN THE X-DIRECTION
930=C          YRECT-WIDTH OF APERTURE IN THE Y-DIRECTION
940=C
950=C          THE GEOMETRIC CENTER OF THE APERTURE IS ALONG THE Z-
960=C          AXIS, WITH X AND Y EQUAL TO ZERO. THUS, THE EXTENT OF
970=C          THE APERTURE IS -XRECT/2 TO +XRECT/2 FOR X.
980=C
990=C          *****
1000=C
1010=C          WHEN THE APERTURE IS CIRCULAR, THE FOLLOWING
1020=C          ENTERED:
1030=C          R-RADIUS OF THE APERTURE. THE POINT WHERE THIS
1040=C          IS CALCULATED IS AT X,Y = 0.
1050=C
1060=C          *****
1070=C

```

```

1080=C      DETERMINE GEOMETRY OF THE APERTURE
1090=C
1100=      IF(ITYPE-1)2700,700,700
1110=2700   CONTINUE
1120=C      IF ITYPE=0, THEN RECTANGULAR
1130=      WRITE(6,580)
1140=580    FORMAT(* *,20X,*THE APERTURE IS RECT. INPUT X,Y DIM.:*)
1150=      WRITE(6,581)
1160=581    FORMAT(* *,30X,*ENTER WIDTH IN X  MM : *)
1170=      READ(5,401)XRECT
1180=      WRITE(6,582)
1190=582    FORMAT(* *,30X,*ENTER WIDTH IN Y  MM : *)
1200=      READ(5,401)YRECT
1210=C      DETERMINE XOMIN AND YOMIN OF APERTURE
1220=      XOMIN=-XRECT/2.0
1230=      YOMIN=-YRECT/2.0
1240=C      DETERMINE XOMAX AND YOMAX OF APERTURE
1250=      XOMAX=XRECT/2.0
1260=      YOMAX=YRECT/2.0
1270=      GOTO 701
1280=700    WRITE(6,590)
1290=590    FORMAT(* *,20X,*APERTURE RADIUS. MM *)
1300=      READ(5,401)R
1310=      XOMIN=-R
1320=      YOMIN=-R
1330=      XOMAX=R
1340=      YOMAX=R
1350=701    CONTINUE
1360=C
1370=C      DETERMINE THE EXTENT OF THE OBSERVATION PLANE
1380=C      AT Z. THE GEOMETRICAL CENTER OF THIS PLANE IS
1390=C      LOCATED AT X1,Y1 = 0.
1400=C
1410=      WRITE(6,600)
1420=600    FORMAT(* *,20X,*ENTER THE DIA OF OBS. PLANE.*)
1430=      WRITE(6,601)
1440=601    FORMAT(* *,30X,*ENTER THE X MINIMUM IN MM : *)
1450=      READ(5,401)X1MIN
1460=      WRITE(6,1111)
1470=1111   FORMAT(* *,30X,*ENTER THE X MAXIMUM VALUE IN MM. *)
1480=      READ(5,401)X1MAX
1490=      WRITE(6,602)
1500=602    FORMAT(* *,30X,*ENTER THE Y MINIMUM IN MM. *)
1510=      READ(5,401)Y1MIN
1520=      WRITE(6,1112)
1530=1112   FORMAT(* *,30X,*ENTER THE Y MAXIMUM VALUE IN MM *)
1540=      READ(5,401)Y1MAX
1550=C
1560=C      PRINTOUT DATA INPUTS AND CALCULATIONS
1570=C
1580=      WRITE(6,603)

```

```

1590=603   FORMAT(* *,10X,*THE FOLLOWING ARE INPUT PARAMETERS*)
1600=      WRITE(6,604)XUMIN,YUMIN
1610=604   FORMAT(* *,20X,*APERTURE=*,*XMIN*,F8.2,*YMIN*,F8.2)
1620=      WRITE(6,605)XUMAX,YUMAX
1630=605   FORMAT(* *,30X,*XMAX*,F8.2,*YMAX*,F8.2)
1640=      WRITE(6,606)XIMIN,YIMIN
1650=606   FORMAT(* *,20X,*OBS. PLANE=*,*XMIN*,F8.2,*YMIN*,F8.2)
1660=      WRITE(6,605)XIMAX,YIMAX
1670=      WRITE(6,607)
1680=607   FORMAT(* *,30X,***** )
1690=      WRITE(6,608)
1700=608   FORMAT(* *,30X,*APPROXIMATIONS TO FRESNEL INTEGRAL*)
1710=      AK=(2*3.14159)/BLAMDA
1720=      AFR=XOMAX**2+YOMAX**2
1730=      ZFR=AK*AFR/2
1740=      WRITE(6,610)ZFR
1750=610   FORMAT(* *,20X,*FAR-FIELD:Z>>*,F10.1,*MM *)
1760=      WRITE(6,611)Z/1000.0
1770=611   FORMAT(* *,20X,*YOUR RANGE=*,F10.1,*METERS *)
1780=      WRITE(6,607)
1790=      WRITE(6,612)
1800=612   FORMAT(* *,20X,*NEW VALUE OF Z: 0-NO.1-YES)
1810=      READ(5,402)INEWZ
1820=      IF(INEWZ-1)2750,750,750
1830=2750   CONTINUE
1840=C
1850=C      ASSUME THAT SPOT SIZE AT APERTURE EQUALS BEAM WAIST
1860=C
1870=C      W=W0
1880=C      NUMERICAL INTEGRATION OF THE FUNCTION F(X,Y)
1890=C      WHERE F(X,Y) IS EXPRESSED AS
1900=C
1910=C       $EXP(-J*PI*(XX1+YY1)/BLAMDA*Z)$ 
1920=C
1930=C      THE INTEGRATION PROCESS WILL BE AS FOLLOWS:
1940=C      1. SET Y1 CONSTANT AT SOME INITIAL VALUE
1950=C      2.VARY X1
1960=C      3.SET Y0 AT SOME INITIAL VALUE
1970=C      4.INTEGRATE OVER X0
1980=C      5.INCREMENT Y0 AND REPEAT 4
1990=C      6.ONCE 10 STEPS ARE COMPLETE, NEXT X1
2000=C      7.ONCE X1 IS COMPLETE, NEXT Y1 UNTIL FINISHED
2010=C
2020=C      INITIALIZE PARAMETERS REQUIRED FOR INTEGRATION
2030=C      X1=XIMIN
2040=C      Y1=0.0
2050=C      STEPX0=(XOMAX-XIMIN)/BC0
2060=C      STEPY1=(YIMAX-YIMIN)/XX1
2070=C      STEPY0=(YOMAX-YOMIN)/BC1
2080=C      STEPX1=(XOMAX-XOMIN)/XX1
2090=C

```



```

2100=C      STEP 11 IN STEPY1 INCREMENTS
2110=      Y1=1
2120=      DO 110 IX1=1,NNN
2130=      V=CMPLX(0.0,0.0)
2140=      VA=CMPLX(0.0,0.0)
2150=      XO=XOMIN
2160=      YO=YOMIN+STEPYO
2170=      DO 120 IYD=1,NBCD
2180=      IF(ITYPE .EQ. 1) GOTO 666
2190=      GOTO 667
2200=666    XOMIN=-SQRT(R**2-YO**2)
2210=      XOMAX=-XOMIN
2220=      XO=XOMIN
2230=      STEPXO=2*XOMAX/BCD
2240=      XRECT=2*R
2250=667    CONTINUE
2260=      XO=XO+STEPXO
2270=      SUM=CMPLX(0.0,0.0)
2280=      SUMA=CMPLX(0.0,0.0)
2290=      DO 130 IXD=2,NBCD
2300=C
2310=C      INTEGRATE OVER XO USING THE TRAPEZOID NUMERICAL
2320=C      INTEGRATION RULE.
2330=C
2340=      CALL FIELD(UOXY,XO,YO,W,Z,ITYPE)
2350=      CALL XYZ(ARG,UOXY,XO,YO,X1,Y1,AK,Z,BLAMBDA,F)
2360=      FX=ARG
2370=      SUM=SUM+FX
2380=      CALL ABERRAC(ABERR,DSEED,XRECT,XO,YO,W,Z)
2390=      FXA=FX*ABERR
2400=      SUMA=SUMA+FXA
2410=130    XO=XO+STEPXO
2420=C
2430=C      NOW DETERMINE THE AREA UNDER THE CURVE IN X AT
2440=C      SOME VALUE OF Y1.
2450=C
2460=C      DETERMINE F(X) INITIAL AND F(X) N+1
2470=C
2480=      CALL XYZ(ARG,UOXY,XOMIN,YO,X1,Y1,AK,Z,BLAMBDA,F)
2490=      FXI=ARG
2500=      CALL XYZ(ARG,UOXY,XOMAX,YO,X1,Y1,AK,Z,BLAMBDA,F)
2510=      FXMAX=ARG
2520=      CALL ABERRAC(ABERR,DSEED,XRECT,XOMIN,YO,W,Z)
2530=      FXAI=FXI*ABERR
2540=      CALL ABERRAC(ABERR,DSEED,XRECT,XOMAX,YO,W,Z)
2550=      FXMAX=FXMAX*ABERR
2560=C
2570=C      DIFFRACTION LIMITED CASE
2580=C
2590=      AREAI=FXI+SUM+FXMAX
2600=      AREA=STEPXO*AREAI/Z

```

```

2610=0
2620=0      APPROXIMATE CASE
2630=0
2640=0      AREA1A=F(X1)+2*F(XM1)+F(XM2)
2650=0      AREA=STEPY0*AREA1A/2
2660=0
2670=0      DETERMINE VOLUME IN STRIP BOUNDED BY AREA OF
2680=0      F(X) AND Y INCREMENT STEPY0
2690=0
2700=0      VOL=STEPY0*AREA
2710=0      VOLA=STEPY0*AREA1A
2720=0      V=V+VOL
2730=0      VA=VA+VOLA
2740=0
2750=0      DETERMINE AREA OF F(X) AT NEXT Y0
2760=0
2770=0      X0=X0MIN
2780=120     Y0=Y0+STEPY0
2790=0
2800=0      THE DOUBLE INTEGRAL AT SOME UVALUE OF X1 AND Y1
2810=0      INTEGRATED OVER ED. THE VALUE
2820=0      OF IRRADIANCE AT X1 AND Y1 WILL NOW BE DETERMINED.
2830=0
2840=0      WHERE IRRADIANCE=CONJUGATE OF VOL X VOLUME
2850=0      CX=CONJG(V)
2860=0      CXA=CONJG(VA)
2870=0      CPX=CX*X
2880=0      CPXA=CXA*VA
2890=0      ALZ=(BLAMDA*Z)**2
2900=0      FX(IY1,IX1)=REAL(CPX)/ALZ
2910=0      FXA(IY1,IX1)=REAL(CPXA)/ALZ
2920=0
2930=0      NEXT VALUE OF X1
2940=0
2950=110     X1=X1+STEPX1
2960=0
2970=0      NOW DETERMINE THE PEAK VALUE OF IRRADIANCE ON
2980=0      AXIS. THIS VALUE WILL BE USED TO NORMALIZE THE
2990=0      IRRADIANCE DISTRIBUTION.
3000=0
3010=0      X1=0.0
3020=0      Y0=Y0MIN+STEPY0
3030=0      VP=CMPLX(0.0,0.0)
3040=0      Y1=0.0
3050=0      DO 140 IY1=1,NBCD
3060=0      IF(IY1.EQ. 1) GO TO 666
3070=0      GO TO 669
3080=666     X0MIN=-SQRT((X1+Z)-(Y0**2))
3090=0      X0MAX=X0MIN
3100=0      STEPX0=2*X0MAX/666
3110=667     CONTINUE

```

AD-A127 412

CHARACTERIZATION OF LASER BEAM QUALITY(U) AIR FORCE
INST OF TECH WRIGHT-PATTESSON AFB OH SCHOOL OF
ENGINEERING A T GUMAHAD DEC 82 AFIT/GEO/PH/82D-4

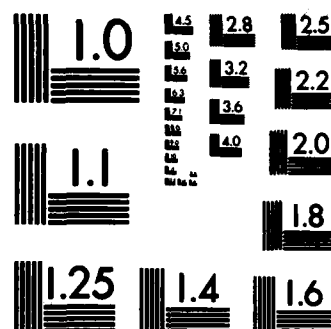
2/2

UNCLASSIFIED

F/G 20/5

NL





MICROCOPY RESOLUTION TEST CHART
NATIONAL BUREAU OF STANDARDS-1963-A

```

3120=      XU=XUMIN
3130=      SPX=CMPLX(0.0,0.0)
3140=      XO=XO+STEPXO
3150=      DO 150 IPX=2,NBCO
3160=      CALL F(ELD(UOXY,XO,YO,W,F,ITYPE)
3170=      CALL XYZ(ARG,UOXY,XO,YO,0.0,0.0,AK,F,BLMDA,F)
3180=      FXP=ARG
3190=      SPX=SPX+FXP
3200=150   XO=XO+STEPXO
3210=      CALL XYZ(ARG,UOXY,XOMIN,YO,0.0,0.0,AK,F,BLMDA,F)
3220=      PMA=ARG
3230=      CALL XYZ(ARG,UOXY,XOMAX,YO,0.0,0.0,AK,F,BLMDA,F)
3240=      PMI=ARG
3250=      A1=PMA+2*SPX+PMI
3260=      A=STEPXO*A1/2
3270=      UPD=STEPYO*A
3280=      VP=VP+VPO
3290=140   YO=YO+STEPYO
3300=      C=CONJG(VP)
3310=      CZ=C*VP
3320=      PEAK=REAL(CZ)/ALZ
3330=C
3340=C      NORMALIZE IRRADIANCE DISTRIBUTION WITH RESPECT TO
3350=C      PEAK INTENSITY OF DIFFRACTION-LIMITED CASE, EVAL-
3360=C      UATED AT X1=0 AND Y1=0.
3370=C
3380=      JY=1
3390=      DO 170 JX=1,NNN
3400=      PLOG(JY,JX)=PX(JY,JX)/PEAK
3410=      PLOGA(JY,JX)=PXA(JY,JX)/PEAK
3420=170   CONTINUE
3430=C
3440=C      REPLACE X1 AND Y1 INTO ARRAYS AX1 AND AY1
3450=C
3460=      AX1(1)=X1MIN
3470=      AY1(1)=0.0
3480=      DO 181 K=2,NNN
3490=      AX1(K)=AX1(K-1)+STEPX1
3500=181   CONTINUE
3510=C
3520=C      PRINT EVERY NTH DATA POINT IN ARRAY
3530=C
3540=      I=1
3550=      WRITE(6,531)AY1(I)
3560=531   FORMAT(*0*,20X,*Y (5:*,F7.2)
3570=      DO 491 N=1,NNN
3580=      DFF(N)=PLOG(I,N)-PLOGA(I,N)
3590=491   WRITE(6,5)AX1(N),PLOG(I,N),PLOGA(I,N),DFF(N)
3600=5     FORMAT(15X,F7.2,3F14.6)
3610=      WRITE(6,933)
3620=933   FORMAT(* *,20X,*PROGRAM COMPLETE*)

```

```

3630= STOP
3640= END
3650=C
3660=C *****
3670=C SUBROUTINE TO EVALUATE F(X) OF INTEGRAL
3680=C
3690= SUBROUTINE XYZ(ARG,UOXY,X0,Y0,X1,Y1,AK,Z,BLAMD,F)
3700= COMPLEX ARG
3710= COMPLEX EA,EB
3720= COMPLEX EA1,EB1
3730= COMPLEX EFCS,EAFC
3740=C
3750=C EXP(J AK/2*Z(X**2+Y**2)
3760=C
3770= ADDA=X0**2
3780= ADDB=Y0**2
3790= ADD=ADDA+ADDB
3800= PRODA=AK*ADD
3810= PROD=PRODA/(2*Z)
3820= EA1=CMPLX(0.0,PROD)
3830= EA=CEXP(EA1)
3840=C
3850=C LENS PHASE TRANSFORMATION FUNCTION
3860=C
3870= PRFCS=PRODA/(2*F)
3880= EFCS=CMPLX(0.0,-PRFCS)
3890= EAFC=CEXP(EFCS)
3900=C
3910=C EXP(-J*2PI/BLAMD*Z(X0X1+Y0Y1)
3920=C
3930= ADD1=(X0*X1)+(Y0*Y1)
3940= PRAD=-2*3.14159*ADD1
3950= PROD1=PRAD/(BLAMD*Z)
3960= EB1=CMPLX(0.0,PROD1)
3970= EB=CEXP(EB1)
3980= ARG=UOXY*EA*EB*EAFC
3990= RETURN
4000= END
4010=C
4020=C *****
4030=C SUBROUTINE TO GENERATE ABERRATION
4040=C
4050= SUBROUTINE ABERRAC(ABERR,DSEED,XRECT,X0,Y0,U,Z)
4060= DOUBLE PRECISION DSEED
4070= DIMENSION RNDM(50)
4080= COMPLEX ABERR, ANUM,ANUM3
4090= DSEED=123457.D0
4100= NR=20
4110= ABSUM=0.
4120= DO 3313 KMN=1,20
4130= ANUMA=(FLUAT(KMN)*2.*3.14159*X0)/XRECT

```

```

4140=      ANUM1=COS(ANUM4)
4150=      CALL GGUST(DSEED,NR,RNDM)
4160=      ANUM2=RNDM(KAN)/5. * ANUM1
4170=      ABSUM=ABSUM + ANUM2
4180=3313  CONTINUE
4190=      ANUM3=CMPLX(0.0,ABSUM)
4200=      ANUM=CEXP(ANUM3)
4210=      ABERR=ANUM
4220=      RETURN
4230=      END
4240=C
4250=C      *****
4260=C      SUBROUTINE TO GENERATE FIELD
4270=C
4280=      SUBROUTINE FIELD(UOXY,XO,YO,W,Z,ITYPE)
4290=      IF(ITYPE.EQ.1)GOTO 800
4300=      RECT=1.0
4310=      CALL FINC(CINC,XO,YO,W)
4320=      UOXY=RECT*CINC
4330=      GOTO 837
4340=800   CIRC=1.0
4350=      CALL FINC(CINC,XO,YO,W)
4360=      UOXY=CIRC*CINC
4370=837   CONTINUE
4380=      RETURN
4390=      END
4400=C
4410=C      *****
4420=C      SUBROUTINE FOR A GAUSSIAN INCIDENT FIELD
4430=C
4440=      SUBROUTINE FINC(CINC,XO,YO,W)
4450=      TOP=XO**2+YO**2
4460=      TOP1=TOP/(W**2)
4470=      CINC=EXP(-TOP1)
4480=      RETURN
4490=      END
4500=*EOR

```

..

APERTURE-XMIN -.50YMIN -.50
 XMAX .50YMAX .50
 OBS. PLANE-XMIN: -6.00YMIN: -6.00
 XMAX 6.00YMAX 6.00

 APPROXIMATIONS TO FRESNEL INTEGRAL
 FAR-FIELD:Z>> 248.2MM
 YOUR RANGE= .2METERS

 NEW VALUE OF Z: 0-NO,1-YES
 Y IS: 0.00

-6.00	.001556	.001795	-.000239
-5.76	.003232	.001119	.002113
-5.52	.003279	.001285	.001794
-5.28	.001119	.002626	-.001507
-5.04	.000015	.007205	-.007190
-4.80	.002000	.015715	-.013715
-4.56	.005568	.024656	-.019088
-4.32	.006568	.028166	-.021597
-4.08	.003397	.023780	-.020384
-3.84	.000107	.015782	-.015675
-3.60	.002399	.011172	-.008773
-3.36	.009954	.011823	-.001869
-3.12	.014852	.012416	.002436
-2.88	.010396	.008369	.002027
-2.64	.001540	.005237	-.003697
-2.40	.002715	.015961	-.013246
-2.16	.021016	.044378	-.023361
-1.92	.042245	.072280	-.030035
-1.68	.040975	.070534	-.029559
-1.44	.013482	.032649	-.019167
-1.20	.002919	.000398	.002521
-.96	.002543	.047804	.034739
-.72	.297032	.223448	.073585
-.48	.606380	.494640	.111740
-.24	.886628	.746648	.139980
.00	1.000000	.849569	.150431
.24	.886628	.746648	.139980
.48	.606380	.494640	.111740
.72	.297032	.223448	.073585
.96	.002543	.047804	.034739
1.20	.002919	.000398	.002521
1.44	.013482	.032649	-.019167
1.68	.040975	.070534	-.029559
1.92	.042245	.072280	-.030035
2.16	.021016	.044378	-.023361
2.40	.002715	.015961	-.013246
2.64	.001540	.005237	-.003697
2.88	.010396	.008369	.002027
3.12	.014852	.012416	.002436
3.36	.009954	.011823	-.001869
3.60	.002399	.011172	-.008773
3.84	.000107	.015782	-.015675
4.08	.003397	.023780	-.020384
4.32	.006568	.028166	-.021597
4.56	.005568	.024656	-.019088
4.80	.002000	.015715	-.013715
5.04	.000015	.007205	-.007190
5.28	.001119	.002626	-.001507
5.52	.003279	.001285	.001794

Appendix B

Least Squares Method of Curve Fitting

```

100=    PROGRAM CRVFIT(INPUT,OUTPUT,TAPE5=INPUT,TAPE6=OUTPUT,TAPE8,TAPE9)
110=    DIMENSION A(55),B(55),C(55),X(55),YJ(55)
120=C    PROGRAM FOR LEAST SQUARES FIT FOR SIGMA AND F
130=C    INITIALIZE VARIABLES
140=    CALL PLOTS
150=    CALL POFF
160=    N=51
170=    NNN=51
180=    EPS=0.001
190=    PI=3.14159
200=    SIGMA=1.
210=    STEPSIG=1.
220=C    READ IN PLOG, PLOGA, AND X. WHERE:
230=C        X - VALUES CORRESPONDING TO OBSERVATION PLANE
240=C        PLOG -IDEAL CASE IRRADIANCE  A
250=C        PLOGA -ABERRATED CASE  B
260=    DO 10 I=1,N
270=    READ(8,*)X(I),A(I),B(I),C(I)
280=10    CONTINUE
290=C
300=C    CALCULATE FIRST VALUE OF FUNCTION G(SIGMA)
310=C
320=    CALL GOSIG(G,A,B,X,SIGMA,N,F)
330=    GFIRST=G
340=12    SIGMA=SIGMA + STEPSIG
350=C
360=C    CALCULATE G(SIGMA) AT SIGMA + STEPSIGMA
370=C
380=    CALL GOSIG(G,A,B,X,SIGMA,N,F)
390=    GPRIME=G
400=    IF(GPRIME*GFIRST)20,30,40
410=40    GFIRST=GPRIME
420=    GOTO 12
430=20    IF(EPS .GE. STEPSIG) GOTO 30
440=    SIGMA=SIGMA - STEPSIG
450=    STEPSIG=STEPSIG/10.
460=    GOTO 12
470=30    CONTINUE
480=    WRITE(6,101)SIGMA**2,F
490=101    FORMAT(20X,*VARIANCE IS:*,F12.5,10X,*F IS:*,F12.5)
500=C
510=C    PRINT OUT FITTED VALUES TO COMPARE WITH ANALYTICAL RESULTS
520=    DO 17 M=1,N
530=    YJ(M)=F*A(M)+(1.-F)*EXP(-0.5*(X(M)/SIGMA)**2)/SQRT(2*PI*SIGMA**2)
540=17    CONTINUE
550=C    PLOT OF DATA POINTS IN THE HP PLOTTER

```

```

560=C
570= CALL FUN
580= CALL PLOT(2.,2.,-3)
590= CALL SCALE(X,7.,NNN,1)
600= CALL SCALE(B,4.,NNN,1)
610= CALL SCALE(YJ,4.,NNN,1)
611= IF(S(NNN+2) .GT. 0.25) GOTO 999
612= GOTO 998
613=999 B(NNN+2)=0.25
614=998 CONTINUE
620= YJ(NNN+1)=B(NNN+1)
630= YJ(NNN+2)=B(NNN+2)
640= CALL AXIS(0.,0.,11HA-AXIS (MM),-11,7..0..X(52),X(53))
650= CALL AXIS(0.,0.,10IRRADIANCE.10,4.,90..B(52).B(53))
660= CALL NEWPEN(1)
670= CALL LINE(X,B.NNN,1,5,4)
680= CALL SYMBOL(6.,1.2,0.1,11H+-ABERRATED,0.,11)
690= CALL NEWPEN(2)
700= CALL LINE(X,YJ,NNN,1,5,3)
710= CALL SYMBOL(6.,1.0,0.1,8H*-FITTED,0.,8)
720= CALL NEWPEN(4)
730= CALL SYMBOL(1.5,4.5,0.2,17HLEAST SQUARES FIT,0.,17)
740= CALL PLOT(-0.5,-0.5,-3)
750= CALL PLOT(0.,5.5,2)
760= CALL PLOT(8.,5.5,2)
770= CALL PLOT(8.,0.,2)
780= CALL PLOT(0.,0.,2)
790= CALL SYMBOL(5.,4.,0.11,11HRECTANGULAR,0.,11)
800= CALL SYMBOL(5.,3.8,0.11,15HLAMBDA=6.328 UM,0.,15)
810= CALL SYMBOL(5.,3.6,0.11,13HDIM X= 1.0 MM,0.,13)
820= CALL PLOT(4.9,4.5,-3)
830= CALL PLOT(0.,-1.0,2)
840= CALL PLOT(2.,-1.,2)
850= CALL PLOT(2.,0.,2)
860= CALL PLOT(0.,0.,2)
870= CALL PLOTE(N)
880= STOP
890= END
900=C *****
910=C *
920=C * SUBROUTINE TO DETERMINE G(SIGMA)
930=C *
940=C *****
950= SUBROUTINE GUSIG(G,A,B,X,SIGMA,N,F)
960= DIMENSION A(55),B(55),X(55)
970= G=0.
980= PI=3.14159
990= CALL FUSIG(F,A,B,X,SIGMA,N)
1000= DO 2 J=1,N
1010= GA=(-B(J)+A(J)*F)*(1.-F)*EXP(-0.5+(X(J)/SIGMA)**2)
1020= GAA=GA/(SQRT(2.*PI)*SIGMA**2)

```

```

1030=      GB=(1.-F)**2*EXP(-(X(J)/SIGMA)**2)/(2.*PI*SIGMA**3)
1040=      GSUM=GAA + GB
1050=      GG=GSUM*((X(J)/SIGMA)**2-1.)
1060=      G=G + GG
1070=2     CONTINUE
1080=      RETURN
1090=      END
1100=C     *****J*****
1110=C     *
1120=C           SUBROUTINE TO DETERMINE F(SIGMA)
1130=C     *
1140=C     *****
1150=      SUBROUTINE FOSIG(F,A,B,X,SIGMA,N)
1160=      DIMENSION A(55),B(55),X(55)
1170=      FN=0.
1180=      FD=0.
1190=      PI=3.14159
1200=      FA1=1./SQRT(2*PI*SIGMA**2)
1210=      DO 1 I=1,N
1220=      FA=A(I)*B(I)-((A(I)+B(I))*EXP(-0.5*(X(I)/SIGMA)**2))*FA1
1230=      FNUM=FA+(EXP(-(X(I)/SIGMA)**2))/(2*PI*SIGMA**2)
1240=      FN=FN + FNUM
1250=      FDA=A(I)**2-(2*A(I)*EXP(-0.5*(X(I)/SIGMA)**2))*FA1
1260=      FDEN=FDA+(EXP(-(X(I)/SIGMA)**2))/(2*PI*SIGMA**2)
1270=      FD=FD + FDEN
1280=1     CONTINUE
1290=      F=FN/FD
1300=      RETURN
1310=      END
1311=*EOR

```

Appendix C

Values of Randomly Generated Coefficients

C(1)	=	0.248
C(2)	=	0.880
C(3)	=	0.914
C(4)	=	0.035
C(5)	=	0.387
C(6)	=	0.976
C(7)	=	0.611
C(8)	=	0.112
C(9)	=	0.105
C(10)	=	0.553
C(11)	=	0.213
C(12)	=	0.843
C(13)	=	0.314
C(14)	=	0.453
C(15)	=	0.603
C(16)	=	0.955
C(17)	=	0.578
C(18)	=	0.159
C(19)	=	0.030
C(20)	=	0.514

VITA

Captain Arsenio T. Gumahad II was born on 11 January 1957 in Manila, the Philippines. He graduated from Cedar Grove Memorial High School, Cedar Grove, New Jersey in 1972. He attended the New Jersey Institute of Technology from which he received the degree of Bachelor of Science in Electrical Engineering in May 1976. Upon graduation, he received a commission in the USAF and was assigned to the Electronic Intelligence Exploitation Branch, 544th Strategic Intelligence Wing, Strategic Air Command, Offutt AFB, Nebraska as an electrical engineer. In June 1981 he was assigned to the School of Engineering, Air Force Institute of Technology, WPAFB, Ohio.

Permanent Address: 59 David Road
Cedar Grove, NJ 07009

UNCLASSIFIED

SECURITY CLASSIFICATION OF THIS PAGE (When Data Entered)

REPORT DOCUMENTATION PAGE		READ INSTRUCTIONS BEFORE COMPLETING FORM
1. REPORT NUMBER AFIT/GEQ/PH/82D-4	2. GOVT ACCESSION NUMBER A127472	3. RECIPIENT'S CATALOG NUMBER
4. TITLE (and Subtitle) CHARACTERIZATION OF LASER BEAM QUALITY		5. TYPE OF REPORT & PERIOD COVERED MS Thesis
7. AUTHOR(s) ARSENIO T. GUMAHAD II Captain USAP		6. PERFORMING ORG. REPORT NUMBER
9. PERFORMING ORGANIZATION NAME AND ADDRESS Air Force Institute of Technology (AFIT-EN) Wright-Patterson AFB, Ohio 45433		8. CONTRACT OR GRANT NUMBER(s)
11. CONTROLLING OFFICE NAME AND ADDRESS AAWD-2 Air Force Avionics Laboratory Wright-Patterson AFB, Ohio 45433		10. PROGRAM ELEMENT, PROJECT, TASK AREA & WORK UNIT NUMBERS
14. MONITORING AGENCY NAME & ADDRESS (if different from Controlling Office)		12. REPORT DATE December 1982
		13. NUMBER OF PAGES 105
		15. SECURITY CLASS. (of this report) Unclassified
		15a. DECLASSIFICATION/DOWNGRADING SCHEDULE
16. DISTRIBUTION STATEMENT (of this Report) Approved for public release; distribution unlimited		
17. DISTRIBUTION STATEMENT (of the abstract entered in Block 20, if different from Report)		
18. SUPPLEMENTARY NOTES Approved for public release; IAW AFB 100-17. LYNN E. WOLAVEN Dean for Research and Professional Development Air Force Institute of Technology (AFIT) Wright-Patterson AFB OH 45433 APR 7 1983 APR 7 1982		
19. KEY WORDS (Continue on reverse side if necessary and identify by block number) Beam Quality Laser Beam Characterization Nondiffraction-limited beams		
20. ABSTRACT (Continue on reverse side if necessary and identify by block number) Current methods of characterizing the quality of laser beams were found to be generally insufficient. Since lasers are gaining more use in many applications, an improved set of quality criteria must now be developed. This thesis report investigated characteristics of random phase aberrations and its effects on the far-field irradiance distribution of lasers. A numerical model was developed to simulate nondiffraction-limited beams. Several simu-		

DD FORM 1 JAN 73 1473

EDITION OF 1 NOV 65 IS OBSOLETE

UNCLASSIFIED

SECURITY CLASSIFICATION OF THIS PAGE (When Data Entered)

UNCLASSIFIED

SECURITY CLASSIFICATION OF THIS PAGE(When Data Entered)

lations were done to study the irradiance profiles for varying degrees of aberrations. It was found that phase aberrated beams can be expressed as the sum of two beams: one is the diffraction-limited beam attenuated by a factor F which is a function of the phase distortion, and the second, a much wider beam whose amplitude and lateral extent is a function of the variance and the form of the phase aberration. By assuming the shape of this 'secondary' beam to be Gaussian, its extent can be measured by calculating the variance of the Gaussian distribution. A numerical code was devised to determine the two parameters by a least squares fitting method, in addition, a list of procedures is included to measure these parameters, experimentally. The report proposes using the attenuation factor and the lateral extent of the beam as figures of merit when characterizing the quality of laser beams.

UNCLASSIFIED

SECURITY CLASSIFICATION OF THIS PAGE(When Data Entered)

END

FILMED

5-83

DTIC